

METHYLMERCAPTOPROPIONATE-COA LIGASE AND  
METHYLTHIOACRYLOYL-COA HYDRATASE FROM THE  
DIMETHYLSULFONIOPROPIONATE DEMETHYLATION PATHWAY

by

HANNAH A. BULLOCK

(Under the Direction of William B. Whitman)

ABSTRACT

The organosulfur compound dimethylsulfoniopropionate (DMSP) is a valuable commodity for both the phytoplankton that produce it and the marine bacteria that degrade it. While phytoplankton use DMSP primarily as an osmolyte, for marine bacteria DMSP is also a source of reduced carbon and sulfur. The enzymes involved in the pathways for bacterial DMSP metabolism, the cleavage and demethylation pathways, were identified in the roseobacter *Ruegeria pomeroyi* DSS-3. These advances have allowed for in-depth studies of the pathways' enzymes, their regulation, and diversity. Characterization of the DmdB methylmercaptopropionate (MMPA)-CoA ligase isozymes, RPO\_DmdB1 and RPO\_DmdB2, from *R. pomeroyi* revealed these enzymes have activity with a range of substrates but have adapted specific regulatory features for catalyzing reactions with the demethylation pathway intermediate MMPA. The DmdB isozymes were differentially regulated with RPO\_DmdB1 being stimulated by increasing ADP levels while RPO\_DmdB2 responded to increasing MMPA. DmdB may also be regulated by acetylation. RPO\_DmdB2 showed reduced activity when acetylated with a protein *N*-acetyltransferase. Multiple deacetylases from *R. pomeroyi* could

reverse the acetylation. The methylthioacryloyl (MTA)-CoA hydratase DmdD catalyzes the final reaction of the demethylation pathway, but is not widely distributed phylogenetically. An alternative enzyme, AcuH, was identified in *R. pomeroyi* and *Ruegeria lacuscaerulensis*. AcuH was present in diverse microorganisms and exhibited activity towards MTA-CoA and the cleavage pathway intermediate acryloyl-CoA. The regulation of the demethylation and cleavage pathways is still under investigation. While ADP influenced the activity of both DmdB and AcuH, the availability of free tetrahydrofolate (THF) and turnover of methyl-THF may also play a regulatory role. The first step of the demethylation pathway utilizes THF and produces methyl-THF. When THF availability was limited, dimethyl sulfide (DMS) production increased indicating elevated use of the cleavage pathway. Additionally, the specific activities of enzymes required for the turnover of methyl-THF were two-fold higher in cell extracts grown on DMSP compared with acetate. Based on the current evidence, the DMSP degradation enzymes have likely been recruited from preexisting metabolic pathways. While DmdB and AcuH clearly function in DMSP metabolism, they have broader substrate specificities allowing them to carrying out a range of reactions for other pathways.

INDEX WORDS: *Ruegeria pomeroyi*, *Ruegeria lacuscaerulensis*, Roseobacters, Phytoplankton, Alphaproteobacteria, Dimethylsulfoniopropionate, DMSP, Methylercaptopropionate, MMPA, Dimethyl sulfide, DMS, Coenzyme A.

METHYLMERCAPTOPROPIONATE-COA LIGASE AND  
METHYLTHIOACRYLOYL-COA HYDRATASE FROM THE  
DIMETHYLSULFONIOPROPIONATE DEMETHYLATION PATHWAY

by

HANNAH A. BULLOCK

B.S., University of New Hampshire, 2010

A Dissertation Submitted to the Graduate Faculty of The University of Georgia in Partial  
Fulfillment of the Requirements for the Degree

DOCTOR OF PHILOSOPHY

ATHENS, GEORGIA

2016

© 2016

HANNAH ALISSA BULLOCK

All Rights Reserved

METHYLMERCAPTOPROPIONATE-COA LIGASE AND  
METHYLTHIOACRYLOYL-COA HYDRATASE FROM THE  
DIMETHYLSULFONIOPROPIONATE DEMETHYLATION PATHWAY

by

HANNAH ALISSA BULLOCK

Major Professor:	William B. Whitman
Committee:	Mary Ann Moran
	Timothy R. Hoover
	Harry A. Dailey

Electronic Version Approved:

Suzanne Barbour  
Dean of the Graduate School  
The University of Georgia  
December 2016

## ACKNOWLEDGEMENTS

First, I would like to thank my advisor, Dr. William B. Whitman, for showing me to how to become not only a better scientist, but a more creative one as well. I would like to thank my doctoral committee; Dr. Mary Ann Moran, Dr. Timothy Hoover, and Dr. Harry Dailey, for their helpful advice over the years. I would also like to thank the many past and present members of the Whitman lab including: Chris Reisch, Felipe Sarmiento, Feng Long, Warren Crabb, Tao Wang, Yixuan Zhu, Zhe Lyu, Hao Shi, Qiuyuan Huang, Taiwo Solomon Akinyemi, Joe Wirth, Suet Yee Chong, Kamlesh Jangid, Amala Malladi, and Courtney Ellison for their help, friendship, and encouragement. Additionally, Dr. Mary Ann Moran and the members of her lab, Andrew Burns, Christa Smith, and Haiwei Luo, have always been there to help me with experiments, data analysis, and to provide insights into the inner workings of *Ruegeria pomeroyi*. I also thank my classmates, Mark Jones, Angela Pack, Lisa Kuhns, Warren Crabb, and Nathan Hartman and the rest of the Microbiology Department.

I would like to thank my family and friends for their continued support over the years. And finally, thank you to my husband, Norman Hassell, for being a constant source of support, encouragement, and friendship.

## TABLE OF CONTENTS

	Page
ACKNOWLEDGEMENTS .....	iv
CHAPTER	
1 INTRODUCTION AND LITERATURE REVIEW .....	1
2 REGULATORY AND FUNCTIONAL DIVERSITY OF METHYLMERCAPTOPROPIONATE COA LIGASES (DMDB) FROM THE DIMETHYLSULFONIOPROPIONATE DEMETHYLATION PATHWAY IN <i>RUEGERIA POMEROYI</i> DSS-3 AND OTHER PROTEOBACTERIA .....	45
3 ACUH FROM <i>RUEGERIA LACUSCAERULENSIS</i> IS A CROTONASE SUPERFAMILY ENZYME WITH ACTIVITY TOWARDS METHYLTHIOACRYLOYL-COA AND ACRYLOYL-COA.....	89
4 POTENTIAL REGULATORS OF DIMETHYLSULFONIOPROPIOANTE DEMETHYLATION IN <i>RUEGERIA POMEROYI</i> DSS-3: TETRAHYDROFOLATE AVAILABILITY AND DMDB ACETYLATION .....	142
5 CONCLUSIONS .....	185

## CHAPTER 1

### INTRODUCTION AND LITERATURE REVIEW

#### **Introduction:**

Dimethylsulfoniopropionate (DMSP) was first identified in 1948 and has since been found to be not only ubiquitous in marine surface waters but also a valuable resource for many marine organisms and an integral part of the global sulfur cycle (1). DMSP is the precursor of the climate-active gas dimethyl sulfide (DMS), which once released into the atmosphere aids in the formation of cloud condensation nuclei (2, 3). Additionally, DMS is the largest natural source of sulfur to the atmosphere, comparable in magnitude to the sulfur dioxide formed during the burning of coal. As DMS oxidation products display a longer residence time in the atmosphere than anthropogenic sulfur dioxide, their contribution to the global sulfur burden is also greater (2, 4).

From an organismal viewpoint, DMSP is equally important. The ability to produce and metabolize DMSP is concentrated into specific classes of life. The main producers of DMSP are phytoplankton, mostly the classes Dinophyceae (dinoflagellates) and Prymnesiophyceae (coccolithophores) (5). DMSP production has also been noted in diatoms (6, 7), the green algae *Ulva intestinalis* (8), corals (9), and certain higher plants like sugarcane (10), and the coastal angiosperms *Spartina alterniflora* (11) and *Wollastonia biflora* (12) (8, 10-12). The basis of the need for DMSP is not entirely understood. Several physiological functions for DMSP in phytoplankton and green algae have been demonstrated, including roles as an osmolyte, antioxidant, predator deterrent, and cryoprotectant (13-16). At present, each of the proposed

pathways for DMSP biosynthesis begins with methionine, although subsequent steps vary (Figure 1-1) (6, 8, 11, 12). The variations in the individual steps of the DMSP biosynthesis pathways seem to indicate that the ability to synthesize DMSP has evolved at least twice since the separation of the green and red algae lineages and the evolution of terrestrial plants (17). The pathways identified for phytoplankton, algae, and corals share similar reactions and intermediates which differ distinctly from those predicted in the coastal angiosperms (Figure 1-1).

The DMSP demethylation and cleavage pathway enzymes are hypothesized to be adapted versions of enzymes that were already contained within bacterial genomes, developed as a result of physiological and environmental pressures (18, 19). In this review, we investigate the likely evolutionary path that led to the development of DMSP biosynthesis and the subsequent development of specialized DMSP catabolic pathways. Bacteria may metabolize DMSP via two pathways, the cleavage pathway or the demethylation pathway (Figure 1-2). The cleavage pathway results in the formation of DMS, while the demethylation pathway produces methanethiol (MeSH). The members of the Alphaproteobacteria, specifically members of the roseobacter clade, appear to be uniquely adapted to utilize this valuable source of reduced carbon and sulfur. Bacteria within the roseobacter clade possess enzymes that specifically and efficiently catalyze reactions of the demethylation and cleavage pathways (19-24). Bacteria are also responsible for the majority of DMSP catabolism via the cleavage pathway (Figure 1-2). There is additional evidence suggesting the use of DMSP as an osmolyte and antioxidant in marine bacteria (19, 25-28). Many microorganisms encode enzymes that share a great deal of similarity to the demethylation pathway enzymes (Figure 1-3) helping to demonstrate the

adaptability and plasticity of microbial enzymes. The many roles of DMSP may have helped to drive the adaptation of existing enzymes for DMSP metabolism

### **Evolution of Modern Phytoplankton**

The first photosynthetic eukaryotes developed as the result of the acquisition of a cyanobacterium endosymbiont by a eukaryotic host, creating a membrane bound plastid (29-31). Further diversification events lead to the formation of three clades from this original photosynthetic eukaryote, the green algae (green plastid lineage), the red algae (red plastid lineage), and the microbial algae glaucophytes (32). These lineages are distinguished by the chlorophyll present in their plastids. All of the plastids contain chlorophyll a, the green plastids also contain chlorophyll b, and the red plastids contain phycobilin (33). Members of the Charophyta branch of the green plastid lineage colonized the land approximately 430 million year ago (mya). The Chlorophyta branch evolved into the green algae species seen today, including the Euglenoids and Chlorarachniophytes (34-36). Meanwhile, today's marine phytoplankton are largely descended from the red plastid lineage. The red plastid lineage phytoplankton, including coccolithophores, diatoms, and most dinoflagellates, first began to increase in abundance after the end-Permian extinction and into the Mesozoic about 250 mya (37, 38).

The coccolithophores and dinoflagellates both began appearing in the fossil record about 250 mya in the Mid Triassic, while diatoms first appeared during the Early Cretaceous, around 150 mya. All three groups saw extensive diversification in the Mesozoic (250-65 mya) (39-44). The red lineage first began to proliferate in the benthic coastal regions, which were the first consistently oxic marine habitats. The breakup of Pangea increased sea levels and the total length of coastal area available for phytoplankton to colonize. This event also allowed nutrients that had

been locked into the interior portions of the continent to reach coastal waters (45, 46). Changes in ocean redox chemistry from more reducing conditions that favored the green plastid lineage prior to the end-Permian extinction to the higher oxidation states of the Mesozoic ocean further contributed to the success of the red plastid lineage (47). Quigg et al., 2003 presents evidence for the role of trace metal availability in the proliferation of the red plastid lineage based on differences in the trace metal composition of members of the red plastid lineage compared with those of the green plastid lineage (48). Members of the green plastid lineage have much higher requirements for iron, zinc, and copper while members of the red plastid lineage have high requirements for manganese, cobalt, and cadmium. It has been predicted that these differences in trace metal requirements reflect differences in their biochemistry (37, 48).

The dominance of the red plastid lineage is such that all but one of the eight major taxa of eukaryotic phytoplankton in the present day oceans contains the red plastid (37). The diversity of the red plastid lineage has greatly expanded as a result of secondary and tertiary endosymbiotic events, which is evident from the presence of multiple membranes surrounding some plastids of modern day phytoplankton. These events involve the engulfment of an algal cell by another eukaryote via endocytosis (31-33, 49), and the majority of the phytoplankton present today are the result of secondary and sometimes tertiary endosymbiotic events (50). Today's phytoplankton play key roles in global nutrient cycles and particularly in the global sulfur cycle as producers of DMSP and DMS (2).

### **Phytoplankton and DMSP**

Marine phytoplankton and algae live in an environment that is continually changing based on shifts in ocean currents. Living in this dynamic environment requires that these organisms adapt continually to varying temperatures, light, and nutrient availability (51-53).

These changes may have been even more magnified in the Paleozoic and Mesozoic oceans.

Abiotic forces have been shown to have a large impact on the population variability of *Emiliania huxleyi* and *Florisphaera profunda* (51). Phytoplankton adapt quickly and relatively readily to environmental changes due to their rapid cell division rates and large population sizes (52-55).

One specific adaptation that may help phytoplankton deal with their ever changing environment is the ability to synthesize and utilize DMSP and DMS. DMSP makes up about 90% of the reduced sulfur found in algae, but much about the regulation of its biosynthesis and uptake is still not well understood (8). Nevertheless, many of the proposed roles for these compounds would be beneficial to phytoplankton trying to survive in an ever changing environment. DMSP is proposed to have roles as an osmolyte (16), an antioxidant (14), and as a means of balancing excess cellular energy (17, 54). Additionally, polar diatoms and algae are thought to produce DMSP as a cryoprotectant (15). This is supported by the higher levels of DMSP seen in sea ice diatoms compared with those from more temperate climates (6, 7). DMSP is also observed to be a predator/grazing deterrent owing to its cleavage to acrylate (17). New studies of coral genus *Acropora* have generated still more uses for DMSP. Reef building coral juveniles increase DMSP production when subject to thermal stress and may also use DMSP as a bacterial signaling molecule, attracting particular microbial communities that are necessary for coral health (9).

The role of DMSP and DMS as antioxidants could be particularly useful for phytoplankton as plastids are typically hyperoxic and produce reactive oxygen species (ROS) during oxygenic photosynthesis. Other stresses like exposure to ultraviolet radiation (UVR) and thermal stress can further increase ROS production (27, 56, 57). The production of ROS by plastids might explain why DMSP and DMS production are observed in both phytoplankton and

land plants. There is evidence to suggest that the final step of DMSP synthesis in the flowering plant *W. biflora* takes place in the plastid (chloroplast) (58). DMSP and DMS are both able to quench HO•. However, since DMS can diffuse through biological membranes it is possible for it to act as an antioxidant nearly anywhere in the cell (14, 27).

Another impetus for the production of DMSP may be the need for an osmolyte that does not contain nitrogen. Nitrogen is often limiting in ocean surface waters, which may in turn limit the production of the nitrogen-containing osmolyte glycine betaine. Additionally, Ito et al., 2011 observed that under conditions where sulfate-limited growth of the marine algae *Ulva pertusa*, the sulfur from Met was used primarily for the synthesis of adenosyl Met and methionyl-tRNA synthetase, rather than for DMSP synthesis (59). However, when the salinity increased; the sulfur from Met was increasingly used for DMSP biosynthesis, and DMSP uptake increased (59).

One additional hypothesis for the origin of DMSP biosynthesis proposes that it developed as a means of dispelling excess energy, carbon and reducing equivalents when growth becomes unbalanced due to nutrient limitation (17). Rapid changes in the ocean environment can require phytoplankton to have an equally rapid response to imbalances between photosynthesis and growth (52-54). Since photon capture cannot be quickly stopped, production of nitrogen or phosphorous poor molecules when growth is limited by these nutrients is a means of consuming extra carbon, energy, and reducing equivalents that cannot be used for protein biosynthesis or cell division. (17, 54, 55). Further, the continued production of DMSP may also serve to regenerate and redistribute nitrogen for the production of new amino acids and to stimulate continued sulfate assimilation by keeping the cellular concentration of methionine and cysteine

low (8, 17). DMSP may have originally been produced as a means of dissipating excess energy and carbon and was then adapted for other functions.

### **Synthesis of DMSP by Marine Phytoplankton and Algae**

The main producers of DMSP are phytoplankton, mostly in the classes Dinophyceae (dinoflagellates) and the Prymnesiophyceae (which includes the coccolithophores). Certain members of the Chrysophyceae and Bacillariophyceae (diatoms) can also produce DMSP (5). DMSP production is less common among the higher plants, though it has been observed in *Spartina* species (11), certain sugarcanes (10), and the flowering plant *Wollastonia biflora* (12, 60). Recently, DMSP production has been observed in members of the coral genus *Acropora* in the absence of their algal endosymbiont *Symbiodinium*, also a known DMSP producer (9).

Very little is known about the biosynthetic pathways for DMSP in marine phytoplankton from the red plastid lineage and coral, and all of the described pathways are from members of the green plastid lineage. Complete pathways have been described in the green algae *Ulva intestinalis* (8), the marine cordgrass *Spartina alterniflora* (11), and *W. biflora* (12, 60) (Figure 1-1). Each pathway identified thus far begins with methionine and includes a deamination reaction, supporting the hypothesis that DMSP biosynthesis is used by these organisms to regenerate nitrogen from methionine. The DMSP biosynthetic pathways of *S. alterniflora* and *W. biflora* are more similar than the pathway in *U. intestinalis*, suggesting that the plant pathways evolved independently from those in marine algae, corals, and phytoplankton. If true, this would indicate that there was strong selective pressure for the evolution of DMSP biosynthetic pathways even in very different organisms.

The DMSP biosynthesis pathways of the major producers in the marine environment are still largely unknown, but they are likely to be similar to the pathway described in *U. intestinalis*.

The *U. intestinalis* pathway begins with methionine and utilizes an aminotransferase, a NADPH-linked reductase, a methyltransferase, and an oxidative decarboxylase to produce DMSP (8, 61). The commitment step is hypothesized to be the third step, the conversion of 4-methylthio-2-hydroxybutyrate (MTHB) to 4-dimethylsulfonio-2-hydroxybutyrate (DMSHB) by a methyltransferase (Figure 1-1). The key intermediate DMSHB has been identified in *U. intestinalis*, *U. pertusa*, *E. huxleyi*, *Tetraselmis sp.*, and *Melosira nummuloides*, indicating that this pathway is present in a range of phytoplankton (8, 17, 59). Lyon et al., identified candidate proteins and genes for this four step pathway in the sea-ice diatom *Fragilariopsis cylindrus* (6). Proteins from the same enzyme classes proposed in the *U. intestinalis* pathway were more abundant when *F. cylindrus* was exposed to conditions that increase DMSP production. However, the activities of these proteins still need to be verified. Orthologs for the genes encoding a NADPH-reductase and an AdoMet-dependent methyltransferase have also been found in the corals *Acropora millepora* and *Acropora digitifera* and in the coral dinoflagellate symbiont *Symbiodinium*, all known DMSP producers. Based on the collective data, Raina et al., hypothesized that the enzymes of the DMSP biosynthetic pathway are conserved between diatoms, alveolates, green algae, and corals (9). Interestingly, a study of the diatom *Thalassiosira pseudonana* did not identify any of the same proteins proposed for the *F. cylindrus* biosynthetic pathway under conditions that increased intracellular DMSP levels (7).

### **DMSP Cleavage by Marine Phytoplankton**

While the demethylation pathway appears to be unique to marine bacteria, several marine phytoplankton lyse DMSP into DMS. Multiple studies have reported significant DMSP lyase activity within phytoplankton blooms and among individual phytoplankton, including *Phaeocystis sp.*, *Heterocapsa triquetra*, *Scropsiella trochoidea*, and several *Symbiodinium* strains

(62-65). To date, while several marine phytoplankton have been observed to produce DMS from DMSP, the genes responsible for this action have not been identified in most cases. It has been known for many years that *E. huxleyi* cleaves DMSP into DMS and acrylate (65), but only recently was the responsible gene, *Alma1*, identified (66). *Alma1* is a member of the aspartate racemase superfamily. Based on sequence similarity, *Alma1* and its orthologs from *E. huxleyi* are present in a wide range of phytoplankton, as well as certain bacteria, highlighting the diversity of this protein (66, 67). However, the *Alma* homologs tested from *E. huxleyi* and *Symbiodinium sp.* had varying levels of activity towards DMSP (66). Other phytoplankton DMSP lyases have yet to be identified.

### **Bacterial Pathways for DMSP Metabolism**

Marine bacteria have developed many uses for DMSP, from a source of reduced sulfur and carbon (25, 68), to use as an osmolyte (14, 28), and potentially a cryoprotectant (15). The details of the bacterial catabolism of DMSP have only recently come to light (Figure 1-2). The characterization of the enzymes involved in the DMSP demethylation pathway, as well as the identification of several DMSP lyases from the DMSP cleavage pathway, have provided new insights into the evolution of these enzymatic activities. The enzymes of the demethylation pathway have likely roots in fatty acid  $\beta$ -oxidation (18, 19, 21). The DMSP lyases are widely distributed and varied in sequence, structure, and activity (23, 24). Many of the enzymes involved in the microbial DMSP catabolic pathways are widespread, particularly among the Proteobacteria (Figure 1-3). Presumably, the relative modern evolution of DMSP biosynthesis provided the impetus for developing these functions. To learn more about how the degradation pathways evolved, the structural and functional characteristics of the DMSP catabolic enzymes were examined to posit how they may have been adapted from existing enzymes.

## Enzymatic Cleavage of DMSP

The enzymatic cleavage of DMSP produces DMS and acrylate. To date, eight DMSP lyases have been identified (Table 1-1). The lyases were recently reviewed in (24). Except DddD which produces 3-hydroxypropionate, these enzymes all carry out the same reaction to form DMS and acrylate even though they differ drastically in sequence and size (23, 69). This variability indicates that the DMSP lyases likely evolved separately. The diversity of the DMSP lyases that have been identified so far indicates that there is a great deal of pressure to evolve this function. There are several reports of DMSP lyase activity being induced by the presence of DMSP. *Ruegeria pomeroyi* DSS-3 and *Roseovarius nubinhibens* *dddP* and *dddQ* expression were induced when cells were pre-grown with DMSP as compared to cells not exposed to DMSP, as was *dddY* in *Alcaligenes faecalis* (70, 71). Further, a field study in Monterey Bay, CA found that expression of *dddP* was increased during mixed-community DMSP-producing phytoplankton blooms (72).

Evidence of the physiological relevance of the two best studied lyases, DddP and DddQ, has been mounting. The *dddP* and *dddQ* genes are the most abundant of the bacterial DMSP lyases in the marine metagenome as determined by the Global Ocean Sampling Expedition (GOS) (73, 74). DddP and DddQ from *R. pomeroyi* DSS-3 and *R. nubinhibens* show a clear role in DMSP cleavage. Labeling studies using  $^{14}\text{C}$  or  $^{13}\text{C}$  labelled DMSP show DMS and acrylate production from *Escherichia coli* extracts expressing the *dddQ* and *dddP* from *R. nubinhibens* and *R. pomeroyi* (73, 75). Additionally, *dddP* and *dddQ* mutants in *R. pomeroyi* produce significantly less DMS when compared with WT cells, 50% less in the case of *dddP* and 97% less in the case of *dddQ*. A *dddQ* mutant from *R. nubinhibens* produced 20% less DMS from DMSP while a *dddP* mutant produced only 10% of the WT levels (71, 73, 75). The structures of

the DMSP lyases may provide insight into their evolutionary roots. The crystal structures of DddP and DddQ from *R. lacuscaerulensis* and DddP from *Roseobacter denitrificans* have been solved (76, 77). Data gathered from the available structures suggests that subtle changes in the active sites of these lyases make sulfur containing substrates, like DMSP, the preferred substrates for these enzymes.

The sequence and structure of DddP most closely resembles that of M24 peptidase (Figure 1-4). Typically, an M24 peptidase hydrolyzes C-N bonds. DddP, however, cleaves C-S bonds (71, 77). Wang and coworkers expressed the recombinant *R. lacuscaerulensis dddP* in *E. coli* and found it displayed no measureable activity towards the M24 peptidase substrate valine-proline, but it did exhibit DMSP lyase activity, producing acrylate and DMS (77). DddP is a homodimeric protein in which one monomer has a metal center containing Fe, while the other monomer generally contains Fe, but may also contain Ni, Zn, or Cu instead (77, 78). The explanation for the change in substrate preference and activity appears to be due to the change of the active ion from Co or Mn coordinated by five residues in the M24 peptidases to Fe coordinated by six residues in DddP. The two metal ions in DddP are coordinated with three aspartates, two glutamates, and a histidine residue, which are conserved in the known functional DddPs (77, 78). The substitution of any of the active site residues for alanine in DddP results in the elimination of DMSP lyase activity, indicating that all six are necessary for activity (75, 77). Additionally, two conserved histidine residues in M24 peptidases that help to bind and stabilize substrates are exchanged for aspartate and phenylalanine in DddP (77, 78). Wang et al., suggest that this change abolishes the peptidase activity of DddP and allows the active site aspartate to act as a nucleophilic base for DMSP cleavage (77). It is further proposed that DddP is a case of divergent evolution from the M24 peptidases as DddPs cluster in a separate clade. In support of

this hypothesis, the M24 peptidase conserved C-domain has up to 31% sequence identity with the C-domain of the *R. lacuscaerulensis* DddP. The N-domain of DddP, by contrast is structurally different than the N-domains of M24 peptidases and allows for the formation of a compact dimer and a smaller catalytic cavity for DMSP binding (77). In conclusion, DddP appears to have acquired specific adaptations for DSMP lyase activity, supporting the assertion that this is its major role.

A structure for DddQ from *R. lacuscaerulensis* has recently been solved (76). DddQ is one of the cupin motif containing DMSP lyases, along with DddW and DddL (23, 24). DddQs have been identified in a number of roseobacters, but they display substantial amino acid sequence variation, even when multiple copies are present in the same organism (73). Despite this variation, certain amino acids in the cupin motifs, two histidines and a glutamate in cupin motif 1, and a histidine in cupin motif 2, are conserved in DddQ, DddW, and DddL. In addition to these conserved amino acids, two tyrosines in motif 1 are highly conserved in all the cupin protein DMSP lyases, but not among other cupin proteins. These conserved active site residues are predicted to play a role in DMSP cleavage as substitution at any of these residues decreased activity towards DMSP (76).

The formation of DMS and acrylate from DMSP is proposed to be the result of a  $\beta$ -elimination reaction (76, 77). The DMSP lyases appear to have developed different catalytic mechanisms for carrying out the same reaction, indicating separate evolutionary paths to this activity. DddP is proposed to implement an ion shift. When DMSP enters the active site, a moveable Fe binds to the carboxyl group of DMSP, stabilizing the molecule in the active site, while two other conserved residues, tryptophan and tyrosine, bind to the sulfur in DMSP. This orientation allows for the abstraction of a proton by aspartate from the alpha carbon of the DMSP

carboxyl group, cleavage of the C-S bond, and the subsequent formation of a double bond between alpha and beta carbons of DMSP to produce acrylate (77, 78). In DddQ, it has been proposed that binding of DMSP to the metal cofactor causes a conserved tyrosine residue to shift closer to the DMSP molecule. This shift allows the oxygen atom of one of the conserved tyrosine residues to interact with the alpha carbon of DMSP. The resultant conformational change enables the abstraction of a proton from the DMSP carboxyl group by the oxygen atom of tyrosine (76). The algal DMSP lyase, Alma1, is proposed to function in a similar manner, abstracting a proton from the carbon adjacent to the carboxylate to cause  $\beta$ -elimination and the subsequent release of DMS and acrylate (66). Further investigations into the structures and mechanisms of the other DMSP lyases, like the algal Alma1 or DddY, may yield still more variability in reaction mechanisms.

Despite promising evidence for the physiological role of the DMSP lyases, none of the currently known lyases have particularly high affinity for DMSP, displaying  $K_m$ s for DMSP in the millimolar range (Table 1-1) (24). The  $K_m$ s for the most widely distributed lyases, DddP and DddQ, are some of the highest (73, 74). The lowest  $K_m$  for DMSP observed thus far is for DddY. The DddYs from *Alcaligenes faecalis* and *Desulfovibrio acrylicus* DddY has  $K_m$ s for DMSP of 1.4 and 0.4 mM, respectively (Table 1-1) (79, 80). Both of these organisms are found in coastal marine sediments and likely obtain DMSP from *Spartina spp.* (81). High  $K_m$  values for DMSP is also shared with the DMSP demethylases (see DmdA below), which is the first committed step of the demethylation pathway. Thus, the low affinities of the lyases may simply reflect the requirement for high intracellular concentrations of DMSP. It is possible that since DMSP may be maintained at high concentrations in the cell for use as an osmolyte, low  $K_m$ s for DMSP are not necessary for DMSP lyases to function effectively *in vivo* (20). Senescence and autolysis of

DMSP producers, like *Spartina* or phytoplankton, can also produce microenvironments with high concentrations of DMSP (82).

DddY is the most unique of the DMSP lyases and was the first to be identified (82). It is the only DMSP lyase that is a periplasmic protein and is not similar to any currently known polypeptides. In addition to the DddYs from *A. faecalis* M3A and *D. acrylicus*, putative DddYs have been identified in several *Shewanella* species and *Acrobacter nitrofigilis* DSM7299. DMS production from DMSP was observed in *Shewanella halifaxensis* HAW-EB4, *Shewanella putrefaciens* CN-32, and *A. nitrofigilis* DSM7299 (81). *S. halifaxensis* and *S. putrefaciens* are found in marine sediments and shale sandstone, respectively, while *A. nitrofigilis* can be found in sediment around *Spartina* roots. It is likely that *dddY* was spread via horizontal gene transfer (HGT). In addition to *dddY*, *A. faecalis* also has acrylate utilization (*acu*) genes that resemble those used for DMSP and acrylate metabolism in other DMSP-utilizing bacteria (81). More in depth studies of DddY have not been undertaken.

### **Bacterial Demethylation of DMSP**

The DMSP demethylation pathway consists of a series of reactions that convert DMSP into methanethiol (MeSH), HS-CoA, CO<sub>2</sub>, and acetaldehyde (18, 19). While DMS production from phytoplankton has been observed, there is no indication that these organisms possess the demethylation pathway. Instead, the demethylation pathway is restricted to the Alphaproteobacteria (Figure 1-3). Based on the current evidence, it seems likely that the individual steps of the demethylation pathway may have evolved independently.

## **DmdA: An Adapted Glycine Cleavage T-protein**

The initial step of the demethylation pathway is mediated by the DMSP demethylase DmdA. This step also commits DMSP metabolism to the demethylation pathway as the demethylation of DMSP precludes the formation of DMS (19, 20, 83). As with the DMSP lyases, the  $K_m$ s for DMSP of the two characterized DmdAs, from *R. pomeroyi* and *Pelagibacter ubique*, are relatively high, 5.4 mM and 13.2 mM, respectively. The deletion of *dmdA* from *Ruegeria pomeroyi*, however, results in a mutant incapable of producing MeSH, indicating that this gene encodes the only protein in *R. pomeroyi* able to perform this reaction (20, 83). Additionally, field measurements indicate that *dmdA* expression is upregulated during blooms of DMSP-producing phytoplankton (72). DmdA in *R. pomeroyi* was initially annotated as a glycine cleavage T-protein (GcvT) (18). However, when analyzed phylogenetically, DmdA-like proteins share sequence identity ranging from 22-26% with GcvT, dimethylglycine oxidase and sarcosine oxidase, but form a separate clade from known GcvTs.

The crystal structure of DmdA from *P. ubique* provides further evidence supporting a common ancestry for DmdA and GcvT (Figure 1-5). Schuller et al., described the structure of DmdA, noting that while DmdA is structurally similar to GcvT, the low sequence similarity between the two indicated that the enzymes are evolutionarily distant (84). Both proteins possess a highly similar tri-domain structure (Figure 1-5) with the conserved residues between the proteins being mainly involved with tetrahydrofolate (THF) binding. Specifically, the residues that bond with the folate moiety and those involved in the ring stacking of THF are highly conserved (20, 84, 85). Despite structural similarity, DmdA and GcvT are mechanistically distinct. DmdA produces 5-methyl-THF from DMSP as the result of a redox-neutral methyl

transfer while GcvT converts glycine to 5,10-methylene-THF (20, 83, 84). Small changes to the THF binding fold in DmdA allow for hydrogen bond formation between amino acid residues in the fold and THF, enabling DmdA to carry out a redox-neutral methyl transfer to produce 5-methyl-THF. Overall, the mechanism of DmdA catalysis appears to be most similar to the *S*-adenosylmethionine SAM-dependent *N*-methyltransferases (84).

Phylogenetic analysis reveals that GcvTs and other similar proteins are nearly universally distributed among the prokaryotes, while DmdA proteins cluster separately. DmdA appears to be most prevalent among members of the Alphaproteobacteria (Figure 1-3) (20, 86). DmdA may have originally been a GcvT, but the development of a new activity and substrate preference has uniquely adapted this enzyme for DMSP metabolism (20). Other organisms without DmdA may simply maintain DMSP as an osmolyte or utilize one of the many DMSP lysases identified so far to metabolize it.

### **The Flexibility of DmdB and DmdC**

Once methylmercaptopropionate (MMPA) is produced by DmdA, it is converted first to MMPA-CoA by the MMPA-CoA ligase or DmdB and then to methylthioacryloyl (MTA)-CoA by the MMPA-CoA dehydrogenase DmdC (18). In contrast to the narrower distribution of DmdA, DmdB and DmdC are found in up to 60% of surface ocean bacteria, assuming one copy per cell, as well as in bacteria from terrestrial environments (Figure 1-3) (19). The DmdB and DmdC enzymes characterized thus far show activity with a wide range of substrates, mostly with short to medium chain length fatty acids and their CoA derivatives (unpublished data)(19, 21) . These enzymes probably did not originate specifically for DMSP metabolism, potentially having been recruited from the pathways of methionine degradation and  $\beta$ -fatty acid oxidation (18, 19).

The ability of DmdB and DmdC to act upon MMPA and MMPA-CoA is a demonstration of the plasticity and flexibility of these enzymes.

*R. pomeroyi* possess more than 20 CoA ligases, but not all are predicted to have activity with MMPA. *R. pomeroyi* has two DmdB isozymes, RPO\_DmdB1 and RPO\_DmdB2 (Table 1-2). RPO\_DmdB1 has a  $K_m$  of 0.08 mM for MMPA but has even lower  $K_m$ s for butyrate and propionate, 0.02 mM and 0.04 mM, respectively. RPO\_DmdB2 has a  $K_m$  for MMPA similar to that of RPO\_DmdB1, 0.07 mM, but this was the lowest  $K_m$  it displayed with any of the substrates tested (Table 1-2) (21). It has been observed that there are distinct differences between the DmdB enzymes from marine and non-marine microorganisms. Particularly, only the DmdBs from marine enzymes showed sensitivity to the presence of DMSP, likely part of the regulation for DMSP metabolism. *R. pomeroyi*'s DmdB isozymes exhibit different regulatory mechanisms to stimulate the enzymes' activity for DMSP metabolism. RPO\_DmdB1 responds to changes in cellular energy charge, while RPO\_DmdB2 responds to MMPA concentration (21). The regulatory mechanisms that have developed for the DmdB isozymes suggest that these enzymes have adapted from general short chain fatty acid CoA ligases to become more specialized for activity with MMPA and DMSP metabolism.

Three DmdC isozymes were identified in *R. pomeroyi* and verified to have activity towards MMPA-CoA (19). The  $K_m$  of one of the DmdC isozymes (SPO3804; DmdC1) from *R. pomeroyi* for MMPA-CoA is low at 0.03 mM. Lower  $K_m$ s were observed for this enzyme with caproyl-CoA, valeryl-CoA, and butyryl-CoA (unpublished data). Thus, MMPA-CoA is not necessarily the preferred substrates for this enzyme. Instead, the substrate specificity of DmdC appears, like DmdB, to be based primarily on the length of the carbon chain of a substrate. Regulation of the DmdC isozymes has not yet been studied.

DmdB and DmdC isozymes are more widely distributed than DmdA, suggesting that this enzyme may be important in organisms that either metabolize only MMPA or possess pathways that form MMPA from substrates other than DMSP. These enzymes are also insensitive to regulation by DMSP, supporting the hypothesis of a different physiological role from the roseobacter DmdBs. Methionine degradation is one potential source of MMPA (87), a side reaction of the methionine salvage pathway can also produce MMPA (88, 89). *Xanthomonas campestris* produces MMPA to induce bacterial blight in cassava (90, 91), and many plants, particularly fruiting plants, produce sulfur volatiles which closely resemble MMPA in structure (e.g. 3-methylthio-propanol, 3-methylthio-propanal, and ethyl-3-methylthio-propionate) (92). These compounds may also be substrates of DmdB.

#### **DMSP Specific Enoyl-CoA Hydratases: DmdD and AcuH**

DmdD, a member of the crotonase superfamily, appears to be uniquely adapted for the metabolism of DMSP. DmdD has a crystal structure largely similar to other crotonases, a hexamer made up of a dimer of trimers. Figure 1-6 shows an overlay of one DmdD monomer with a monomer of rat liver enoyl CoA hydratase (ECH) The main difference is that in DmdD the C-terminal loops of one of the trimers is oriented so that it can interact with the phosphate groups of CoA (Figure 1-6). DmdD is similar to the rat liver ECH, sharing 32% amino acid identity (22). The same glutamate residues that are conserved in the rat liver ECHs and are important for catalysis are also conserved in DmdD. However, DmdD is not nearly as efficient as ECH at catalyzing the hydration of crotonyl-CoA, with a catalytic efficiency of  $2100 \text{ mM}^{-1}\text{s}^{-1}$  compared with the typical  $45000\text{-}119000 \text{ mM}^{-1}\text{s}^{-1}$  of other crotonases. DmdD instead displays a  $K_m$  of  $0.008 \text{ mM}$  for MTA-CoA and a high catalytic efficiency,  $5400 \text{ mM}^{-1}\text{s}^{-1}$  (22, 93, 94). This greater catalytic efficiency only applies to reactions with MTA-CoA and appears to be due, at

least in part, to the structure of MTA-CoA. The combination of the double bond and sulfur atom in MTA-CoA seem key for high rates DmdD hydrolysis activity as reactions with MMPA-CoA and crotonyl-CoA occur at lower rates (22).

While DmdD is highly efficient at catalyzing the hydration of MTA-CoA, it is not widely distributed (19). DmdD is lacking in the majority of marine bacteria that utilize the demethylation pathway (possess DmdA) (Figure 1-3). An ortholog of DmdD, named AcuH, has been identified in *R. lacuscaerulensis* and *R. pomeroyi* (Bullock et al., 2016, unpublished). AcuH is a hydratase with high activity toward acryloyl-CoA, but also displays activity toward MTA-CoA. While AcuH is less efficient than DmdD at hydrolyzing MTA-CoA, it is far more common, being found in a wide range of microorganisms, including in the roseobacter clade (Figure 1-3). Based on amino acid sequence identity, DmdD and AcuH are both likely ECHs that have been adapted to function in the DMSP demethylation pathway. *R. pomeroyi* DmdD and AcuHs from *R. pomeroyi* and *R. lacuscaerulensis* have similar catalytic efficiencies for crotonyl-CoA, within the range of 2000-3800  $\text{mM}^{-1}\text{s}^{-1}$  (Table 1-3). However, recombinant AcuH from *R. lacuscaerulensis* and *R. pomeroyi* display very different catalytic efficiencies for MTA-CoA of 11.5  $\text{mM}^{-1}\text{s}^{-1}$  and 0.1  $\text{mM}^{-1}\text{s}^{-1}$ , respectively. These are drastically lower than the 5400  $\text{mM}^{-1}\text{s}^{-1}$  observed for *R. pomeroyi* DmdD (Table 1-3) (22) (Bullock et al., manuscript in preparation). The result of the lower catalytic efficiency of AcuH is demonstrated by the inability of an *R. pomeroyi* DmdD deletion strain to grow on MMPA as a sole carbon source. This confirms that the catalytic efficiency of the *R. pomeroyi* AcuH is not sufficient to power the demethylation pathway. By contrast, the recombinant *R. lacuscaerulensis* AcuH complements a *R. pomeroyi* *dmdD* deletion, allowing slow growth on MMPA comparable to the growth of wild-type *R. lacuscaerulensis* (Bullock et al., manuscript in preparation). AcuH in many cases may not

possess sufficient activity with MTA-CoA to allow for growth on DMSP or MMPA as a sole substrate. AcuH could, however, allow for metabolism of DMSP and MMPA via the demethylation pathway when mixed carbon sources are available, while catalyzing the hydrolysis of MTA-CoA at a low rate.

AcuH-like enzymes are distributed across all domains of life, including many organisms unlikely to utilize DMSP or metabolize MTA-CoA. AcuH is predicted to function in the cleavage pathway as it efficiently hydrolyzes acryloyl-CoA (Figure 1-2) (Bullock et al 2016, manuscript in preparation). Interestingly, while DmdD has no activity towards acryloyl-CoA both the *R. lacuscaerulensis* and *R. pomeroyi* AcuHs have high catalytic efficiencies ( $7.4 \times 10^6 \text{ mM}^{-1} \text{ s}^{-1}$  and  $4.9 \times 10^6 \text{ mM}^{-1} \text{ s}^{-1}$ , respectively) for this substrate (Table 1-3) (Bullock et al., manuscript in preparation). Clearly, AcuH is more specialized for activity with acryloyl-CoA, or crotonyl-CoA rather than MTA-CoA. This is true for a number of putative AcuHs that have been analyzed. AcuH is a more versatile enzyme than DmdD and has maintained more of its similarity to ECH, as is evident by its level of activity toward crotonyl-CoA and acryloyl-CoA (Bullock et al., manuscript in preparation). Since AcuH may function in both the cleavage and the demethylation pathways, it gives the cells metabolic flexibility. DmdD, by contrast, has adapted specifically to function in the demethylation pathway, allowing organisms which possess DmdD to utilize DMSP more efficiently.

### **Conclusion: Evolution of DMSP Metabolism**

It is unclear what the original impetus for the development of DMSP biosynthetic pathway may have been. The proposed roles for DMSP in marine phytoplankton as an osmolyte, antioxidant, predator deterrent, cryoprotectant, and as an energy overflow mechanism would provide great benefit, particularly in consistently changing marine environments. If DMSP was

originally produced as part of an overflow mechanism for dealing with unbalanced growth due to nutrient limitation, the other benefits provided by this compound may have selected for the maintenance of this pathway.

DMSP likely first became abundant in ocean environments about 250 mya in conjunction with the increasing abundance of dinoflagellates and coccolithophores. The dinoflagellates appear to be the key players. Based on a comparison of literature reports for 95 DMSP producing species (Table 1-4), it was determined that dinoflagellates produce the highest amounts of DMSP, with intracellular concentrations ranging from 0.00011 to 14.7 pmol/cell. In particular, *Alexandrium minutum* and *Protoperidinum* produced 14.2 and 14.7 pmol DMSP/cell respectively. Diatoms have intracellular DMSP concentrations ranging from 0.0006-0.257 pmol/cell, while haptophytes (coccolithophores) contained from 0.00037-0.148 pmol DMSP/cell (Unpublished data from H. Luo) (95). The case may be made for the co-evolution of the marine roseobacter and the DMSP producing-phytoplankton. Members of the roseobacter clade are abundant in coastal waters and are one of the main bacterial groups enriched during DMSP-producing phytoplankton blooms (96-98). The roseobacter ancestor is predicted to have undergone a genome expansion around 250 mya, the same time as the increase in abundance and diversification of the dinoflagellates and coccolithophores (99, 100). Thus, the radiation of the dinoflagellates and coccolithophores may have provided new environments for members of the roseobacter clade, in much the same way that the breakup of Pangea and changes in ocean redox chemistry created new environments for the proliferation of members of the red plastid lineage (47, 48, 99).

As DMSP became more readily available in the environment, marine organisms, like *R. pomeroyi* and other roseobacters, likely adapted to utilize this compound as a source of carbon,

as well as reduced sulfur. In this process, organisms would likely have adapted proteins already encoded for in their genomes to utilize this new compound with exposure to DMSP driving the evolution of function. Examples of this can be seen in the enzymes DmdA and DmdD from the demethylation pathway and DddP from the cleavage pathway. Each of these enzymes have become more specialized to function in DMSP metabolism, particularly DmdA and DmdD. AcuH adopted a different strategy and can function as both a MTA-CoA hydratase in the demethylation pathway and an acryloyl-CoA hydratase in the cleavage pathway. DmdB and DmdC maintained activity with a wide range of substrates while adapting to function efficiently in DMSP metabolism as well.

Enzymes are known to diverge from a parental function to develop new substrate specificities. Enzymes maintain a certain core set of amino acid residues that are required for functionality and structure but also leave room for variation and change in the remaining amino acids. This can lead to new functions and substrate specificities (101). Likely, this is the reason the amino acid sequences and structures of the proteins that catalyze the DMSP catabolic reactions do not vary greatly from their non-DMSP degrading counter parts. It is a common view that enzymes families have evolved via the duplication of a gene encoding a multifunctional and multispecific enzyme that then undergoes an alteration in substrate specificity (102). We see several possible cases of this within the DMSP catabolic proteins. The enzymes of the DMSP demethylation and cleavage pathway are simply examples of the various processes of enzyme adaptation and evolution.

## References

1. **Challenger F, Simpson MI.** 1948. Studies on biological methylation; a precursor of the dimethyl sulphide evolved by *Polysiphonia fastigiata*; Dimethyl-2-carboxyethylsulphonium hydroxide and its salts. *J. Chem. Soc.* **43**:1591-1597.
2. **Lovelock JE, Maggs RJ, Rasmussen Ra.** 1972. Atmospheric dimethyl sulfide and natural sulfur cycle. *Nature* **237**:452-453.
3. **Hatakeyama S, Okuda M, Akimoto H.** 1982. Formation of sulfur-dioxide and methanesulfonic-acid in the photo-oxidation of dimethyl sulfide in the air. *Geophys. Res. Lett.* **9**:583-586.
4. **Chin M, Jacob DJ.** 1996. Anthropogenic and natural contributions to tropospheric sulfate: A global model analysis. *J. Geophys. Res.* **101**:18691-18699.
5. **Keller M.** 1989. Dimethyl sulfide production and marine phytoplankton. *Biological Oceanography* **6**:375-382.
6. **Lyon BR, Lee PA, Bennett JM, DiTullio GR, Janech MG.** 2011. Proteomic analysis of a sea-ice diatom: salinity acclimation provides new insight into the dimethylsulfoniopropionate production pathway. *Plant Physiol.* **157**:1926-1941.
7. **Kettles NL, Kopriva S, Malin G.** 2014. Insights into the regulation of DMSP synthesis in the diatom *Thalassiosira pseudonana* through APR activity, proteomics and gene expression analyses on cells acclimating to changes in salinity, light and nitrogen. *PLoS One* **9**:e94795.
8. **Gage DA, Rhodes D, Nolte KD, Hicks WA, Leustek T, Cooper AJ, Hanson AD.** 1997. A new route for synthesis of dimethylsulphonio propionate in marine algae. *Nature* **387**:891-894.
9. **Raina JB, Tapiolas DM, Foret S, Lutz A, Abrego D, Ceh J, Seneca FO, Clode PL, Bourne DG, Willis BL, Motti CA.** 2013. DMSP biosynthesis by an animal and its role in coral thermal stress response. *Nature* **502**:677-680.
10. **Paquet L, Rathinasabapathi B, Saini H, Zamir L, Gage DA, Huang ZH, Hanson AD.** 1994. Accumulation of the compatible solute 3-dimethylsulfoniopropionate in sugarcane and its relatives, but not other gramineous crops. *Aust. J. of Plant Physiol.* **21**:37-48.
11. **Kocsis MG, Nolte KD, Rhodes D, Shen TL, Gage DA, Hanson AD.** 1998. Dimethylsulfoniopropionate biosynthesis in *Spartina alterniflora*. Evidence that S-methylmethionine and dimethylsulfoniopropylamine are intermediates. *Plant Physiol.* **117**:273-281.

12. **Hanson AD, Rivoal J, Paquet L, Gage DA.** 1994. Biosynthesis of 3-dimethylsulfoniopropionate in *Wollastonia biflora* (L.) DC. Evidence that S-methylmethionine is an intermediate. *Plant Physiol* **105**:103-110.
13. **Wolfe GV, Steinke M.** 1997. Grazing-activated chemical defense in a unicellular marine alga. *Nature* **387**:894-897.
14. **Sunda W, Kieber DJ, Kiene RP, Huntsman S.** 2002. An antioxidant function for DMSP and DMS in marine algae. *Nature* **418**:317-320.
15. **Karsten U, Kuck K, Vogt, C. Kirst, GO.** 1996. Dimethylsulphoniopropionate production in phototrophic organisms and its physiological function as a cryoprotectant., p. 143-153. *In* Kiene RV, PT. Keller, MD. Kirst, GO. (ed.), *Biological and Environmental Chemistry of DMSP and Related Sulphonium Compounds*. Plenum Press, New York.
16. **Kirst GO, Thiel C, Wolff H, Nothnagel J, Wanzek M, Ulmke R.** 1990. Dimethylsulfoniopropionate (DMSP) in icealgae and its possible biological role. *Mar. Chem.* **35**:381-388.
17. **Stefels J.** 2000. Physiological aspects of the production and conversion of DMSP in marine algae and higher plants. *J. Sea Res.* **43**:183-197.
18. **Reisch CR, Moran MA, Whitman WB.** 2011. Bacterial catabolism of dimethylsulfoniopropionate (DMSP). *Front. Microbiol* **2**:172.
19. **Reisch CR, Stoudemayer MJ, Varaljay VA, Amster IJ, Moran MA, Whitman WB.** 2011. Novel pathway for assimilation of dimethylsulphoniopropionate widespread in marine bacteria. *Nature* **473**:208-211.
20. **Reisch CR, Moran MA, Whitman WB.** 2008. Dimethylsulfoniopropionate-dependent demethylase (DmdA) from *Pelagibacter ubique* and *Silicibacter pomeroyi*. *J. Bacteriol.* **190**:8018-8024.
21. **Bullock HA, Reisch CR, Burns AS, Moran MA, Whitman WB.** 2014. Regulatory and functional diversity of methylmercaptopropionate coenzyme A ligases from the dimethylsulfoniopropionate demethylation pathway in *Ruegeria pomeroyi* DSS-3 and other proteobacteria. *J. Bacteriol.* **196**:1275-1285.
22. **Tan D, Crabb WM, Whitman WB, Tong L.** 2013. Crystal structure of DmdD, a crotonase superfamily enzyme that catalyzes the hydration and hydrolysis of methylthioacryloyl-CoA. *PLoS One* **8**:e63870.
23. **Curson AR, Todd JD, Sullivan MJ, Johnston AW.** 2011. Catabolism of dimethylsulphoniopropionate: microorganisms, enzymes and genes. *Nat. Rev. Microbiol.* **9**:849-859.

24. **Johnston AW, Green RT, Todd JD.** 2016. Enzymatic breakage of dimethylsulfoniopropionate-a signature molecule for life at sea. *Curr. Opin. Chem. Biol.* **31**:58-65.
25. **Kiene RL, Linn LJ, Bruton, JA.** 2000. New and important roles for DMSP in marine microbial communities. *J. Sea Res.* **43**:209-224.
26. **Simo RA, Archer SD, Pedros-Alio C, Gilpin L, Stelfox-Widdicombe, CE.** 2002. Coupled dynamics of dimethylsulfoniopropionate and dimethyl sulfide cycling and the microbial food web in surface waters of the North Atlantic. *Limnol. and Oceanogr.* **47**:53-61.
27. **Lesser MP.** 2006. Oxidative stress in marine environments: Biochemistry and physiological ecology. *Annu. Rev. Physiol.* **68**:253-278.
28. **Salgado P, Kiene R, Wiebe W, Magalhaes C.** 2014. Salinity as a regulator of DMSP degradation in *Ruegeria pomeroyi* DSS-3. *J. Microbiol.* **52**:948-954.
29. **Bhattacharya D, Medlin L.** 1998. Algal phylogeny and the origin of land plants. *Plant Physiol.* **116**:9-15.
30. **Yoon HS, Hackett JD, Ciniglia C, Pinto G, Bhattacharya D.** 2004. A molecular timeline for the origin of photosynthetic eukaryotes. *Mol. Biol. Evol.* **21**:809-818.
31. **Palmer JD.** 2003. The symbiotic birth and spread of plastids: How many time and whodunit. *Journal Phycology* **39**:4-11.
32. **Delwiche CF.** 1999. Tracing the thread of plastid diversity through the tapestry of life. *Am. Nat.* **154**:S164-S177.
33. **Keeling PJ.** 2010. The endosymbiotic origin, diversification and fate of plastids. *Phil. Trans. R. Soc. Biol. Sci* **365**:729-748.
34. **Lewis LA, McCourt RM.** 2004. Green algae and the origin of land plants. *Am. J. Bot.* **91**:1535-1556.
35. **McCourt RM, Delwiche CF, Karol KG.** 2004. Charophyte algae and land plant origins. *Trends Ecol. Evol.* **19**:661-666.
36. **Sanderson MJ.** 2003. Molecular data from 27 proteins do not support a Precambrian origin of land plants. *Am. J. Bot.* **90**:954-956.
37. **Falkowski PG, Katz ME, Knoll AH, Quigg A, Raven JA, Schofield O, Taylor FJ.** 2004. The evolution of modern eukaryotic phytoplankton. *Science* **305**:354-360.

38. **Falkowski PG, Schofield O, Katz ME, van de Schootbrugge B, Knoll A.** 2004. Why Is the Land Green and the Ocean Red? p. 429-453. *In* H. Thierstein and J. Young (eds.) *Coccolithophores-From molecular processes to global impact*. Elsevier, Amsterdam.
39. **Bown PR, Lees J, Young JR.** 2004. Calcareous nannoplankton diversity and evolution through time. p. 481-508. *In* H. Thierstein and J. Young (eds.) *Coccolithophores-From molecular processes to global impact*. Springer-Verlag, Berlin.
40. **Harwood DM, Nikolaev VA.** 1995. Cretaceous diatoms: morphology, taxonomy, biostratigraphy. Paleontological Society, Lawrence, KS.
41. **Moldowan JM Dahl J, Jacobson SR, Huizinga BJ, Fago FJ, Shetty R, Watt DS, Peters, KE.** 1996. Chemostratigraphic reconstruction of biofacies: Molecular evidence linking cyst-forming dinoflagellates with pre-Triassic ancestors. *Geology* **24**:159-162.
42. **Moldowan JM, Jacobson S.** 2000. Chemical signals for early evolution of major taxa: biosignatures and taxon-specific biomarkers. *International Geology Review* **42**:805-812.
43. **Moldowan JM, Talyzina NM.** 1998. Biogeochemical evidence for dinoflagellate ancestors in the Early Cambrian. *Science* **281**:1168-1170.
44. **Stover LE, Brinkhuis H, Damassa SP, de Verteuil L, Helby RJ.** 1996. Mesozoic-Tertiary dinoflagellates, acritarchs and prasinophytes. *Amer. Assoc. Strat, Palynol. Found* **2**:641-750.
45. **Haq BU, Hardenbol J, Vail PR.** 1987. Chronology of fluctuating sea levels since the triassic. *Science* **235**:1156-1167.
46. **Vail PR, Mitchum RM, Thompson III S.,** 1977. Seismic stratigraphy and global changes of sea level, part 4: Global cycles of relative changes of sea level. *Am. Assoc. Pet. Geol.* **26**:51-52.
47. **Whitfield M.** 2001. Interactions between phytoplankton and trace metals in the ocean. *Advances in Marine Biology* **41**:3-128.
48. **Quigg A, Finkel ZV, Irwin AJ, Rosenthal Y, Ho TY, Reinfelder JR, Schofield O, Morel FM, Falkowski PG.** 2003. The evolutionary inheritance of elemental stoichiometry in marine phytoplankton. *Nature* **425**:291-294.
49. **Archibald JM, Keeling PJ.** 2002. Recycled plastids: a 'green movement' in eukaryotic evolution. *Trends Genet.* **18**:577-584.
50. **Archibald JM.** 2009. The puzzle of plastid evolution. *Curr. Biol.* **19**:R81-88.
51. **Cortes MY, Bollmann J, Thierstein HR.** 2001. Coccolithophore ecology at the HOT station HOT, Hawaii. *Deep Sea Research II* **48**:1957-1981

52. **Allen AE, Vardi A, Bowler C.** 2006. An ecological and evolutionary context for integrated nitrogen metabolism and related signaling pathways in marine diatoms. *Curr Opin. Plant Biol.* **9**:264-273.
53. **Wagner H Jakob T, Wilhelm C.** 2005. Balancing the energy flow from captured light into biomass under fluctuating light conditions. *New Phytologist* **169**:95-108.
54. **Allen AE.** 2005. Defining the molecular basis for energy balance in marine diatoms under fluctuating environmental conditions. *J. Phycol.* **6**:1073-1076.
55. **Simo R.** 2001. Production of atmospheric sulfur by oceanic plankton: biogeochemical, ecological and evolutionary links. *Trends Ecol. Evol.* **16**:287-294.
56. **Asada K, Takahashi M.** 1987. Production and scavenging of active oxygen in photosynthesis. p 227-287. *In* DJ Kyle, CB Osmond, CJ Arntzen (eds.) *Photoinhibition*. Elsevier, Amsterdam.
57. **Fridovich I.** 1998. Oxygen toxicity: a radical explanation. *J. Exp. Biol.* **201**:1203-1209.
58. **Trossat C, Nolte KD, Hanson AD.** 1996. Evidence that the pathway of dimethylsulfoniopropionate biosynthesis begins in the cytosol and ends in the chloroplast. *Plant Physiol.* **111**:965-973.
59. **Ito T, Asano Y, Tanaka Y, Takabe T.** 2011. Regulation of biosynthesis of dimethylsulfoniopropionate and its uptake in sterile mutant of *Ulva pertusa* (Chlorophyta). *J. Phycol.* **47**:517-523.
60. **James F, Paquet L, Sparace SA, Gage DA, Hanson AD.** 1995. Evidence implicating dimethylsulfoniopropionaldehyde as an intermediate in dimethylsulfoniopropionate biosynthesis. *Plant Physiol.* **108**:1439-1448.
61. **Summers PS, Nolte KD, Cooper AJL, Borgeas H, Leustek T, Rhodes D, Hanson AD.** 1998. Identification and stereospecificity of the first three enzymes of 3-dimethylsulfoniopropionate biosynthesis in a chlorophyte alga. *Plant Physiol.* **116**:369-378.
62. **Stefels J, Dijkhuizen L, Gieskes WWC.** 1995. DMSP-lyase activity in a spring phytoplankton bloom off the Dutch coast, related to *Phaeocystis* sp. abundance. *Mar. Ecol. Prog. Ser.* **123**:235-243.
63. **Niki T, Kunugi M, Kohata K, Otsuki A.** 1997. Annual monitoring of DMS-producing bacteria in Tokyo Bay, Japan in relation to DMSP. *Mar. Ecol. Prog. Ser.* **156**:17-24.
64. **Niki T, Kunugi K, Otsuki A.** 2000. DMSP-lyase activity in five marine phytoplankton species: its potential importance in DMS production. *Mar. Biol.* **136**:759-764.

65. **Yoch DC.** 2002. Dimethylsulfoniopropionate: its sources, role in the marine food web, and biological degradation to dimethylsulfide. *Appl. Environ. Microbiol.* **68**:5804-5815.
66. **Alcolombri U, Ben-Dor S, Feldmesser E, Levin Y, Tawfik DS, Vardi A.** 2015. Marine Sulfur Cycle. Identification of the algal dimethyl sulfide-releasing enzyme: A missing link in the marine sulfur cycle. *Science* **348**:1466-1469.
67. **Yost DM, Mitchelmore C.** 2009. Dimethylsulfoniopropionate (DMSP) lyase activity in different strains of the symbiotic alga *Symbiodinium microadriaticum*. *Mar. Ecol. Prog. Ser.* **386**:61-70.
68. **Kiene RP, Linn LJ, Gonzalez J, Moran MA, Bruton JA.** 1999. Dimethylsulfoniopropionate and methanethiol are important precursors of methionine and protein-sulfur in marine bacterioplankton. *Appl. Environ. Microbiol.* **65**:4549-4558.
69. **Todd JD, Curson AR, Nikolaidou-Katsaraidou N, Brearley CA, Watmough NJ, Chan Y, Page PC, Sun L, Johnston AW.** 2010. Molecular dissection of bacterial acrylate catabolism--unexpected links with dimethylsulfoniopropionate catabolism and dimethyl sulfide production. *Environ. Microbiol.* **12**:327-343.
70. **Todd JD, Rogers R, Li YG, Wexler M, Bond PL, Sun L, Curson AR, Malin G, Steinke M, Johnston AW.** 2007. Structural and regulatory genes required to make the gas dimethyl sulfide in bacteria. *Science* **315**:666-669.
71. **Todd JD, Curson AR, Dupont CL, Nicholson P, Johnston AW.** 2009. The *dddP* gene, encoding a novel enzyme that converts dimethylsulfoniopropionate into dimethyl sulfide, is widespread in ocean metagenomes and marine bacteria and also occurs in some Ascomycete fungi. *Environ. Microbiol.* **11**:1376-1385.
72. **Varaljay VA, Robidart J, Preston CM, Gifford SM, Durham BP, Burns AS, Ryan JP, Marin R, Kiene RP, Zehr JP, Scholin CA, Moran MA.** 2015. Single-taxon field measurements of bacterial gene regulation controlling DMSP fate. *ISME J.* **9**:1692.
73. **Todd JD, Curson AR, Kirkwood M, Sullivan MJ, Green RT, Johnston AW.** 2011. DddQ, a novel, cupin-containing, dimethylsulfoniopropionate lyase in marine roseobacters and in uncultured marine bacteria. *Environ. Microbiol.* **13**:427-438.
74. **Rusch DB, Halpern AL, Sutton G, Heidelberg KB, Williamson S, Yooseph S, Wu D, Eisen JA, Hoffman JM, Remington K, Beeson K, Tran B, Smith H, Baden-Tillson H, Stewart C, Thorpe J, Freeman J, Andrews-Pfannkoch C, Venter JE, Li K, Kravitz S, Heidelberg JF, Utterback T, Rogers YH, Falcon LI, Souza V, Bonilla-Rosso G, Eguiarte LE, Karl DM, Sathyendranath S, Platt T, Bermingham E, Gallardo V, Tamayo-Castillo G, Ferrari MR, Strausberg RL, Neilson K, Friedman R, Frazier M, Venter JC.** 2007. The Sorcerer II Global Ocean Sampling expedition: northwest Atlantic through eastern tropical Pacific. *PLoS Biol* **5**:e77.

75. **Kirkwood M, Le Brun NE, Todd JD, Johnston AW.** 2010. The *dddP* gene of *Roseovarius nubinhibens* encodes a novel lyase that cleaves dimethylsulfoniopropionate into acrylate plus dimethyl sulfide. *Microbiology* **156**:1900-1906.
76. **Li C, Wei T, Zhang S, Chen X, Gao X, Wang P, Xie B, Su H, Qin Q, Zhang X, Yu J, Zhang H, Zhou B, Yang P, Zhang Y.** 2013. Molecular insight into bacterial cleavage of oceanic dimethylsulfoniopropionate into demethyl sulfide. *PNAS* **111**:1026-1031.
77. **Wang P, Chen XL, Li CY, Gao X, Zhu DY, Xie BB, Qin QL, Zhang XY, Su HN, Zhou BC, Xun LY, Zhang YZ.** 2015. Structural and molecular basis for the novel catalytic mechanism and evolution of DddP, an abundant peptidase-like bacterial dimethylsulfoniopropionate lyase: a new enzyme from an old fold. *Mol. Microbiol.* **98**:289-301.
78. **Hehemann JH, Law A, Redecke L, Boraston AB.** 2014. The structure of RdDddP from *Roseobacter denitrificans* reveals that DMSP lyases in the DddP-family are metalloenzymes. *PLoS One* **9**:e103128.
79. **de Souza MP, Yoch DC.** 1996. Differential metabolism of dimethylsulfoniopropionate and acrylate in saline and brackish intertidal sediments. *Microb. Ecol.* **31**:319-330.
80. **van der Maarel M, van Bergeijk S, van Werkhoven A, Laverman A, Meijer W, Stam W, Hansen T.** 1996. Cleavage of dimethylsulfoniopropionate and reduction of acrylate by *Desulfovibrio acrylicus* sp. nov. *Arch. Microbiol.* **166**:109-115.
81. **Curson AR, Sullivan MJ, Todd JD, Johnston AW.** 2011. DddY, a periplasmic dimethylsulfoniopropionate lyase found in taxonomically diverse species of Proteobacteria. *ISME J* **5**:1191-1200.
82. **de Souza MP, Yoch DC.** 1995. Comparative physiology of dimethyl sulfide production by dimethylsulfoniopropionate lyase in *Pseudomonas doudoroffii* and *Alcaligenes* sp. strain M3A. *Appl. Environ. Microbiol.* **61**:3986-3991.
83. **Howard EC, Henriksen JR, Buchan A, Reisch CR, Burgmann H, Welsh R, Ye W, Gonzalez JM, Mace K, Joye SB, Kiene RP, Whitman WB, Moran MA.** 2006. Bacterial taxa that limit sulfur flux from the ocean. *Science* **314**:649-652.
84. **Schuller DJ, Reisch CR, Moran MA, Whitman WB, Lanzilotta WN.** 2012. Structures of dimethylsulfoniopropionate-dependent demethylase from the marine organism *Pelagabacter ubique*. *Protein Sci.* **21**:289-298.
85. **Lee HH, Kim DJ, Ahn HJ, Ha JY, Suh SW.** 2004. Crystal structure of T-protein of the glycine cleavage system: Cofactor binding, insights into H-protein recognition, and molecular basis for understanding nonketotic hyperglycinemia. *J. Biol. Chem.* **279**:50514-50523.

86. **Moran MA, Reisch CR, Kiene RP, Whitman WB.** 2012. Genomic insights into bacterial DMSP transformations. *Ann. Rev. Mar. Sci.* **4**:523-542.
87. **Steele RD, Benevenga NJ.** 1979. The metabolism of 3-methylthiopropionate in rat liver homogenates. *J. Biol. Chem.* **254**:8885-8890.
88. **Albers E.** 2009. Metabolic characteristics and importance of the universal methionine salvage pathway recycling methionine from 5'-methylthioadenosine. *IUBMB Life* **61**:1132-1142.
89. **Sekowska A, Denervaud V, Ashida H, Michoud K, Haas D, Yokota A, Danchin A.** 2004. Bacterial variations on the methionine salvage pathway. *BMC Microbiol.* **4**:9.
90. **Ewbank EM, H.** 1990. Conversion of methionine to phytotoxic 3-methylthiopropionic acid by *Xanthomonas campestris* pv. *manihotis*. *J. of Gen. Microbiol.* **136**:1185-1189.
91. **Perreaux D, Marate H, Meyer JA.** 1982. Identification of 3(methylthio) propionic acid as a blight inducing toxin produced by *Xanthomonas campestris* pv. *manihotis* *in vitro*. *Physiol. Plant Path.* **20**:313-319.
92. **Gonda I, Lev S, Bar E, Sikron N, Portnoy V, Davidovich-Rikanati R, Burger J, Schaffer AA, Tadmor Y, Giovannonni JJ, Huang M, Fei Z, Katzir N, Fait A, Lewinsohn E.** 2013. Catabolism of L-methionine in the formation of sulfur and other volatiles in melon (*Cucumis melo* L.) fruit. *Plant J.* **74**:458-472.
93. **Feng Y, Hofstein HA, Zwahlen J, Tonge PJ.** 2002. Effect of mutagenesis on the stereochemistry of enoyl-CoA hydratase. *Biochemistry* **41**:12883-12890.
94. **Kiema TR, Engel CK, Schmitz W, Filppula SA, Wierenga RK, Hiltunen JK.** 1999. Mutagenic and enzymological studies of the hydratase and isomerase activities of 2-enoyl-CoA hydratase. *Biochemistry* **38**:2991-2999.
95. **Caruana A, Malin G.** 2014. The variability in DMSP content and DMSP lyase activity in marine dinoflagellates. *Prog. Oceanogr.* **120**:410-424.
96. **Moran MA, Belas R, Schell MA, Gonzalez JM, Sun F, Sun S, Binder BJ, Edmonds J, Ye W, Orcutt B, Howard EC, Meile C, Palefsky W, Goesmann A, Ren Q, Paulsen I, Ulrich LE, Thompson LS, Saunders E, Buchan A.** 2007. Ecological genomics of marine Roseobacters. *Appl. Environ. Microbiol.* **73**:4559-4569.
97. **Zubkov MV, Fuchs BM, Archer SD, Kiene RP, Amann R, Burkill PH.** 2001. Linking the composition of bacterioplankton to rapid turnover of dissolved dimethylsulphoniopropionate in an algal bloom in the North Sea. *Environ. Microbiol.* **3**:304-311.

98. **Gonzalez JM, Simo R, Massana R, Covert JS, Casamayor EO, Pedros-Alio C, Moran MA.** 2000. Bacterial community structure associated with a dimethylsulfoniopropionate-producing North Atlantic algal bloom. *Appl. Environ. Microbiol.* **66**:4237-4246.
99. **Luo H, Csuros M, Hughes AL, Moran MA.** 2013. Evolution of divergent life history strategies in marine alphaproteobacteria. *MBio.* **4**: e00373-13.
100. **Luo H, Moran MA.** 2014. Evolutionary ecology of the marine Roseobacter clade. *Microbiol. Mol. Biol. Rev.* **78**:573-587.
101. **Perona JJ, Craik CS.** 1997. Evolutionary divergence of substrate specificity within the chymotrypsin-like serine protease fold. *J. Biol. Chem.* **272**:29987-29990.
102. **Noda-Garcia L, Camacho-Zarco A, Medina-Ruiz S, Gaytan P, Carrillo-Tripp M, Fulop V, Barona-Gomez F.** 2013. Evolution of substrate specificity in a recipient's enzyme following horizontal gene transfer. *Molecular Biology and Evolution* **30**:2024-2034.
103. **Kocsis MG, Hanson AD.** 2000. Biochemical evidence for two novel enzymes in the biosynthesis of 3-dimethylsulfoniopropionate in *Spartina alterniflora*. *Plant Physiol.* **123**:1153-1161.
104. **Reisch CR, Crabb WM, Gifford SM, Teng Q, Stoudemayer MJ, Moran MA, Whitman WB.** 2013. Metabolism of dimethylsulphoniopropionate by *Ruegeria pomeroyi* DSS-3. *Mol. Microbiol.* **89**:774-791.
105. **Alcolombri U, Laurino P, Lara-Astiaso P, Vardi A, Tawfik DS.** 2014. DddD is a CoA-transferase/lyase producing dimethyl sulfide in the marine environment. *Biochemistry* **53**:5473-5475.
106. **Curson AR, Rogers R, Todd JD, Brearley CA, Johnston AW.** 2008. Molecular genetic analysis of a dimethylsulfoniopropionate lyase that liberates the climate-changing gas dimethylsulfide in several marine alpha-proteobacteria and *Rhodobacter sphaeroides*. *Environ. Microbiol.* **10**:757-767.
107. **Todd JD, Kirkwood M, Newton-Payne S, Johnston AW.** 2012. DddW, a third DMSP lyase in a model Roseobacter marine bacterium, *Ruegeria pomeroyi* DSS-3. *ISME J.* **6**:223-226.
108. **Brummett AE, Schnicker NJ, Crider A, Todd JD, Dey M.** 2015. Biochemical, kinetic, and spectroscopic characterization of *Ruegeria pomeroyi* DddW--A mononuclear iron-dependent DMSP lyase. *PLoS One* **10**:e0127288.
109. **Sun J, Todd JD, Thrash JC, Qian Y, Qian MC, Temperton B, Guo J, Fowler EK, Aldrich JT, Nicora CD, Lipton MS, Smith RD, De Leenheer P, Payne SH, Johnston**

- AW, Davie-Martin CL, Halsey KH, Giovannoni SJ.** 2016. The abundant marine bacterium *Pelagibacter* simultaneously catabolizes dimethylsulfoniopropionate to the gases dimethyl sulfide and methanethiol. *Nature Microbiol.* **1**:16065.
110. **Engel CK, Mathieu M, Zeelen JP, Hiltunen JK, Wierenga RK.** 1996. Crystal structure of enoyl-coenzyme A (CoA) hydratase at 2.5 angstroms resolution: a spiral fold defines the CoA-binding pocket. *The EMBO J.* **15**:5135-5145.

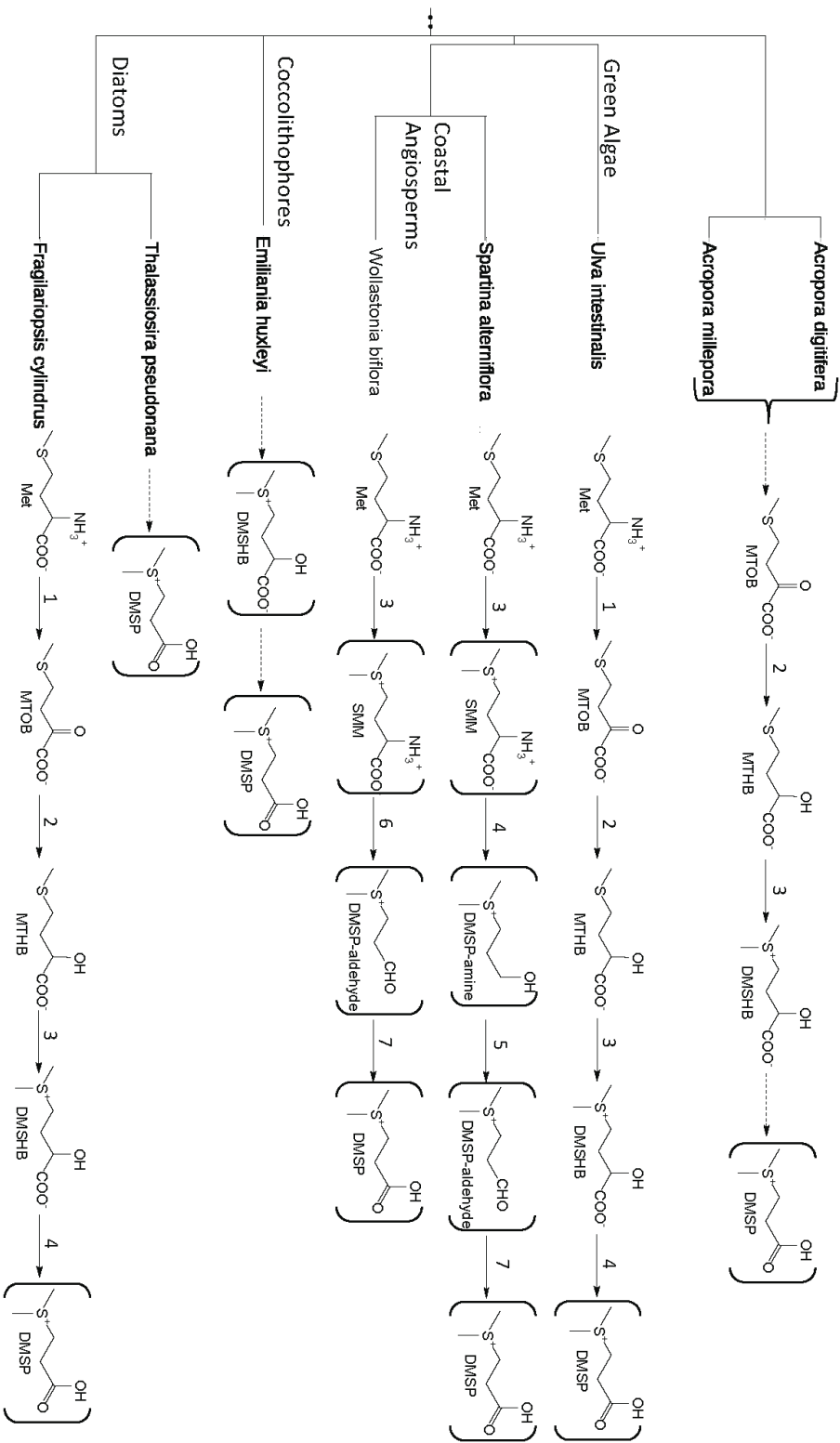


**Figure 1-1.** Proposed DMSP biosynthetic pathways. Structures in brackets have been detected and verified. Complete arrows signify reactions that are identified or predicted based on the observed intermediates. Dotted arrows signify unknown reactions. 1, aminotransferase; 2, NADPH-reductase; 3, methyltransferase; 4, decarboxylase; 5, oxidase; 6, decarboxylase/transaminase; 7, dehydrogenase. MTOB: 4-methylthio-2-oxobutyrate, MTHB: 4-methylthio-2-hydroxybutyrate, DMSHB: 4-dimethylsulfonio-2-hydroxybutyrate, SMM: S-methyl-L-methionine. (6, 9, 11, 12, 60, 61, 103)

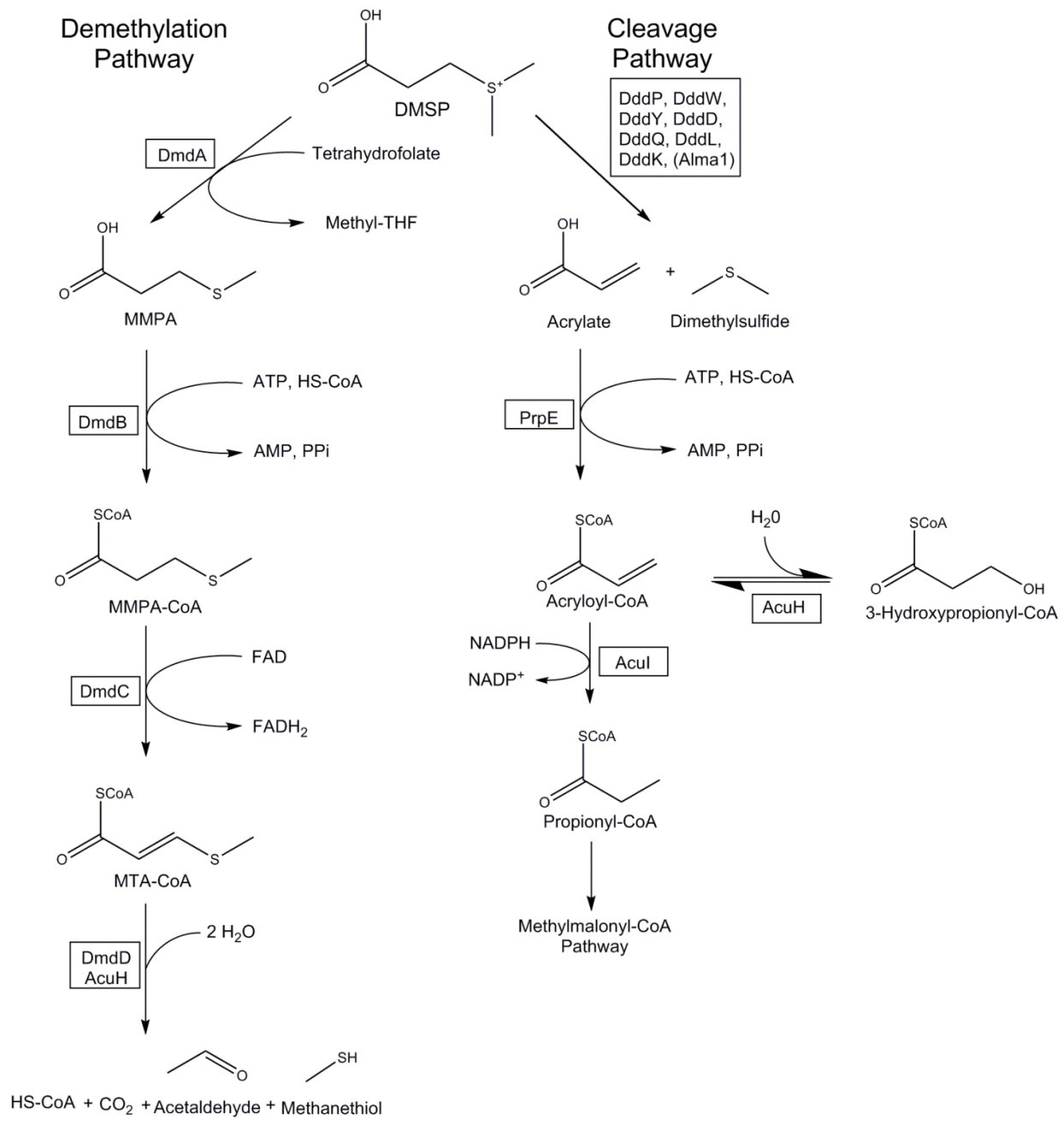


**Figure 1-2.** Bacterial DMSP demethylation and cleavage pathways. Revised from (19, 104)

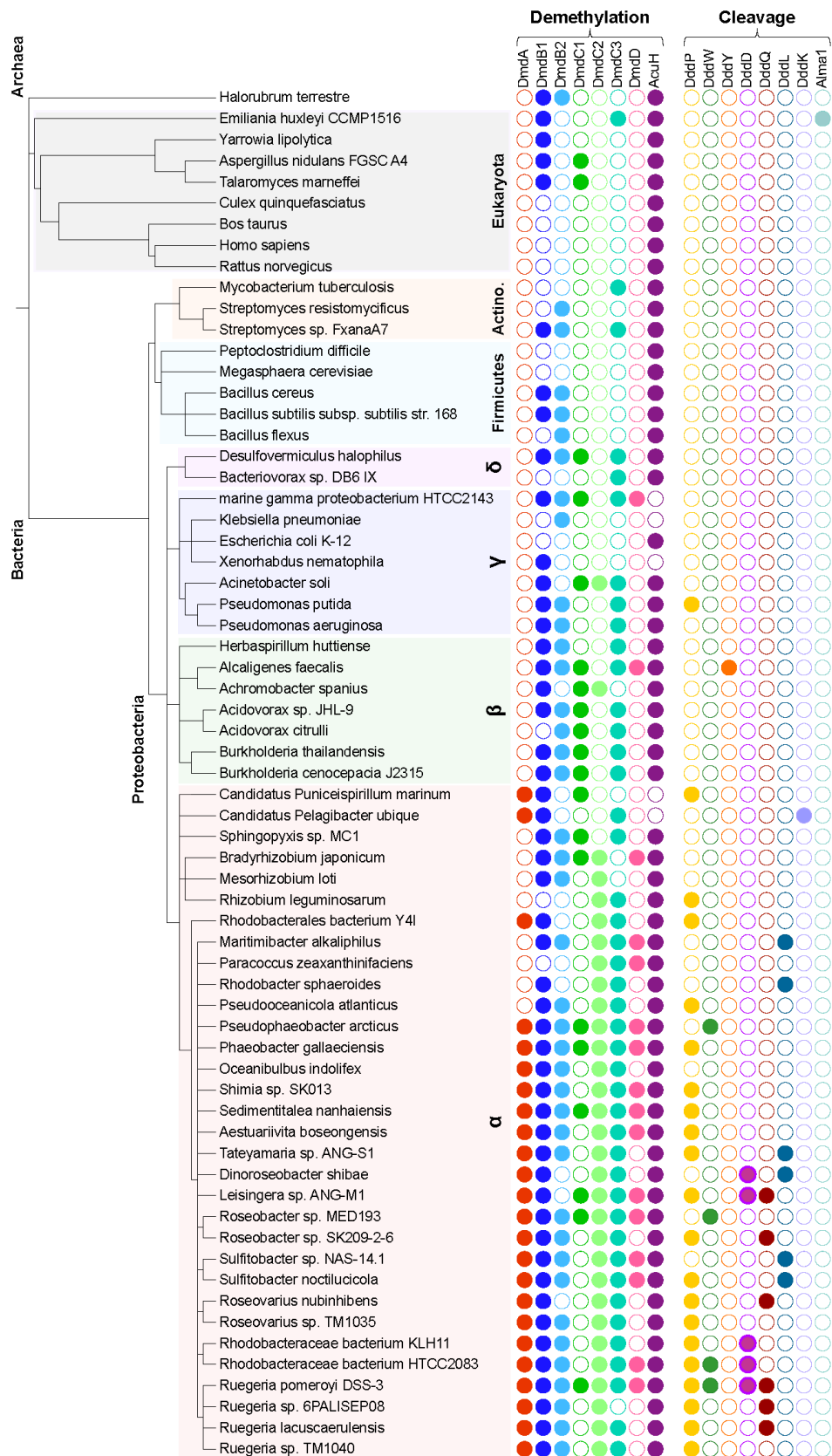


**Figure 1-3.** Phylogenetic species tree representing the diversity of organisms that possess enzymes from the DMSP demethylation pathway and the DMSP lyases. Colored filled circles represent the presence of the indicated protein. Protein designations and query sequences are as follows: From *R. pomeroyi*, DmdA (SPO1913); DmdB1 (SPO0677); DmdB2 (SPO2045); DmdC1 (SPO3805); DmdC2 (SPO0298); DmdC3 (SPO2915); DmdD (SPO3804); and AcuH (SL1157\_0807) from *R. lacuscaerulensis*. DMSP lyase protein designations and query sequences are *R. pomeroyi* DddP (SPO2299), DddW (SPO0453), DddQ (SPO1596), DddD (SPO1703); *A. faecalis* DddY (ADT64689.1); *R. sphaeroides* DddL (RSP1433), *P. ubique* DddK (SAR11\_0394); *E. huxleyi* Alma1 (XP\_005784450). The e value cut off used in all cases was  $< e^{-70}$  with the exception of DddW (cut off of  $< e^{-40}$ ) and dddQ (cut off of  $< e^{-30}$ ).

**Table 1-1.** Identified DMSP lyases

Protein	Organism	$K_m$ with DMSP	Reference
DddY	<i>A. faecalis</i>	1.4 mM	(80-82)
	<i>D. acrylicus</i>	0.4 mM	
DddD	<i>Marinomonas</i>	67 uM (acetyl-CoA)	(70, 105)
DddL	<i>Sulfitobacter</i> EE-36	ND <sup>a</sup>	(106)
DddP	<i>R. lacuscaerulensis</i>	17 mM	(71, 75, 77)
	<i>R. nubinhibens</i>	14 mM	
DddW	<i>R. pomeroyi</i>	8.7 mM	(107, 108)
DddQ	<i>R. lacuscaerulensis</i>	22 mM	(73, 76)
DddK	<i>P. ubique</i> HTCC1062	82 mM	(109)
Alma1	<i>E. huxleyi</i>	9.0 mM	(66)

<sup>a</sup> No data

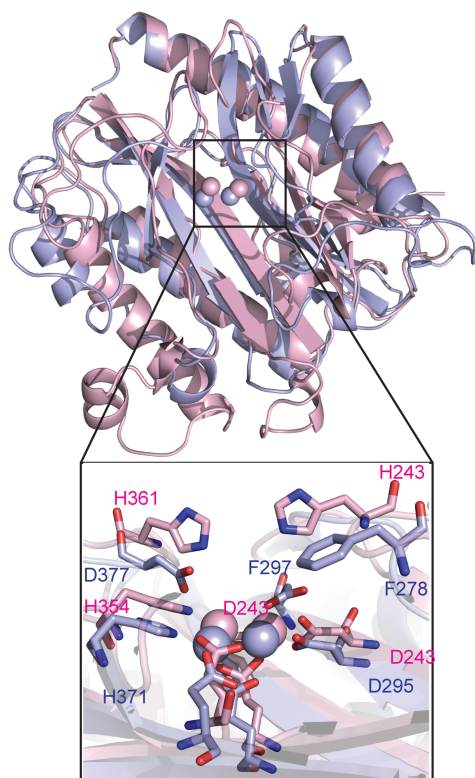


**Figure 1-4.** Overlay of the C-domains of the *R. lacuscaerulensis* DddP structure (light blue) and the aminopeptidase P structure (light pink) with an inset overlaying the active sites of each protein. Reproduced from (77).

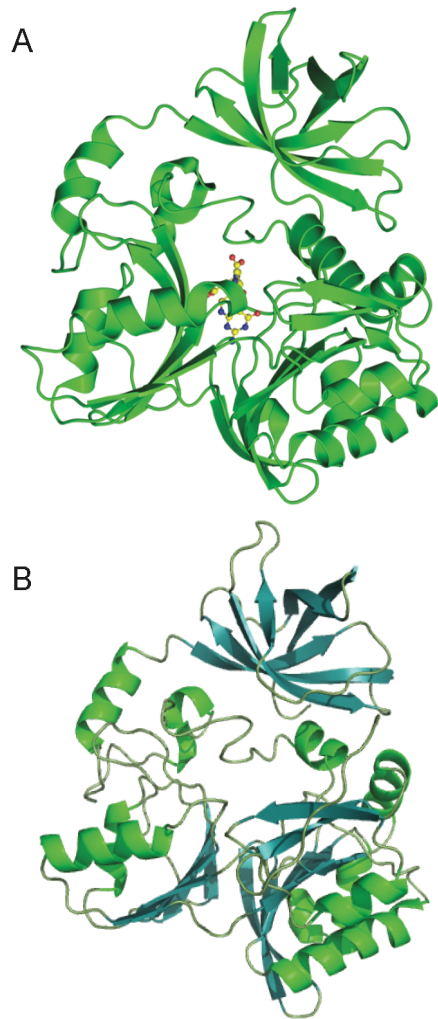


**Figure 1-5.** Crystal structures of glycine cleavage T-protein from *Thermotoga maritima* (A) (85) and DmdA monomer from *P. ubique* (B) (84) showing shared tri-domain structure.

**Table 1-2.** Apparent kinetic constants for *P. ubiquus* HTCC1062 and *R. pomeroiyi* DSS-3 DmdBs<sup>a</sup>

	RPO_DmdB1	RPO_DmdB2
MMPA		
$K_m$	0.08 ±0.02	0.07 ±0.02
$V_{max}$	19.3 ±3.3	15.4 ±2.5
$k_{cat}$	18.7	14.9
$k_{cat}/K_m$	233	213
Butyrate		
$K_m$	0.02 ±0.01	0.12 ±0.03
$V_{max}$	14.9 ±3.6	7.4 ±2.1
$k_{cat}$	14.4	7.2
$k_{cat}/K_m$	1031	71
Propionate		
$K_m$	0.04 ±0.01	3.11 ±1.13
$V_{max}$	11.2 ±2.5	3.8±1.4
$k_{cat}$	10.8	3.7
$k_{cat}/K_m$	271	1.2
Acrylate		
$K_m$	0.9 ±0.2	5.25 ±2.1
$V_{max}$	10.5 ±2.0	1.0 ±0.2
$k_{cat}$	14.3	1.0
$k_{cat}/K_m$	16	0.2

<sup>a</sup> $K_m$  (mM) and  $V_{max}$  ( $\mu\text{mol min}^{-1} \text{mg}^{-1}$ ) shown ( $\pm$  SE) from three independent experiments.  $k_{cat}$  is expressed in units of  $\text{s}^{-1}$  and  $k_{cat}/K_m$  in units of  $\text{mM}^{-1} \text{s}^{-1}$ .

Reproduced from (21).

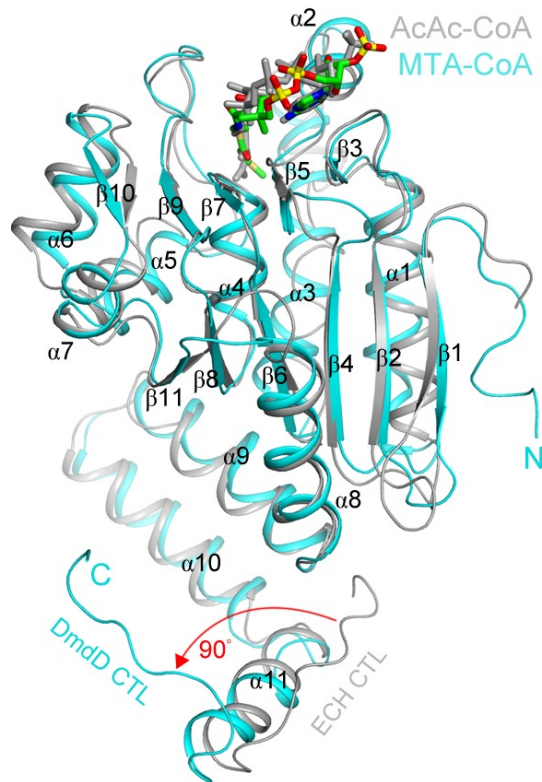


**Figure 1-6.** Comparison of the structures of *R. pomeroyi* DmdD (E121A mutant) monomer (cyan) with MTA-CoA (green) and the rat liver ECH monomer (grey) in complex with acetoacetyl-CoA (grey) (110). The red line indicates a difference in the conformation of the C-terminal loop between the two structures. Figure reproduced from (22).

**Table 1-3.** Apparent kinetic constants of RL\_AcuH, RPO\_AcuH, and RPO\_DmdD with different substrates.

Substrate	Enzyme	$K_m$ (mM) <sup>a</sup>	$k_{cat}$ (s <sup>-1</sup> )	$k_{cat}/K_m$ (mM <sup>-1</sup> s <sup>-1</sup> )
	RL_AcuH	1.1 ± 0.1	12.6 ± 0.6	11.5
MTA-CoA	RPO_AcuH	1.3 ± 0.1	0.2 ± 0.01	0.1
	RPO_DmdD <sup>b</sup>	0.008	44	5.5 x10 <sup>3</sup>
Crotonyl-CoA	RL_AcuH	0.23 ± 0.02	890 ± 68	3.8 x10 <sup>3</sup>
	RPO_AcuH	0.12 ± 0.01	220 ± 9	2.0 x10 <sup>3</sup>
	RPO_DmdD	0.02	42	2.1 x10 <sup>3</sup>
Acryloyl-CoA	RL_AcuH	0.06 ± 0.01	4.2 ± 1.0 x10 <sup>5</sup>	7.4 x10 <sup>6</sup>
	RPO_AcuH	0.07 ± 0.02	3.6 ± 0.8 x10 <sup>5</sup>	5.0 x10 <sup>6</sup>
	RPO_DmdD	ND	ND	ND

<sup>a</sup> $K_m$  and  $k_{cat}$  (±SD) are representative of three independent experiments. The  $k_{cat}$  was calculated on the basis of the monomer molecular weight.

<sup>b</sup>The kinetics of RPO\_DmdD were obtained from (22). The  $k_{cat}$  of the RPO\_DmdD for acryloyl-CoA was below the limit of detection, <1.4 x 10<sup>-4</sup> s<sup>-1</sup>.

**Table 1-4.** Levels of DMSP production for different phytoplankton groups<sup>a</sup>.

No. of species	Common names	Concentration of DMSP (median pmol /cell)	Range (pmol /cell)
40	Dinoflagellates	0.1725	0.00011-14.7
15	Diatoms	0.00745	0.0006-0.257
9	Chlorophytes	0.001	0.00015-0.012
4	Golden algae	$8.36 \times 10^{-4}$	0.000149-0.02
14	Haptophytes	0.0158	0.000373-0.148
1	Cryptophytes	0.0213	0.0213
1	Rhodophyta	0.00231	0.00231
1	Cynaobacteria	$8.94 \times 10^{-6}$	$7.45 \times 10^{-6}$ - $1.04 \times 10^{-5}$
6	Coral	0.0826	0.021-3.331
4	zooxanthellae	0.14	0.048-0.285

<sup>a</sup> Unpublished data from H. Luo, University of Hong Kong.

CHAPTER 2  
REGULATORY AND FUNCTIONAL DIVERSITY OF METHYLMERCAPTOPROPIONATE  
COA LIGASES (DMDB) FROM THE DIMETHYLSULFONIOPROPIONATE  
DEMETHYLATION PATHWAY IN *RUEGERIA POMEROYI* DSS-3  
AND OTHER PROTEOBACTERIA<sup>1</sup>

---

<sup>1</sup>Bullock, H.A., C.R. Reisch, A.S. Burns, M.A. Moran, W.B. Whitman. 2014. Regulatory and functional diversity of methylmercaptopropionate CoA ligases (DmdB) from the dimethylsulfoniopropionate demethylation pathway in *Ruegeria pomeroyi* DSS-3 and other proteobacteria. *Journal of Bacteriology*. 196:1275-1285. Reprinted here with permission of the publisher.

## Abstract

The organosulfur compound dimethylsulfoniopropionate (DMSP) is produced by phytoplankton and is ubiquitous in the surface ocean. Once released from phytoplankton, marine bacteria degrade DMSP by either the cleavage pathway to form the volatile gas dimethylsulfide (DMS) or the demethylation pathway, yielding methanethiol (MeSH), which is readily assimilated or oxidized. The enzyme DmdB, a methylmercaptopropionate (MMPA)-CoA ligase, catalyzes the second step in the demethylation pathway and is a major regulatory point. The two forms of DmdB present in the marine roseobacter *Ruegeria pomeroyi* DSS-3, RPO\_DmdB1 and RPO\_DmdB2, and the single form in the SAR11 clade bacterium *Pelagibacter ubique* HTCC1062, PU\_DmdB1, were characterized in detail. DmdB enzymes were also examined from *Ruegeria lacuscaerulensis* ITI-1157, *Pseudomonas aeruginosa* PAO1, and *Burkholderia thailandensis* E264. The DmdB enzymes separated into two phylogenetic clades. All enzymes had activity with MMPA and were sensitive to inhibition by salts, but there was no correlation between the clades and substrate specificity or salt sensitivity. All *Ruegeria* spp. enzymes were inhibited by physiological concentrations (70 mM) of DMSP. However, ADP reversed the inhibition of RPO\_DmdB1, suggesting that this enzyme was responsive to cellular energy charge. MMPA reversed the inhibition of RPO\_DmdB2 as well as both *R. lacuscaerulensis* ITI-1157 DmdB enzymes, suggesting that a complex regulatory system exists in marine bacteria. In contrast, the DmdBs of the non-DMSP metabolizing *P. aeruginosa* PAO1 and *B. thailandensis* E264 were not inhibited by DMSP, suggesting that DMSP inhibition is a specific adaptation of DmdBs from marine bacteria.

## Introduction

Dimethylsulfoniopropionate (DMSP) is ubiquitous in the ocean, where its degradation impacts global carbon and sulfur cycles. Marine phytoplankton produce DMSP as an osmolyte, predator deterrent, and antioxidant (1-3). It accounts for 10% of carbon fixed by marine phytoplankton in some parts of the ocean and 12-103 Tg of reduced sulfur each year (4-6). The significance of DMSP is partially due to its role as a precursor to the climatically active gas dimethylsulfide (DMS), but it is also a major carbon and energy source for microorganisms (6, 7). DMS is the main biogenic source of sulfur to the atmosphere, with emissions ranging from 0.6-1.6 Tg of sulfur per year (8, 9). Once in the atmosphere, DMS is oxidized and enhances the formation of cloud condensation nuclei (CCN) (1, 6, 10).

DMSP is metabolized by marine bacteria via one of two competing pathways, the cleavage or the demethylation pathway (11, 12). Certain microorganisms, such as *R. pomeroyi* DSS-3, possess both pathways (11, 13). Approximately 10% of DMSP is degraded via the cleavage pathway, resulting in the formation of DMS and acrylate (14-16). However, the majority of DMSP is degraded by the demethylation pathway, which forms methyl-tetrahydrofolate (methyl-THF), methanethiol (MeSH), CO<sub>2</sub>, and acetaldehyde (Figure 2-1) (11). In this pathway, DMSP is demethylated to form MMPA, precluding the formation of DMS and allowing DMSP to be used as both a carbon and reduced sulfur source by bacterioplankton (7, 11, 14). Four previously uncharacterized enzymes catalyze this pathway, DmdA, DmdB, DmdC, and DmdD (11). In *R. pomeroyi* DSS-3, a model organism for DMSP metabolism, there are two forms of the demethylation pathway methylmercaptopropionate CoA ligase enzyme DmdB, RPO\_DmdB1 and RPO\_DmdB2 (Figure 2-1). These isozymes are representative of each of the two phylogenetic clades of DmdB, B1 and B2. The ubiquitous SAR11 clade bacterium

*Pelagibacter ubique* HTCC1062 possesses a single form of this enzyme, a member of the B1 clade designated PU\_DmdB1 (Figure 2-2) (11).

The goals of the current work are to gain better understanding of the DmdB isozymes involved in the demethylation pathway. Marine bacteria use DMSP as a carbon and sulfur source, incorporating 15-40% of DMSP-S for amino acid and protein synthesis (7, 15, 16). DMSP may also be an osmolyte and antioxidant for bacteria as well as phytoplankton (17). DMSP being used in any of these capacities may alter the regulation of the pathways or the isozymes (7, 14, 17). To gain further insights into the roles and regulation of the DmdB isozymes, the purified recombinant PU\_DmdB1, RPO\_DmdB1, and RPO\_DmdB2 enzymes were further characterized. To determine if functional characteristics of DmdB enzymes were predictable based upon their clade designation, four additional members of the two DmdB clades were also purified and characterized. Two enzymes from *Ruegeria lacuscaerulensis* ITI-1157 (RL\_DmdB1 and RL\_DmdB2) were chosen to represent a sister organism to *R. pomeroyi* DSS-3. The enzymes from *Pseudomonas aeruginosa* PAO1 (PA\_DmdB1), and *Burkholderia thailandensis* E264 (BTH\_DmdB2) were chosen to represent non-marine organisms capable of metabolizing MMPA to MeSH (11). As a group, the enzymes represent a range of amino acid identities of 86-51 % within and 35-33 % between the clades (Table 2-1).

## **Materials and Methods**

**Materials/Substrate Synthesis.** MMPA, marketed as 3-(methylthio) propionic acid (L12861), was purchased from Alfa Aesar (Ward Hill, MA). DMSP was synthesized as described previously by Chambers *et al.* 1987 from dimethyl sulfide and acrylic acid (Sigma Aldrich) (18).

**Expression of Recombinant Proteins.** The genes from *R. pomeroyi* DSS-3 (RPO\_DmdB1: SPO0677 YP\_165932.1, RPO\_DmdB2: SPO2045 YP\_167275.1) (19, 20), *P. aeruginosa* PAO1 (PA\_DmdB1: PA4198 NP\_252887.1) (21), *R. lacuscaerulensis* ITI-1157 (RL\_DmdB1: SL1157\_1815 WP\_005981195.1, RL\_DmdB2: SL1157\_2728 WP\_005982887.1) (20, 22), and *B. thailandensis* E264 (BTH\_DmdB2: BTH\_I2141 YP\_442662.1) (23) were PCR amplified from genomic DNA. The *P. ubiquus* HTCC1062 gene PU\_DmdB1 (SAR11\_0248: YP\_265673.1) (24) was previously synthesized using *Escherichia coli* codon usage by the GenScript Corporation (11). Amplified genes were cloned into the pET101 expression vector per Invitrogen recommended methods. Constructed plasmids and relevant primers are summarized in Tables 2-2 and 2-3. Clones were then transformed into BL21 (DE3) or Rosetta (DE3) *E. coli* cells for protein expression. *P. aeruginosa* PAO1, *R. lacuscaerulensis* ITI-1157, and *B. thailandensis* E264 *dmdB* genes were cloned to include the 6x histidine tag from the pET101 vector. The recombinant proteins were given the RPO, PU, RL, PA, or BTH designations before the gene product name to allow for a clear indication of the genus and species of the source bacterium.

Cells for protein expression were grown in Luria Bertani (LB) broth at 30°C until an optical density at 600 nm of 0.4-0.5 was reached. Cultures were then induced with 0.1 mM IPTG (isopropyl-β-D-thiogalactopyranoside) and incubated for 4 hours at 30°C. Cultures were harvested by centrifugation at 8,000 X g for 10 min, and pellets were washed with 50 mM Tris (pH 7.5). Cells resuspended in 50 mM Tris were lysed by French Press or sonication. Lysed cells were centrifuged at 17,000 X g for 5 min to remove cell debris.

**Chromatography Techniques.** Six forms of column chromatography were used to purify the various DmdB enzymes. Fractions including the DmdB proteins were assayed for the

formation of MMPA-CoA by the HPLC-based assay described below. A Q-Sepharose (GE Healthcare) column (1.6 by 7 cm) was used for anion exchange chromatography. The column was equilibrated with 50 mM Tris (pH 7.5), and proteins were eluted using a linear gradient from 0 M NaCl to 1 M NaCl at a flow rate of 2 ml min<sup>-1</sup>. A phenyl Superose (GE Healthcare) column (1.0 by 10 cm) was equilibrated with 50 mM Tris (pH 7.5) plus 1.7 M (NH<sub>4</sub>)<sub>2</sub>SO<sub>4</sub>, and proteins were eluted with a linear gradient from 1.7 M to 0 M (NH<sub>4</sub>)<sub>2</sub>SO<sub>4</sub> at a flow rate of 1 ml min<sup>-1</sup>. A HiTrap Blue HP (GE Healthcare) column (1.6 by 2.5 cm) was used as an affinity chromatography step. The column was equilibrated with 50 mM KHPO<sub>4</sub> (pH 7.5), and proteins were eluted with a linear gradient of KCl increasing from 0 to 2 M KCl at a flow rate of 1 ml min<sup>-1</sup>. A CHT ceramic hydroxyapatite type 1 (Bio-Rad) column (1.0 by 7.0 cm) was equilibrated with 5 mM NaHPO<sub>4</sub> (pH 7.5) plus 150 mM NaCl. Proteins were eluted with a linear gradient from 5 mM to 500 mM NaHPO<sub>4</sub> plus 150 mM NaCl at a flow rate of 0.5 ml min<sup>-1</sup>. Gel filtration was performed using a Sephacryl (25)S200 HR (GE Healthcare) column (1.6 by 34 cm) equilibrated with 50 mM Tris (pH 7.5) and 250 mM NaCl. Proteins were eluted in the same buffer at a flow rate of 0.75 ml min<sup>-1</sup>.

**Purification of PU\_DmdB1.** Extracts of 2.3 g protein containing recombinant PU\_DmdB1 were applied to a Q-Sepharose anion exchange column. Active fractions eluted from 0.21-0.26 M NaCl. Active fractions were pooled, adjusted to 1.7 M (NH<sub>4</sub>)<sub>2</sub>SO<sub>4</sub> using solid (NH<sub>4</sub>)<sub>2</sub>SO<sub>4</sub>, and applied to a phenyl Superose hydrophobic interaction column. Active fractions eluted from 0.35-0.28 M (NH<sub>4</sub>)<sub>2</sub>SO<sub>4</sub>. These fractions were pooled and concentrated at 6,000 X g for 15 min using Amicon Ultra-4 10K centrifugal filter units (Millipore) to remove excess (NH<sub>4</sub>)<sub>2</sub>SO<sub>4</sub>. Protein samples were diluted two times with 50 mM KHPO<sub>4</sub> (pH 7.5) and then applied to the HiTrap Blue column (GE Healthcare). Active fractions eluted from 0.75-1.0 M

KCl. These fractions were concentrated using the Amicon Ultra-4 10K centrifugal filter units and brought up to 2 ml using 100 mM HEPES (pH 7.5). The enzyme was then stored at -20 °C.

**Purification of RPO\_DmdB1.** Extracts of 2.5 g protein containing recombinant RPO\_DmdB1 were applied to a Q-Sepharose anion exchange column, and active fractions were pooled and concentrated as above. Active fractions from the Q-Sepharose column eluted from 0.42-0.46 M NaCl. Protein samples were diluted two times using 50 mM KHPO<sub>4</sub> (pH 7.5) and then applied to the HiTrap Blue column. Fractions containing RPO\_DmdB1 eluted from 1.0-1.2 M KCl. Active fractions were pooled, concentrated as before, and applied to the gel filtration Sephacryl S200 HR column. Final protein samples were concentrated as above, brought to 2 ml using 100 mM KHPO<sub>4</sub> (pH 7.5), and stored at -20 °C.

**Purification of RPO\_DmdB2.** Extracts of 2.7g protein containing recombinant RPO\_DmdB2 were applied to a Q-Sepharose anion exchange column, and active fractions were pooled and concentrated as described previously. Active fractions eluted from 0.46-0.50 M NaCl. Protein samples were diluted two times using 50 mM NaHPO<sub>4</sub> (pH 7.5) and then applied to the CHT ceramic hydroxyapatite type 1 column. Active fractions eluted from 0.06-0.08 M NaHPO<sub>4</sub>. These fractions were pooled, concentrated as before, and applied to the HiTrap Blue column. Active fractions from the HiTrap Blue column eluted from 1.3-1.5 M KCl. Final protein samples were concentrated, brought to 2 ml using 100 mM KHPO<sub>4</sub> (pH 7.5), and stored at -20°C.

**Purification of His-tagged DmdBs.** His-tagged DmdBs from *R. lacuscaerulensis* ITI-1157, *P. aeruginosa* PAO1, and *B. thailandensis* E264 were purified using a His Trap HP (Ge Healthcare) column (7 by 25 mm). The column was equilibrated with 20 mM NaHPO<sub>4</sub> (pH 7.5) plus 5 mM imidazole, and proteins were eluted using a linear imidazole gradient from 5 to 500 mM imidazole at a flow rate of 0.5 ml min<sup>-1</sup>. In all cases, the desired protein eluted from 0.11 to

0.16 M imidazole. The NaHPO<sub>4</sub> buffer was exchanged with 100 mM KHPO<sub>4</sub> (pH 7.5) using Amicon Ultra-4 10K centrifugal filter units. Final protein samples were concentrated as described above, brought to 2 mL using 100 mM KHPO<sub>4</sub> (pH 7.5), and stored at -20 °C.

**Protein Concentration and Purity.** Protein concentrations were determined using either the Bio-Rad Bradford reagent or the BCA Protein Assay Kit (Thermo Scientific) with bovine serum albumin standard. These methods yielded similar results for these proteins. Protein purity was assessed using SDS-PAGE gels and the Gel Pro Analyzer program version 4.0 from Media Cybernetics, L.P.

**SDS-PAGE.** Sodium dodecyl sulfate-polyacrylamide gel electrophoresis (SDS-PAGE) was accomplished using Mini-PROTEAN TGX Precast Gels (Bio-Rad) 4-15% polyacrylamide gradient mini-gels. Gels were stained using Simply Blue Safe Stain (Invitrogen). SDS-PAGE images of purified recombinant DmdB enzymes are shown in Figures 2-3 and 2-4.

**Enzyme Assays.** Two types of enzyme assays were performed. In both assays, one unit was defined as one μmol product formed min<sup>-1</sup>, and specific activity was defined as one unit per mg<sup>-1</sup> of protein. All enzyme assays were performed at room temperature because preliminary studies of PU\_DmdB1 and RPO\_DmdB2 possessed good activity at this temperature. Their activities at 10°C to 30°C were nearly the same as room temperature.

In the first assay, product formation was analyzed using a Waters Alliance 2695 HPLC using a Hypersil Gold C18 Reverse Phase column with a 3 μm particle size (4.6 by 150 mm; Thermo Scientific). The column was developed with a linear gradient from 3% to 25% acetonitrile with 50 mM ammonium acetate at a flow rate of 1.0 min ml<sup>-1</sup> over 10 minutes. This HPLC assay was less sensitive to interference by salts and contained fewer potential effectors, such as ADP. Thus, it was used to perform kinetic experiments, salt sensitivity analysis with 0.4

M salts, DMSP sensitivity, and specific activity analyses. Unless stated otherwise, the HPLC assay contained 2 mM ATP, 2 mM MgCl<sub>2</sub>, 2 mM MMPA, 0.1 mM CoA, and 100 mM HEPES buffer (pH7.5) in total volume of 100 µl. Assays were run for 2 min and quenched by the addition of 4 µl of 85% phosphoric acid. The HPLC assay was linear over the two-minute time course.

A spectrophotometric coupled-assay was used for all other experiments (26). ATP, MgCl<sub>2</sub>, and MMPA were all supplied at 2 mM, CoA at 0.3 mM, phosphoenolpyruvate at 3 mM, and NADH at 0.1 mM in 100 mM HEPES buffer (pH 7.5). One unit of rabbit myokinase (Sigma) and two units of pyruvate kinase/lactate dehydrogenase (Sigma) were used. At these levels, the coupling enzymes were not rate-limiting. The reaction was initiated by the addition of either MMPA or ATP, and reaction progress was monitored at 340 nm. Rates were calculated using the NADH extinction coefficient of 6,220 M<sup>-1</sup>cm<sup>-1</sup>(27). This assay was used for the determination of substrates specificity and pH optima. Substrate specificity was examined by replacing MMPA with 2 mM of each substrate tested. Initial screening of substrates using the HPLC assay showed that no other products were formed than the expected CoA-thioesters, which confirmed the identity and purity of the substrates.

Apparent Michaelis-Menten kinetic constants were calculated by varying one of three substrates (MMPA or the fatty acid, CoA, or ATP) while keeping the other two at the concentrations of the standard assay. MMPA, butyrate, propionate, and acrylate were varied from 0.01 mM to 20 mM. ATP was varied from 0.01 to 2 mM, and CoA was varied from 0.005 to 0.2 mM. Kinetic data analyses, other calculations, and statistical analyses were performed using SigmaPlot 11.0 (Systat Software Inc.).

The pH optimum was determined using the following buffers and pH values: sodium HEPES (6.5, 7.0, 7.5, and 8.0), Tris-Base (8.0, 8.5, and 9.0), sodium 2-(N-morpholino)ethanesulfonic acid (MES) (5.5, 6.0, and 6.5), 1,3-bis(Tris)propane (6.5, 7.0, 7.5, 8.0, 8.5, and 9.0), sodium 3-(N-morpholino)propanesulfonic acid (MOPS) (6.5, 7.0, and 7.5), and sodium 2-(cyclohexylamino)ethanesulfonic acid (CHES) (8.5, 9.0, 9.5, 10.0). Controls established that the coupling enzymes were not rate-limiting in each of the buffers. All proteins had the highest activity in 100 mM HEPES, as compared with 100 mM Tris, MES, CHES, MOPS, and Bis-Tris-Propane (data not shown). For this reason, subsequent assays were performed using 100 mM HEPES at a pH of 7.5 for PU\_DmdB1 and RPO\_DmdB2, and pH 7.0 for RPO\_DmdB1.

**Native Molecular Weight.** The native molecular weights of the enzymes were determined using a Sephacryl S200 HR gel filtration column, as described above.  $\beta$ -Amylase (200 kDa), alcohol dehydrogenase (150 kDa), bovine albumin (66 kDa), carbonic anhydrase (29 kDa), and cytochrome C (12.4 kDa) served as molecular weight standards.

**Phylogenetic Analysis.** The DmdB from *P. ubiquus* HTCC1062 (SAR11\_0248:PU\_DmdB1) was used as a query sequence for the BLASTp search. The PU\_DmdB1 sequence was queried against the genomes of *Escherichia coli* BL21(DE3), *Burkholderia thailandensis*, *Deinococcus radiodurans*, *Dinoroseobacter shibae*, marine  $\gamma$ -proteobacteria HTCC2143, SAR11 HIMB59,  $\alpha$ -proteobacteria HIMB114, *Myxoxoxus xanthus*, *Pseudomonas aeruginosa*, *Pseudoalteromonas atlantica*, *P. ubiquus* HTCC7211, *P. ubiquus* HTCC1062, *Puniceispirillum marinum* IMCC1322, SAR11 HIMB5, *Ruegeria lacuscaerulensis* 1157, and *Ruegeria pomeroyi* DSS-3. Sequences with an expected value  $< e^{-10}$  were aligned

using the MUSCLE algorithm, and the phylogenetic tree was built using the maximum likelihood method in MEGA 5.2. Bootstrap values of 100 were used for the analysis.

**Chemostat Cultures.** *R. pomeroyi* DSS-3 was grown in carbon-limited chemostats containing marine basal medium (MBM)(12, 28) with 6 mM acetate, 2 mM DMSP, 4 mM MMPA, or 3 mM methionine as the sole carbon source. The concentration of each carbon source was chosen to ensure that all four chemostats obtained similar cell densities at the chosen growth rate. Although tested empirically, the concentrations chosen reflect the number of electrons available for growth on each substrate. Chemostats were maintained at 30°C with a dilution rate of 0.0416 h<sup>-1</sup> and a 14 h doubling time. Five exchanges of the 144 ml chemostat volume were completed prior to collection of the first sample. Subsequently, 100 ml samples were taken daily from each chemostat, centrifuged immediately at 8,000 x g for 10 minutes, and stored at -80 ° C for RNA extraction.

**RNA Extraction and mRNA Enrichment.** RNA extractions from chemostat samples were performed using the Illustra RNAspin Mini kit (GE Life Sciences). Two samples from each chemostat were further treated with the MICROBExpress Bacterial mRNA Enrichment kit (Ambion) and Terminator 5'-phosphate-dependent exonuclease (Epicenter) to enrich the mRNA and deplete rRNA.

**Sequencing and Read Mapping to the *R. pomeroyi* DSS-3 Genome.** The TruSeq RNA Sample Preparation Kit v2 (Illumina) was used to form cDNA from the enriched mRNA samples, add barcodes to each cDNA sample, and prepare the Illumina library for sequencing. The enriched mRNA and Illumina libraries were quantified using a 2100 Bioanalyzer (Agilent). RNA samples included two biological replicates, with the exception of the acetate RNA sample which had only one biological sample, and a technical replicate. Sequencing was performed by

the Genome Services Laboratory at the Hudson Alpha Institute for Biotechnology, Huntsville, Alabama on a single lane of the SE50 HiSeq 2000 sequencer. High coverage was attained from the resultant nearly two million 50 bp reads. Reads were mapped to the *R. pomeroyi* DSS-3 genome using Bowtie2 (29). Differential expression was determined using the CuffDiff program from the Cufflinks package. P-values for differential expression were calculated using a negative binomial distribution using CuffDiff (29, 30). Between 2.4 and 5.4 % of the reads from each sample mapped exactly once to the *R. pomeroyi* DSS-3 genome and were used for further analyses. The other 95% of reads mapped identically to multiple places in the genome, in particular rRNA islands.

## Results

**DmdBs are Dimers with MMPA-CoA Ligase Activity.** The genes encoding the DmdB isozymes were recombinantly expressed in *E. coli* BL21(DE3) and purified to over 90% purity (Figures 2-3, 2-4). The PU\_DmdB1 enzyme was stable at -20 °C for up to six months when stored in 100 mM HEPES. The RPO\_DmdB1 and RPO\_DmdB2 enzymes were stable in a solution of 100 mM KHPO<sub>4</sub> at -20 °C for up to two months. The M<sub>r</sub>s of the isozyme subunits, as determined by SDS-PAGE, were consistent with the predicted molecular weights based on their amino acids sequences (19, 24). The native M<sub>r</sub>s as determined by gel filtration chromatography were consistent with these proteins being dimers (Table 2-4).

The specific activity of the PU\_DmdB1 with MMPA was nearly two-fold higher than those of RPO\_DmdB1 and RPO\_DmdB2 (Table 2-4). *P. ubique* HTCC1062 is an oligotroph with a minimal genome that encodes only four other CoA-ligase type enzymes, while *R. pomeroyi* DSS-3 is an opportunist that maintains 26 CoA-ligase homologs (19, 24).

Selection for greater efficiency in the oligotrophs potentially results in higher specific activity enzymes. The isozymes all exhibited a similar pH range for optimal activity (Table 2-4).

**DmdBs Show Varying Activities in the Presence of Salts.** The DmdB isozymes responded differently to the presence of some salts (Table 2-5). To determine if the responses were characteristic of the clades, they were examined in more detail. Because  $Mg^{2+}$  was required for activity, divalent cations were not tested. In most cases, the enzymes were either inhibited by salts or showed no change in activity. However, LiCl and  $NH_4Cl$  stimulated RPO\_DmdB2, RL\_DmdB1, and RL\_DmdB2. This stimulation was sufficient to yield specific activities comparable to that of PU\_DmdB1 in the absence of salt. The other effects of salts were complex. For instance,  $Cl^-$  stimulated both RL\_DmdB1 and PA\_DmdB1, and  $Na^+$  inhibited both the PA\_DmdB1 and BTH\_Dmd2, but even in these cases the counter-ions played significant roles. Moreover, the response to salts for members of the same DmdB clade possessed no more similarity than responses of members of different clades. Even though the *R. pomeroyi* DSS-3 and *R. lacuscaerulensis* ITI-1157 DmdB2s possessed 86% amino acid sequence identity, their responses to salts were very different. Thus, the salt response was highly individual among these enzymes.

**DmdBs Have Activity with MMPA and Short Chain Fatty Acids.** All of the recombinant DmdBs possessed high MMPA-CoA ligase activity (Table 2-6). In addition, all of the enzymes were active with carboxylic acids up to six carbons in length, indicating they were short chain fatty acid CoA ligases. The highest activities were observed with MMPA or substrates between three and five carbons in length. DMSP was included in these tests, but no activity for any of the enzymes was detected at a sensitivity of 0.1% of the MMPA-CoA ligase activity (data not shown). Two of the three DmdB clade 2 enzymes tested, RPO\_DmdB2 and

BTH\_DmdB2, had their highest activity under these conditions with MMPA and little to no activity with acetate. None of the DmdB clade 1 enzymes had their highest activity with MMPA. RPO\_DmdB1 had similar levels of activity with MMPA and crotonate. PU\_DmdB1 had the highest activity with butyrate, almost twice of that with MMPA. However, as shown below, the levels of CoA used in these tests were below the  $K_m$  for MMPA-dependent but not the butyrate-dependent ligase activity of this enzyme. Thus, the values reported here do not necessarily reflect the maximum activities for these substrates. RL\_DmdB1 and PA\_DmdB1 had high levels of activity with acetate and propionate. However, there were no consistent differences between the clade 1 and 2 enzymes.

**Kinetic Analysis of DmdB Reveals Substrate Preferences.** The DmdB isozymes PU\_DmdB1, RPO\_DmdB1, and RPO\_DmdB2 all possessed low apparent Michaelis-Menten constants and high catalytic efficiencies ( $k_{cat}/K_m$ ) for MMPA, consistent with their roles in DMSP metabolism (Table 2-7). Of the three enzymes, PU\_DmdB1 had the lowest  $K_m$  and the highest catalytic efficiency for MMPA and all three fatty acid substrates tested. The catalytic efficiencies of this enzyme for MMPA, butyrate and propionate were within the range expected for physiological activities. In contrast, the catalytic efficiencies of RPO\_DmdB1 and RPO\_DmdB2 were similar for MMPA,  $233 \text{ mM}^{-1} \text{ s}^{-1}$  and  $213 \text{ mM}^{-1} \text{ s}^{-1}$  respectively. Moreover, the higher catalytic efficiencies for butyrate ( $1031 \text{ mM}^{-1} \text{ s}^{-1}$ ) and propionate ( $271 \text{ mM}^{-1} \text{ s}^{-1}$ ) of RPO\_DmdB1 were consistent with these activities being physiologically relevant (31, 32). RPO\_DmdB2 possessed much lower values for these fatty acids, consistent with the conclusion that this DmdB was a specialized MMPA-CoA ligase.

The apparent  $K_m$ s of the DmdB isozymes for ATP and CoA also depended to some extent on whether the substrate was MMPA or butyrate (Table 2-8). PU\_DmdB1 had a higher  $K_m$  for

CoA with MMPA (0.58 mM) than with butyrate (0.11 mM). As cellular levels of CoA are typically between 0.01-0.6 mM, PU\_DmdB1 may have a lower activity with MMPA when other substrates, like butyrate, are available and the CoA pool is limited (33, 34).

**DMSP Inhibition of Marine DmdBs.** During growth on DMSP, *R. pomeroyi* DSS-3 maintains an intracellular concentration of 70 mM DMSP (12). However, DMSP strongly inhibited both RPO\_DmdB1 and RPO\_DmdB2 (Figure 2-5). While internal concentrations of DMSP in *P. ubique* HTCC1062 are not known, PU\_DmdB1 was also inhibited. The inhibition of RPO\_DmdB1 and RPO\_DmdB2 was so severe that no activity would be expected under the cellular concentrations of DMSP. Similar to the *R. pomeroyi* DSS-3 enzymes, RL\_DmdB1 and RL\_DmdB2 were also sensitive to DMSP. In contrast, the DmdB enzymes from non-marine organisms, PA\_DmdB1 and BTH\_DmdB2, were not inhibited by DMSP (Figure 2-6). This result suggests that DMSP sensitivity is a specific adaptation of the DmdBs from marine bacteria.

**ADP and MMPA Relieved Inhibition by DMSP in *R. pomeroyi* DSS-3.** ADP relieved the DMSP inhibition of RPO\_DmdB1 (Figure 2-7). ATP, which is a substrate of the MMPA-CoA ligase reaction, had no effect on DMSP inhibition (data not shown). AMP inhibited RPO\_DmdB1, yielding 50% inhibition at concentrations greater than 0.1 mM, presumably due to product inhibition (data not shown). In the presence of 50 mM DMSP, up to 65% of RPO\_DmdB1 activity was regained at 4 mM ADP, which was comparable to the cellular concentration in *E. coli* during energy limitation (Figure 2-7) (35). In contrast, ADP had no effect on the DMSP inhibition of RPO\_DmdB2, indicating that it was regulated differently. However, MMPA concentrations above 2 mM relieved the DMSP inhibition of RPO\_DmdB2, and 80% activity was regained at a MMPA concentration of 8 mM (Figure 2-7).

The reversals of DMSP inhibition by ADP or MMPA were not properties of the *R. lacuscaerulensis* and *P. ubique* DmdB enzymes. Additions of ADP concentration above 0.5 mM inhibited PU\_DmdB1's activity by 50% even in the absence of DMSP. This inhibition was enhanced in the presence of DMSP. Additions of increasing concentrations of MMPA to the PU\_DmdB1 assays had no effect on the level of DMSP inhibition (data not shown). Similarly, the addition of MMPA above 8 mM restored only 25% of RL\_DmdB1 activity and 35% of RL\_DmdB2 activity (Figure 2-7). ADP had no effect on DMSP inhibition of these enzymes. However, it is not known if *R. lacuscaerulensis* or *P. ubique* accumulate DMSP to high levels, and the response of *R. pomeroyi* DSS-3 to DMSP may be specific to its DmdBs.

**RPO\_ *dmdB1* and RPO\_ *dmdB2* Are Differentially Expressed Depending on Carbon Source.** RNA extracted from chemostat grown cells given four different sole carbon sources was analyzed for variations in RPO\_ *dmdB1* and RPO\_ *dmdB2* expression levels. Cells were grown in chemostats containing 2 mM DMSP, 4 mM MMPA, 3 mM methionine or 6 mM acetate as the sole source of carbon. DmdB activity was expected to be required for metabolism of all of these substrates except acetate, while DmdA was required only for the catabolism of DMSP. As expected, the steady state levels of RPO\_ *dmdA* were only elevated during growth on DMSP (Table 2-9). RPO\_ *dmdB1* exhibited overall lower steady state levels of mRNA than RPO\_ *dmdB2* for all substrates except acetate (Table 2-9). Although the levels of the RPO\_ *dmdB1* transcripts increased during growth on DMSP and methionine, it was always lower than those of RPO\_ *dmdB2*. For that reason, RPO\_ *dmdB2* appeared to be the major DmdB during growth on compounds leading to MMPA formation (Table 2-9).

## Discussion

DmdB is an acyl-CoA ligase that catalyzes the second reaction of the DMSP demethylation pathway. In this study, DmdB enzymes from *R. pomeroyi* DSS-3 and *P. ubique* HTCC1062 were characterized *in vitro* to gain insight into their functional roles and regulation. Four additional DmdB orthologs from *R. lacuscaerulensis* ITI-1157, *P. aeruginosa* PAO1, and *B. thailandensis* E264 were also evaluated for functional similarity to the *P. ubique* HTCC1062 DmdB and *R. pomeroyi* DSS-3 isozymes. Phylogenetic analysis showed that these enzymes are part of a family which forms two distinct clades, with amino acid sequence similarity varying from 33% between members of different clades and up to 86% among members of the same clade (11). All enzymes catalyzed the MMPA-CoA ligase reaction with a high activity, but members of each clade varied greatly in other characteristics.

All seven enzymes possessed broad substrate specificities encompassing a range of short chain fatty acids and MMPA. This verified that the members of both DmdB clades can catalyze the MMPA-CoA ligase reaction as predicted. However, the activity levels of the DmdB enzymes with fatty acids varied greatly, revealing no pattern between enzymes from the same clade. The same was true for the effect of salt ions on enzyme activity. This study emphasizes the broad ranging activities and functional characteristics of the CoA ligase enzymes. Thus, the level of amino acid sequence similarity between two enzymes does not accurately predict many of the functional characteristics beyond the general range of substrates. For that reason, more isozymes from other bacteria were not characterized. This result is consistent with studies of CoA ligases from *Burkholderia xenovorans* and *Geobacillus thermodenitrificans*, which found sequence and even structural similarity did not necessarily infer functional similarity (36, 37). In the case of the two benzoate-CoA ligases from *B. xenovorans*, the activities and affinities of the two

enzymes varied even though the active sites in both enzymes were highly conserved and they shared 83% amino acid sequence identity overall (37). This was further demonstrated with the long-chain acyl CoA ligase derived from rat liver, yeast, and *E. coli*. These CoA ligases have 48-51% sequence identity but vary in substrate specificities and sensitivity to inhibitors (25, 38, 39).

The DmdB enzymes investigated here appear to be adapted to the individual life style of the bacterium regardless of the phylogenetic clade. For instance, PU\_DmdB1 from the obligate oligotroph *P. ubique* HTCC1062 possesses many features absent from other members of the DmdB1 clade. At 1.3 Mbp, this microorganism has one of the smallest genomes of any free living bacterium and may be under extreme selection pressure to maximize its growth efficiency (24). This hypothesis is consistent with the properties of its DmdB. The high specific activity of the enzyme may minimize the amount of enzyme needed to maintain physiological levels of activity, while the broad substrate specificity may allow a single enzyme to perform multiple functions. This would also reduce the number of genes encoding this family of enzymes, consistent with the *P. ubique* HTCC1062 genome only encoding five CoA ligase-like enzymes (24). In comparison, the opportunitroph *R. pomeroyi* DSS-3 has a genome of 4.1 Mb, plus a 0.4 Mb megaplasmid, and encodes 26 CoA ligases (19). Likewise, the high affinity of the PU\_DmdB1 for substrates may allow the cell to lower the pool sizes of intermediates, lowering the difference between intracellular and extracellular concentrations to reduce the energy needed for transport and minimize leakage across the cytoplasmic membrane.

DMSP may be an important regulatory effector of the DmdB enzymes from marine bacteria. All of the enzymes from marine bacteria were sensitive to concentrations of DMSP well below the 70 mM DMSP found to accumulate in *R. pomeroyi* DSS-3 (12). In contrast, the two enzymes from terrestrial bacteria were not affected by DMSP. Neither of these bacteria possesses

*dmdA* homologs, and they are unlikely to metabolize or encounter DMSP. For that reason, DMSP sensitivity appears to be a specific adaptation in marine bacteria. However, only *R. pomeroyi* DSS-3 is known to accumulate high intracellular concentrations of DMSP, and mechanisms to reverse DMSP inhibition were only clearly identified in the DmdBs from this bacterium. Thus, the physiological significance of DMSP inhibition in other marine bacteria is not certain at this time.

The presence of two DmdB isozymes in *R. pomeroyi* DSS-3 raises additional questions concerning their regulation. Indeed, the levels of both RPO\_*dmdB1* and RPO\_*dmdB2* transcripts increased during growth on DMSP even though the intracellular levels of DMSP would be expected to be strongly inhibitory for both enzymes. This suggests that there is a complex regulatory network for their activity, and a working model of DmdB regulation has been developed to illustrate how the properties of the DmdB isozymes might affect DMSP metabolism (Figure 2-8).

The central question is how cells can possess high levels of the enzymes in a catabolic pathway, such as DmdA and DmdB, when they also maintain very high levels of the substrate DMSP. RPO\_*DmdB1* increased activity in response to increasing ADP levels, indicating that the enzyme is sensitive to the energy charge of the cell. Energy charge is a measurement of the amount of metabolic energy contained in the adenylate pool, described by the ratio  $[(ATP) + \frac{1}{2}(ADP)] / [(ATP) + (ADP) + (AMP)]$  (40). During normal cellular growth the majority of the adenylate pool is ATP, and an energy charge of about 0.9 is common (41). When the cell is energy and carbon limited, ADP and AMP accumulate, causing a decrease in energy charge (40). Documented cellular concentrations of ADP are between 0.8 and 3 mM in *E. coli*, within the range of ADP concentrations sufficient to reverse DMSP inhibition of RPO\_*DmdB1* activity (42,

43). In this model, as DMSP accumulates to high levels presumably for use as an osmolyte, it can also serve as a pool of readily available carbon and energy in the cell (1, 7, 12). Should other carbon and energy sources become depleted, the levels of ADP would increase, RPO\_DmdB1 activity would increase, and MMPA (and DMSP) would be degraded as an energy source. This conclusion is supported by the increased level of RPO\_ *dmdB1* transcripts during growth on DMSP but not on MMPA.

Based upon the high levels of transcripts during growth on DMSP, RPO\_DmdB2 appears to be the major form of DmdB utilized during growth on DMSP. This conclusion is supported by kinetic analysis which confirms that RPO\_DmdB2 has a higher specificity for MMPA than RPO\_DmdB1. However, RPO\_DmdB2 is expected to only become active when levels of MMPA are sufficient to relieve the inhibition caused by high intracellular concentrations of DMSP. Thus, MMPA appears to be a second important effector for the regulation of DMSP demethylation. Because DmdA activity is not directly affected by MMPA, presumably the DmdA reaction and the accumulation of MMPA are controlled by the availability of free THF and the turnover of methyl-THF (12). Methyl-THF is probably rapidly oxidized to provide electrons for respiration. This hypothesis is consistent with the increased levels of transcripts for the enzymes involved in methyl-THF oxidation observed during growth with DMSP and MMPA (unpublished data). Methyl-THF also provides C1 intermediates for biosynthesis of purine nucleotides and methionine (44, 45). In the case of DMSP demethylation, when methyl-THF is rapidly metabolized during growth on DMSP, free THF is available for DmdA, leading to increased levels of MMPA. As MMPA accumulates, RPO\_DmdB2 becomes active, and MMPA metabolism could provide an additional source of electrons for respiration and carbon for biosynthesis. This could lower the demand for methyl-THF, decrease levels of free THF, and

decrease the rate of MMPA formation. Thus, the rate of MMPA metabolism may feedback on the rate of DMSP consumption via the levels of free THF. In addition, MMPA metabolism leads to the formation of MeSH and acetaldehyde, which is toxic. MeSH oxidation also leads to the formation of hydrogen peroxide, which may cause oxidative stress and inhibit growth (46, 47). In this variation of the model, growth inhibition by oxidative stress and acetaldehyde toxicity limits methyl-THF metabolism, leading to a decrease in the levels of MMPA and lower RPO\_DmdB2 activity, preventing the further metabolism of DMSP. Because DMSP is also a potent antioxidant, its accumulation would also be protective (2, 17).

The potential for DMSP metabolism to lead to oxidative stress may also explain the response of RPO\_DmdB1 to ADP. In this model, DMSP is needed as a carbon and energy source when other sources are depleted but also to protect against oxidative and osmotic stress. Although speculative, this model illustrates the need for cells to balance the multiple demands for DMSP as an osmolyte and antioxidant during its metabolism with its value as a carbon and sulfur source. Because DMSP inhibition of the DmdBs from *R. lacuscaerulensis* ITI-1157 is also affected by the levels of MMPA, this may be a more general model for DMSP regulation in marine bacteria. However, it is not yet known if this bacterium accumulates high levels of DMSP, so this conclusion is less certain at this time.

While DMSP is likely the main source of MMPA in marine bacteria, the methionine salvage pathway may provide another source of MMPA (48, 49). During the transformation of 1,2-dihydroxy 3-oxomethylthiopentene, if the aci-reductone dioxygenase is bound to Ni<sup>2+</sup> instead of Fe<sup>2+</sup>, MMPA is formed rather than 4-methylthio-2-oxobutyrate (48, 50). This pathway may also be the source of MMPA in non-marine microorganisms, such as *P. aeruginosa* PAO1 and *B. thailandensis* E264. The physiological relevance of this off-pathway has not yet been

demonstrated, however, *Klebsiella pneumonia*-derived aci-reductone dioxygenases bound to  $\text{Fe}^{2+}$  and  $\text{Ni}^{2+}$  have been purified and studied (51, 52). The role of MMPA in methionine salvage is supported by the expression data indicating that RPO\_ *dmdB1* and RPO\_ *dmdB2* are highly expressed during growth on methionine. Furthermore, during growth on methionine *R. pomeroyi* DSS-3 produced MeSH (unpublished observation), suggesting a link between the methionine salvage and demethylation pathways that still needs to be investigated.

In conclusion, DmdB appears to be a major regulatory point in DMSP metabolism by *R. pomeroyi* DSS-3. However, regulation of DmdB activity by itself is not sufficient to explain what is likely to be a complex system balancing the cellular requirements for carbon and sulfur for growth, maintaining the cellular osmotic balance, and protection from oxidative stress. Further study will be necessary to fully understand all of the regulatory aspects of DMSP demethylation and the enzymes involved. Nevertheless, the work here provides valuable insight into the regulation of the DmdB isozymes and expands our knowledge of this multifaceted regulatory system.

### **Acknowledgements**

We would like to acknowledge the National Science Foundation (grant MCB-1158037) for providing the funding for this project.

## References

1. **Stefels J.** 2000. Physiological aspects of the production and conversion of DMSP in marine algae and higher plants. *J. Sea Res.* **43**:183-197.
2. **Sunda W, Kieber DJ, Kiene RP, Huntsman S.** 2002. An antioxidant function for DMSP and DMS in marine algae. *Nature* **418**:317-320.
3. **Steinke M, Wolfe GV, Kirst GO.** 1998. Partial characterization of dimethylsulfoniopropionate (DMSP) lyase isozymes in 6 strains of *Emiliania huxleyi*. *Mar. Ecol. Prog. Ser.* **175**:215-225.
4. **Reisch CR, Moran MA, Whitman WB.** 2011. Bacterial catabolism of dimethylsulfoniopropionate (DMSP). *Front. in Microbiol.* **2**:172.
5. **Simo R, Pedros-Alio C, Malin G, Grimalt JO.** 2000. Biological turnover of DMS, DMSP and DMSO in contrasting open-sea waters. *Mar. Ecol. Prog. Ser.* **203**:1-11.
6. **Simo R, Archer SD, Pedros-Alio C, Gilpin L, Stelfox-Widdicombe CE.** 2002. Coupled dynamics of dimethylsulfoniopropionate and dimethylsulfide cycling and the microbial food web in surface waters of the North Atlantic. *Limnol. Oceanogr.* **47**:53-61.
7. **Kiene RP, Linn LJ, Bruton JA.** 2000. New and important roles for DMSP in marine microbial communities. *J. Sea Res.* **43**:209-224.
8. **Andreae MO.** 1990. Ocean-atmosphere interactions in the global biogeochemical sulfur cycle. *Mar. Chem.* **30**:1-29.
9. **Bruhl C, Lelieveld J, Crutzen PJ, Tost H.** 2012. The role of carbonyl sulphide as a source of stratospheric sulphate aerosol and its impact on climate. *Atmos. Chem. Phys.* **12**:1239-1253.
10. **Charlson RJ, Lovelock JE, Andreae MO, Warren SG.** 1987. Oceanic phytoplankton, atmospheric sulfur, cloud albedo and climate. *Nature* **326**:655-661.
11. **Reisch CR, Stoudemayer MJ, Varaljay VA, Amster IJ, Moran MA, Whitman WB.** 2011. Novel pathway for assimilation of dimethylsulphoniopropionate widespread in marine bacteria. *Nature* **473**:208-211.
12. **Reisch CR, Moran MA, Whitman WB.** 2008. Dimethylsulfoniopropionate-dependent demethylase (DmdA) from *Pelagibacter ubique* and *Silicibacter pomeroyi*. *J. Bacteriol.* **190**:8018-8024.
13. **Gonzalez JM, Kiene RP, Moran MA.** 1999. Transformation of sulfur compounds by an abundant lineage of marine bacteria in the alpha-subclass of the class Proteobacteria. *Appl. Environ. Microbiol.* **65**:3810-3819.

14. **Howard EC, Henriksen JR, Buchan A, Reisch CR, Burgmann H, Welsh R, Ye W, Gonzalez JM, Mace K, Joye SB, Kiene RP, Whitman WB, Moran MA.** 2006. Bacterial taxa that limit sulfur flux from the ocean. *Science* **314**:649-652.
15. **Kiene RP, Linn LJ, Gonzalez J, Moran MA, Bruton JA.** 1999. Dimethylsulfoniopropionate and methanethiol are important precursors of methionine and protein-sulfur in marine bacterioplankton. *Appl. Environ. Microbiol.* **65**:4549-4558.
16. **Kiene RP, Linn LJ.** 2000. The fate of dissolved dimethylsulfoniopropionate (DMS) in seawater: tracer studies using <sup>35</sup>S-DMS. *Geochim. Cosmochim. Acta.* **64**:2797-2810.
17. **Lesser MP.** 2006. Oxidative stress in marine environments: biochemistry and physiological ecology. *Annu. Rev. Physiol.* **68**:253-278.
18. **Chambers ST, Kunin CM, Miller D, Hamada A.** 1987. Dimethylthetin can substitute for glycine betaine as an osmoprotectant molecule for *Escherichia coli*. *J. Bacteriol.* **169**:4845-4847.
19. **Moran MA, Buchan A, Gonzalez JM, Heidelberg JF, Whitman WB, Kiene RP, Henriksen JR, King GM, Belas R, Fuqua C, Brinkac L, Lewis M, Johri S, Weaver B, Pai G, Eisen JA, Rahe E, Sheldon WM, Ye WY, Miller TR, Carlton J, Rasko DA, Paulsen IT, Ren QH, Daugherty SC, Deboy RT, Dodson RJ, Durkin AS, Madupu R, Nelson WC, Sullivan SA, Rosovitz MJ, Haft DH, Selengut J, Ward N.** 2004. Genome sequence of *Silicibacter pomeroyi* reveals adaptations to the marine environment. *Nature* **432**:910-913.
20. **Yi H, Lim YW, Chun J.** 2007. Taxonomic evaluation of the genera *Ruegeria* and *Silicibacter*: a proposal to transfer the genus *Silicibacter* Petrusdottir and Kristjansson 1999 to the genus *Ruegeria* Uchino et al. 1999. *Int. J. Syst. Evol. Micr.* **57**:815-819.
21. **Stover CK, Pham XQ, Erwin AL, Mizoguchi SD, Warrenner P, Hickey MJ, Brinkman FSL, Hufnagle WO, Kowalik DJ, Lagrou M, Garber RL, Goltry L, Tolentino E, Westbrook-Wadman S, Yuan Y, Brody LL, Coulter SN, Folger KR, Kas A, Larbig K, Lim R, Smith K, Spencer D, Wong GKS, Wu Z, Paulsen IT, Reizer J, Saier MH, Hancock REW, Lory S, Olson MV.** 2000. Complete genome sequence of *Pseudomonas aeruginosa* PAO1, an opportunistic pathogen. *Nature* **406**:959-964.
22. **Zinser BA, Ferriera SF, Johnson JJ, Kravitz SK, Beeson KB, Sutton GS, Roger YHR, Friedman RF, Frazier MF, Venter JC.** 2008. *Silicibacter lacuscaerulensis* ITI-1157 Genome Sequence. EMBL/GenBank/DDBJ databases.
23. **Kim HS, Schell MA, Yu Y, Ulrich RL, Sarria SH, Nierman WC, DeShazer D.** 2005. Bacterial genome adaptation to niches: divergence of the potential virulence genes in three *Burkholderia* species of different survival strategies. *BMC Genomics* **6**:174

24. **Giovannoni SJ, Tripp HJ, Givan S, Podar M, Vergin KL, Baptista D, Bibbs L, Eads J, Richardson TH, Noordewier M, Rappe MS, Short JM, Carrington JC, Mathur EJ.** 2005. Genome streamlining in a cosmopolitan oceanic bacterium. *Science* **309**:1242-1245.
25. **Black PN, Zhang Q, Weimar JD, DiRusso CC.** 1997. Mutational analysis of a fatty acyl-coenzyme A synthetase signature motif identifies seven amino acid residues that modulate fatty acid substrate specificity. *J. Biol. Chem.* **272**:4896-4903.
26. **Shimizu S, Inoue K, Tani Y, Yamada H.** 1979. Enzymatic microdetermination of serum free fatty acids. *Anal. Biochem.* **98**:341-345.
27. **Bergmeyer H, Hagen A.** 1972. *New Principle of Enzymatic Analysis.* Fresenius Z. Anal. Chem. **261**:333-&.
28. **Gonzalez JM, Mayer F, Moran MA, Hodson RE, Whitman WB.** 1997. *Microbulbifer hydrolyticus* gen nov, sp nov, and *Marinobacterium georgiense* gen nov, sp nov, two marine bacteria from a lignin-rich pulp mill waste enrichment community. *Int. J. Syst. Bacteriol.* **47**:369-376.
29. **Langmead B, Salzberg SL.** 2012. Fast gapped-read alignment with Bowtie 2. *Nat. Methods* **9**:357-359.
30. **Trapnell C, Hendrickson DG, Sauvageau M, Goff L, Rinn JL, Pachter L.** 2013. Differential analysis of gene regulation at transcript resolution with RNA-seq. *Nat. Biotechnol.* **31**:46-53.
31. **Kumari S, Tishel R, Eisenbach M, Wolfe AJ.** 1995. Cloning, characterization, and functional expression of *Acs*, the gene which encodes acetyl-coenzyme A synthetase in *Escherichia coli*. *J. Bacteriol.* **177**:2878-2886.
32. **Watkins PA, Lu JF, Steinberg SJ, Gould SJ, Smith KD, Braiterman LT.** 1998. Disruption of the *Saccharomyces cerevisiae* FAT1 gene decreases very long-chain fatty acyl-CoA synthetase activity and elevates intracellular very long-chain fatty acid concentrations. *J. Biol. Chem.* **273**:18210-18219.
33. **Chohnan S, Furukawa H, Fujio T, Nishihara H, Takamura Y.** 1997. Changes in the size and composition of intracellular pools of nonesterified coenzyme A and coenzyme A thioesters in aerobic and facultatively anaerobic bacteria. *Appl. Environ. Microbiol.* **63**:553-560.
34. **Jackowski S, Rock C.** 1986. Consequences of reduced intracellular coenzyme A content in *Escherichia coli*. *J. Bacteriol.* **166**:866-871.

35. **Buckstein MH, He J, Rubin H.** 2008. Characterization of nucleotide pools as a function of physiological state in *Escherichia coli*. *J. Bacteriol.* **190**:718-726.
36. **Dong YP, Du HQ, Gao CX, Ma T, Feng L.** 2012. Characterization of two long-chain fatty acid CoA ligases in the Gram-positive bacterium *Geobacillus thermodenitrificans* NG80-2. *Microbiol. Res.* **167**:602-607.
37. **Bains J, Boulanger MJ.** 2007. Biochemical and structural characterization of the paralogous benzoate CoA Ligases from *Burkholderia xenovorans* LB400: Defining the entry point into the novel benzoate oxidation (box) pathway. *J. Mol. Biol.* **373**:965-977.
38. **Black PN, Dirusso CC, Metzger AK, Heimert TL.** 1992. Cloning, sequencing, and expression of the *fadD* gene of *Escherichia coli* encoding acyl coenzyme A synthetase. *J. Biol. Chem.* **267**:25513-25520.
39. **Caviglia JM, Li LO, Wang SL, DiRusso CC, Coleman RA, Lewin TM.** 2004. Rat long chain acyl-CoA synthetase 5, but not 1, 2, 3, or 4, complements *Escherichia coli fadD*. *J. Biol. Chem.* **279**:11163-11169.
40. **Atkinson DE.** 1968. Energy charge of adenylate pool as a regulatory parameter . interaction with feedback modifiers. *Biochemistry* **7**:4030-4034.
41. **Bennett BD, Kimball EH, Gao M, Osterhout R, Van Dien SJ, Rabinowitz JD.** 2009. Absolute metabolite concentrations and implied enzyme active site occupancy in *Escherichia coli*. *Nat. Chem. Biol.* **5**:593-599.
42. **Albe KR, Butler MH, Wright BE.** 1990. Cellular concentrations of enzymes and their substrates. *J. Theor. Biol.* **143**:163-195.
43. **Henry CS, Broadbelt LJ, Hatzimanikatis V.** 2007. Thermodynamics-based metabolic flux analysis. *Biophys. J.* **92**:1792-1805.
44. **Nagy PL, Marolewski A, Benkovic SJ, Zalkin H.** 1995. Formyltetrahydrofolate hydrolase, a regulatory enzyme that functions to balance pools of tetrahydrofolate and one-carbon tetrahydrofolate adducts in *Escherichia coli*. *J. Bacteriol.* **177**:1292-1298.
45. **Huang EY, Mohler AM, Rohlman CE.** 1997. Protein expression in response to folate stress in *Escherichia coli*. *J. Bacteriol.* **179**:5648-5653.
46. **Kim JS, Kim YC, Lee DS, and Yang, JW.** 2000. Isolation and purification of methyl mercaptan oxidase from *Rhodococcus rhodochrous* for mercaptan detection. *Biotechnol. Bioprocess Eng.* **5**:465-468.
47. **Gould WD, Kanagawa T.** 1992. Purification and properties of methyl mercaptan oxidase from *Thiobacillus thioparus* TK-M. *J. Gen. Microbiol.* **138**:217-221.

48. **Albers E.** 2009. Metabolic characteristics and importance of the universal methionine salvage pathway recycling methionine from 5'-methylthioadenosine. *IUBMB Life* **61**:1132-1142.
49. **Sekowska A, V D, Ashida H, Michoud K, Haas D, Yokota A, Danchin A.** 2004. Bacterial variations on the methionine salvage pathway. *BMC Microbiol.* **4**:9.
50. **Dai Y, Wensink PC, Abeles RH.** 1999. One protein, two enzymes. *J. Biol. Chem.* **274**:1193-1195.
51. **Dai Y, Pochapsky TC, Abeles RH.** 2001. Mechanistic studies of two dioxygenases in the methionine salvage pathway of *Klebsiella pneumoniae*. *Biochemistry* **40**:6379-6387.
52. **Al-Mjeni F, Ju T, Pochapsky TC, Maroney MJ.** 2002. XAS investigation of the structure and function of Ni in acireductone dioxygenase. *Biochemistry* **41**:6761-6769.

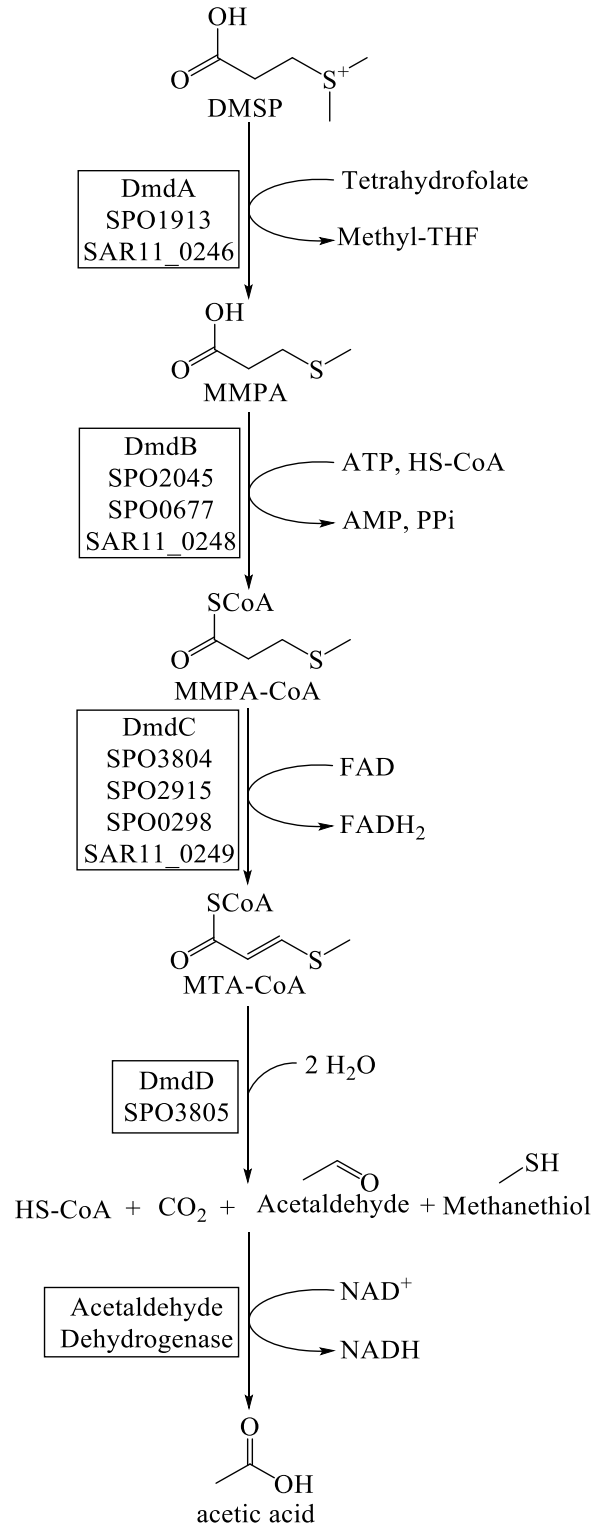


**Figure 2-1:** DMSP demethylation pathway from *R. pomeroyi* DSS-3 and *P. ubique* HTCC1062

(11).

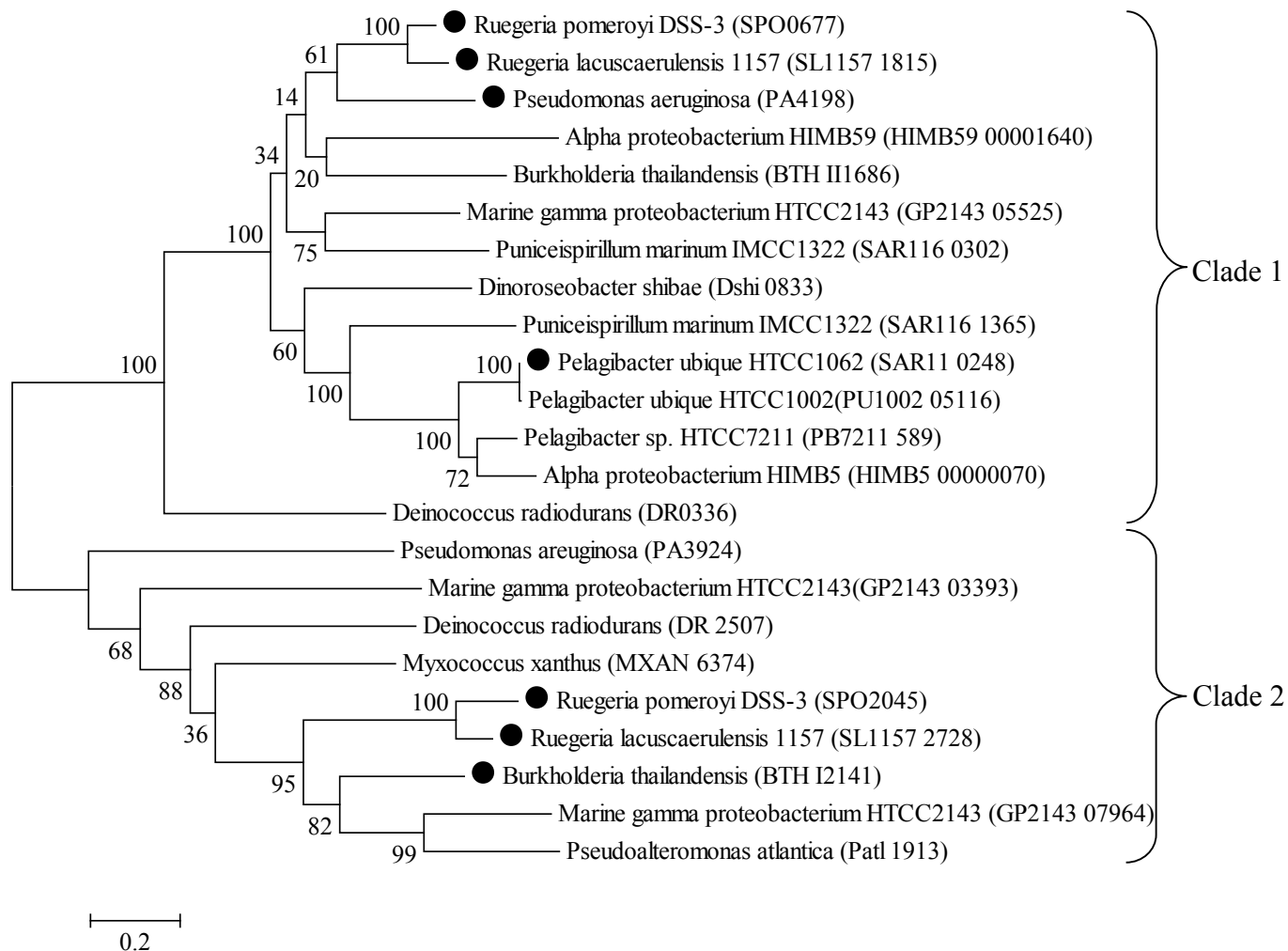


**Figure 2-2:** Phylogenetic tree displaying the two DmdB clades. The phylogenetic tree was constructed using the maximum likelihood method in MEGA 5.2. DmdBs investigated for this study are indicated (•). Nomenclature for DmdBs used in this study is as follows: BTHI2141: BTH\_DmdB2; PA4198: PA\_DmdB1; SAR11\_0248: PU DmdB1; SL1157 1815: RL\_DmdB1; SL1157 2728: RL\_DmdB2; SPO0677: RPO\_DmdB1; SPO2045: RPO\_DmdB2.

**Table 2-1.** Percent amino acid identity of the DmdB enzymes from the two clades.

	PU_	RPO_	RPO_	RL_	RL_	PA_	BTH_
	DmdB1	DmdB1	DmdB2	DmdB1	DmdB2	DmdB1	DmdB2
PU	100%	54%	32%	55%	33%	51%	33%
DmdB1							
	RPO_	100%	34%	86%	33%	65%	35%
DmdB1							
	RPO_	100%	33%	82%	34%	55%	
DmdB2							
	RL_	100%	32%	64%	35%		
DmdB1							
	RL_	100%	32%	56%			
DmdB2							
	PA_	100%	33%				
DmdB1							
	BTH_	100%					
DmdB2							

**Table 2-2.** Plasmids used for recombinant expression in this study

Plasmid	Vector	Genotype	Reference
pCRR205	pET101	SAR11_0248 (PU_DmdB1)	Reisch 2011
pCRR208	pET101	SPO_0677 (RPO_DmdB1)	Reisch 2011
pCRR203	pET101	SPO_2045 (RPO_DmdB2)	Reisch 2011
pHAB101	pET101	SL1157_1815 (RL_DmdB1)	This work
pHAB102	pET101	SL1157_2728 (RL_DmdB2)	This work
pHAB103	pET101	PA4198 (PA_DmdB1)	This work
pHAB104	pET101	BTH_I2141 (BTH_DmdB2)	This work

**Table 2-3.** Primer sequences used for construction of recombinant expression plasmids in this study.

Gene	Primer name and sequence (5' to 3')	Purpose
SL1157_1815	SL1157_1815 Fwd:	Cloning
	CACCATGGCGACCCACAACATCTA	SL1157_1815
	SL1157_1815 Rev:	into pET101
	GCCCAACGCCCGCGCCTGTTCCTGA	
SL1157_2728	SL1157_2728 Fwd:	Cloning
	CACCATGCTGGGACAGATGATGAC	SL1157_2728
	SL1157_2728 Rev:	into pET101
	CCCCGTCAGGGCGTCCTTGAA	
PA_4198	PA_4198 Fwd:	Cloning
	CACCATGTCGATCTTCGAACAGGGT	PA_4198
	PA_4198 Rev:	into pET101
	GAGGGCGGCGGCCCACTCGCGCAGCA	
BTH_I2141	BTH_I2141 Fwd:	Cloning
	CACCATGTTGCTGACCGGTAAGTTAG	BTH_I2141
	BTH_I2141 Rev:	into pET101
	CGCGTCGACCGCCGTCGGCAACA	

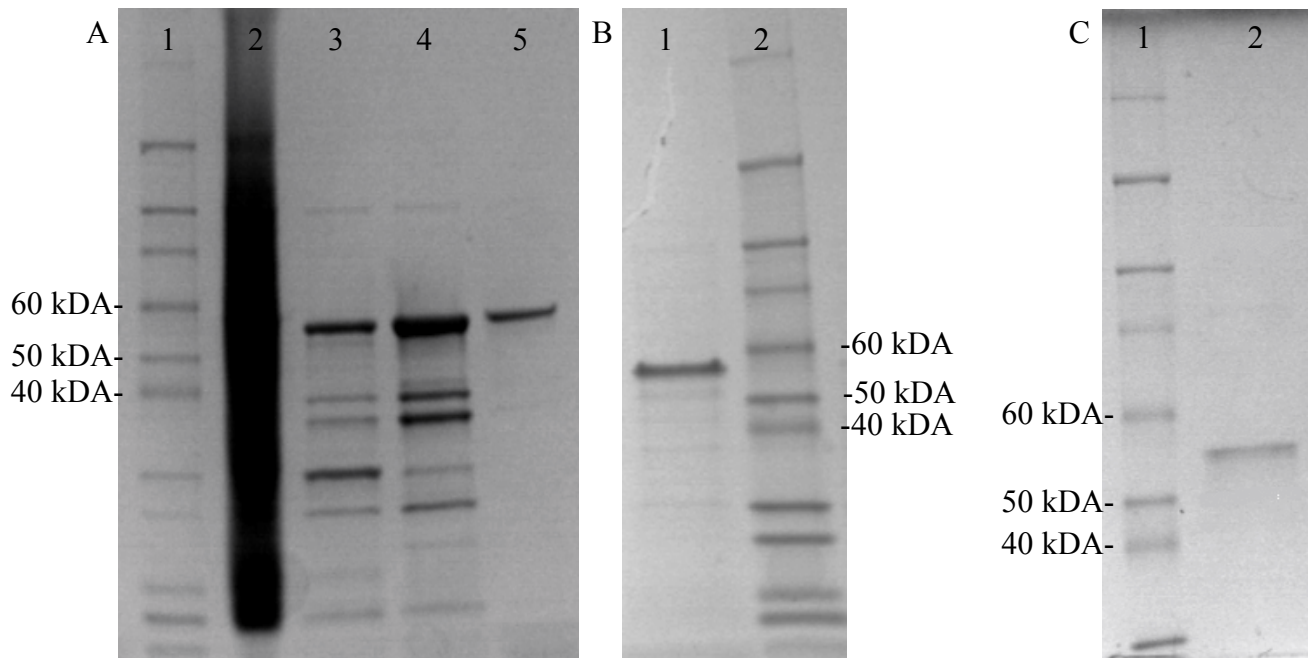


**Figure 2-3.** SDS-PAGE of purified recombinant PU\_DmdB1 from *P.ubique* HTCC1062 and RPO\_DmdB1 and RPO\_DmdB2 from *R. pomeroyi* DSS-3. A) PU\_DmdB1 Lane 1: Novex sharp prestained protein ladder 3.5-260 kDA (Invitrogen). Lane 2: Crude cell extract from recombinant *E. coli*. Lane 3: Q-Sepharose eluate. Lane 4: Phenyl Superpose eluate. Lane 5: Hitrap Blue eluate. B) RPO\_DmdB1 Lane 1: Sephacryl S-200 eluate. Lane 2: Novex sharp prestained protein ladder. C) RPO\_DmdB2 Lane 1: Novex sharp prestained protein ladder. 2: HiTrap Blue eluate.

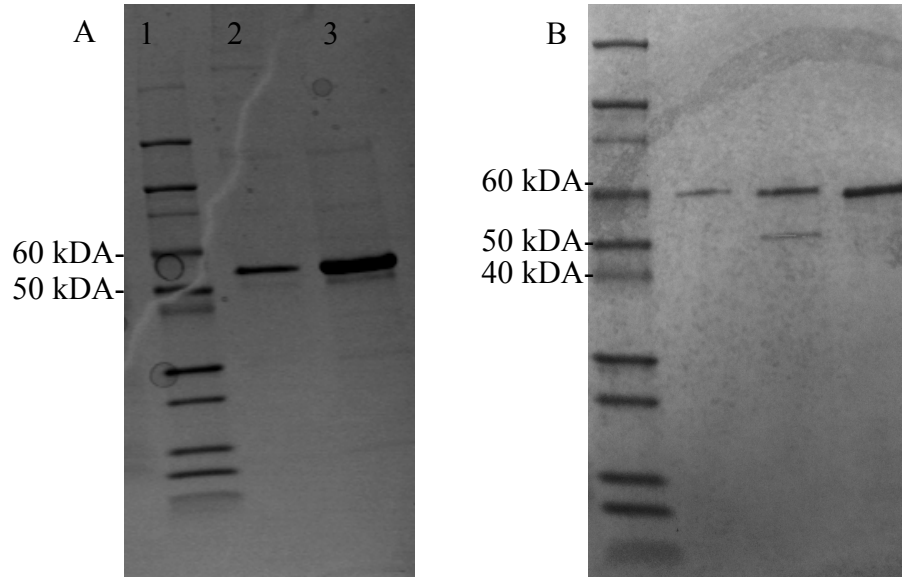


**Figure 2-4.** SDS-PAGE of purified recombinant RL DmdB1 and RL\_DmdB2 from *R. lacuscaerulensis* ITI-1157, BTH\_DmdB2 from *B. thailandensis* E264, and PA\_DmdB1 from *P. aeruginosa* PAO1. A) RL\_DmdB1 and RL\_DmdB2 Lane 1: Novex sharp prestained protein ladder 3.5-260 kDa (Invitrogen). Lane 2: RL\_DmdB1 HisTrap eluate Lane 3: RL\_DmdB2 eluate B) BTH\_DmdB2 PA DmdB1. Lane 1: Novex sharp prestained protein ladder 3.5-260 kDa (Invitrogen). Lane 2: BTH\_DmdB2 HisTrap eluate. Lane 3: PA\_DmdB1 His Trap eluate (1) Lane 4: PA\_DmdB1 HisTrap eluate (2).

**Table 2-4.** General characteristics of the recombinant DmdB isozymes from *P. ubiquus*HTCC1062 and *R. pomoyi* DSS-3

	PU_DmdB1	RPO_DmdB1	RPO_DmdB2
Molecular Weight			
Predicted	61,000	59,000	59,000
Observed Denatured	59,000	62,000	58,000
Observed Native	108,000	112,000	122,000
Purity	93%	90%	92%
Specific Activity ( $\mu\text{mol min}^{-1} \text{mg}^{-1}$ )	28	15	16
pH			
Optimum	7.5	7.0	7.5
Range	6.0-8.5	6.0-8.0	6.5-9.0

**Table 2-5.** Effect of salts on the activity of the DmdB isozymes<sup>a</sup>

Salt	Relative activity (%)						
	PU_ DmdB1	RPO_ DmdB1	RPO_ DmdB2	RL_ DmdB1	RL_ DmdB2	PA_ DmdB1	BTH_ DmdB2
No Salt	(100)	(100)	(100)	(100)	(100)	(100)	(100)
LiCl	9	41	301	135	138	97	13
NH <sub>4</sub> Cl	68	6	210	164	50	95	45
KCl	92	30	45	104	141	103	27
NaCl	43	40	50	86	90	49	8
Na Acetate	39	14	34	32	12	17	55
K Acetate	84	27	49	44	103	15	93
Li <sub>2</sub> SO <sub>4</sub>	8	18	18	43	59	19	8
(NH <sub>4</sub> ) <sub>2</sub> SO <sub>4</sub>	86	25	154	57	71	50	7
K <sub>2</sub> SO <sub>4</sub>	84	32	157	95	10	104	133
Na <sub>2</sub> SO <sub>4</sub>	40	32	117	42	34	36	16

<sup>a</sup> All salts were used at a concentration of 0.4 M. The HPLC based assay was used to avoid salt effects on coupling enzymes. Relative activity ( $\mu\text{mol min}^{-1} \text{mg}^{-1}$ ) values expressed as a percentage of the total specific activity as measured without salt additions (100%). The standard errors are for three independent experiments and were within 3%. Specific activities in units  $\text{mg}^{-1}$  of protein ( $\pm$  SE) defined as 100% were: PU\_DmdB1:  $26 \pm 3$ ; RPO\_DmdB1:  $17 \pm 2$ ; RPO\_DmdB2:  $16 \pm 3$ ; RL\_DmdB1:  $21 \pm 3$ ; RL\_DmdB2:  $18 \pm 2$ ; PA\_DmdB1:  $31 \pm 2$ ; and BTH\_DmdB2:  $25 \pm 4$ .

**Table 2-6.** Substrate specificities of the DmdB isozymes<sup>a</sup>

Substrate	Relative activity (%)						
	PU_DmdB1	RPO_DmdB1	RPO_DmdB2	RL_DmdB1	RL_DmdB2	PA_DmdB1	BTH_DmdB2
MMPA	(100)	(100)	(100)	(100)	(100)	(100)	(100)
Acetate	10	0.0 <sup>b</sup>	10	151	0.0 <sup>b</sup>	110	0.0
Propionate	13	77	16	126	72	124	45
Acrylate	50	79	56	6	29	65	15
Butyrate	160	36	73	81	113	121	93
Isobutyrate	13	30	12	10	7	48	5
Crotonate	2	109	63	32	41	63	87
Methylbutyrate	8	10	39	20	18	24	23
Valerate	18	31	51	49	179	91	68
Isovalerate	8	19	14	15	5	18	4
Hexanoate	5	17	27	17	62	12	94
Caprylate	0.0 <sup>b</sup>	0.0 <sup>b</sup>	0.0 <sup>b</sup>	0.0 <sup>b</sup>	0.0 <sup>b</sup>	0.0 <sup>b</sup>	1
Caprate	0.0 <sup>b</sup>	0.0 <sup>b</sup>	0.0 <sup>b</sup>	0.0 <sup>b</sup>	0.0 <sup>b</sup>	0.0 <sup>b</sup>	0.0 <sup>b</sup>

<sup>a</sup> Relative activity values expressed as a percentage of the total specific activity as measured with MMPA (100%). All standard errors are from three independent experiments and are within 3 %.

Specific activities in units mg<sup>-1</sup> of protein ( $\pm$  SE) defined as 100% were: PU\_DmdB1: 28  $\pm$ 1;

RPO\_DmdB1: 15  $\pm$ 3; RPO\_DmdB2: 17  $\pm$ 3; RL\_DmdB1: 24  $\pm$ 2; RL\_DmdB2: 16  $\pm$ 2;

PA\_DmdB1: 32  $\pm$ 2; and BTH\_DmdB2: 25  $\pm$ 4. <sup>b</sup> < 0.1%

**Table 2-7.** Apparent kinetic constants for *P. ubiquus* HTCC1062 and *R. pomeroyi* DSS-3 DmdBs<sup>a</sup>

	PU_DmdB1	RPO_DmdB1	RPO_DmdB2
MMPA			
$K_m$	0.04 ±0.01	0.08 ±0.02	0.07 ±0.02
$V_{max}$	31.4 ±5.3	19.3 ±3.3	15.4 ±2.5
$k_{cat}$	29.4	18.7	14.9
$k_{cat}/K_m$	735	233	213
Butyrate			
$K_m$	0.01 ±0.01	0.02 ±0.01	0.12 ±0.03
$V_{max}$	46.8 ±7.7	14.9 ±3.6	7.4 ±2.1
$k_{cat}$	43.8	14.4	7.2
$k_{cat}/K_m$	3370	1031	71
Propionate			
$K_m$	0.04 ±0.02	0.04 ±0.01	3.11 ±1.13
$V_{max}$	18.9 ±3.0	11.2 ±2.5	3.8 ±1.4
$k_{cat}$	17.7	10.8	3.7
$k_{cat}/K_m$	505	271	1.2
Acrylate			
$K_m$	0.44 ±0.04	0.9 ±0.2	5.25 ±2.1
$V_{max}$	23.8 ±5.3	10.5 ±2.0	1.0 ±0.2
$k_{cat}$	22.3	14.3	1.0
$k_{cat}/K_m$	50	16	0.2

<sup>a</sup> $K_m$  (mM) and  $V_{max}$  ( $\mu\text{mol min}^{-1} \text{mg}^{-1}$ ) shown ( $\pm$  SE) from three independent experiments.  $k_{cat}$  is expressed in units of  $\text{s}^{-1}$  and  $k_{cat}/K_m$  in units of  $\text{mM}^{-1} \text{s}^{-1}$ .

**Table 2-8.** Apparent kinetic constants for *P. ubiquus* HTCC1062 and *R. pomeroyi* DSS-3 DmdBs for ATP and CoA in the presence of MMPA and butyrate<sup>a</sup>

	PU_DmdB1	RPO_DmdB1	RPO_DmdB2
MMPA/ATP			
$K_m^a$	0.03 ±0.01	0.01 ±0.005	0.03 ±0.01
$V_{max}^b$	24.4 ±4.3	18.9 ±4.2	7.6 ±2.3
MMPA/CoA			
$K_m$	0.58 ±0.02	0.01 ±0.007	0.02 ±0.01
$V_{max}$	46.1 ±5.8	18.4 ±3.4	15.4 ±2.5
Butyrate/ATP			
$K_m$	0.06 ±0.02	0.01 ±0.007	0.08 ±0.03
$V_{max}$	24.0 ±4.4	12.4 ±2.6	3.8 ±1.4
Butyrate/CoA			
$K_m$	0.11 ±0.03	0.14 ±0.05	0.02 ±0.01
$V_{max}$	52.2 ±3.5	8.5 ±2.7	3.6 ±0.7

<sup>a</sup>  $K_m$  (mM) and <sup>b</sup>  $V_{max}$  ( $\mu\text{mol min}^{-1} \text{mg}^{-1}$ ) shown plus SE values from three independent experiments.

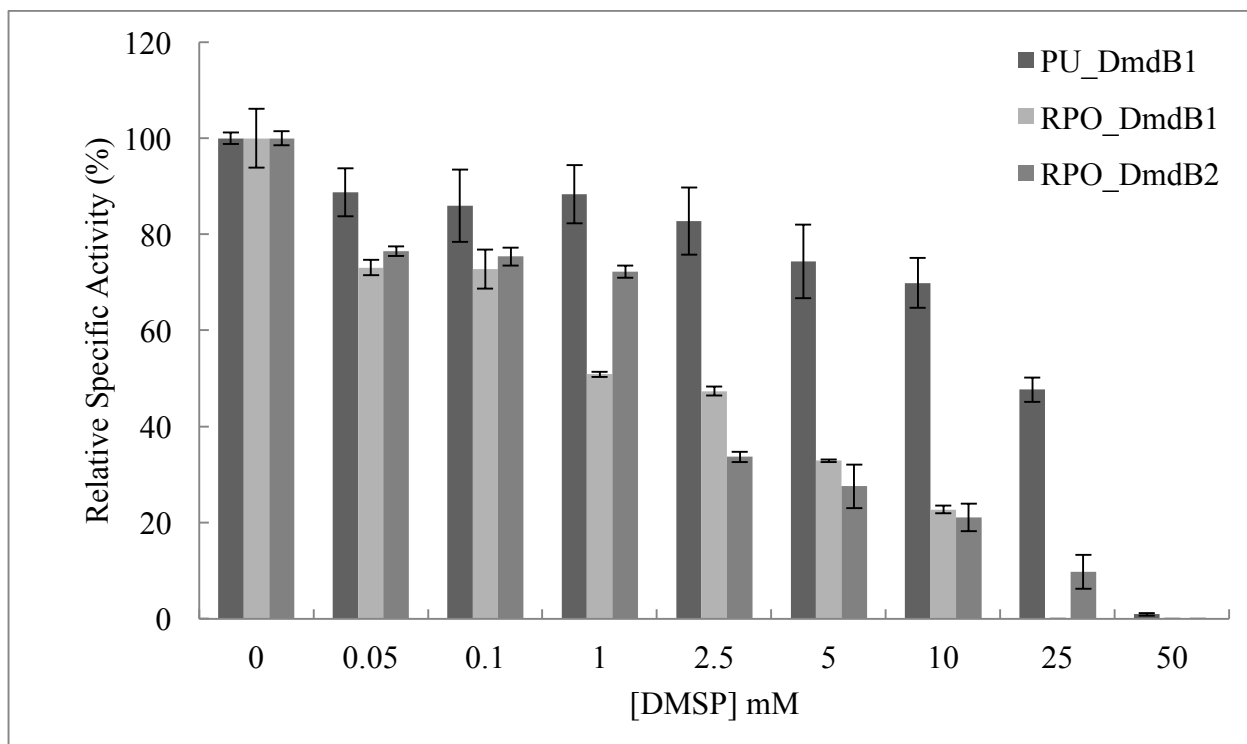


**Figure 2-5.** Inhibition of the MmpA-CoA ligases in the presence of DMSP for the DmdB isozymes from *P. ubique* HTCC1062 and *R. pomeroyi* DSS-3. Relative activity values expressed as a percentage of the total measured activity in the absence of DMSP (100%). Specific activities in units  $\text{mg}^{-1}$  of protein defined as 100% were: PU\_DmdB1:  $31 \pm 1$ ; RPO\_DmdB1:  $18 \pm 4$ ; RPO\_DmdB2:  $15 \pm 2$ . Errors are  $\pm$ SE of three replicates.

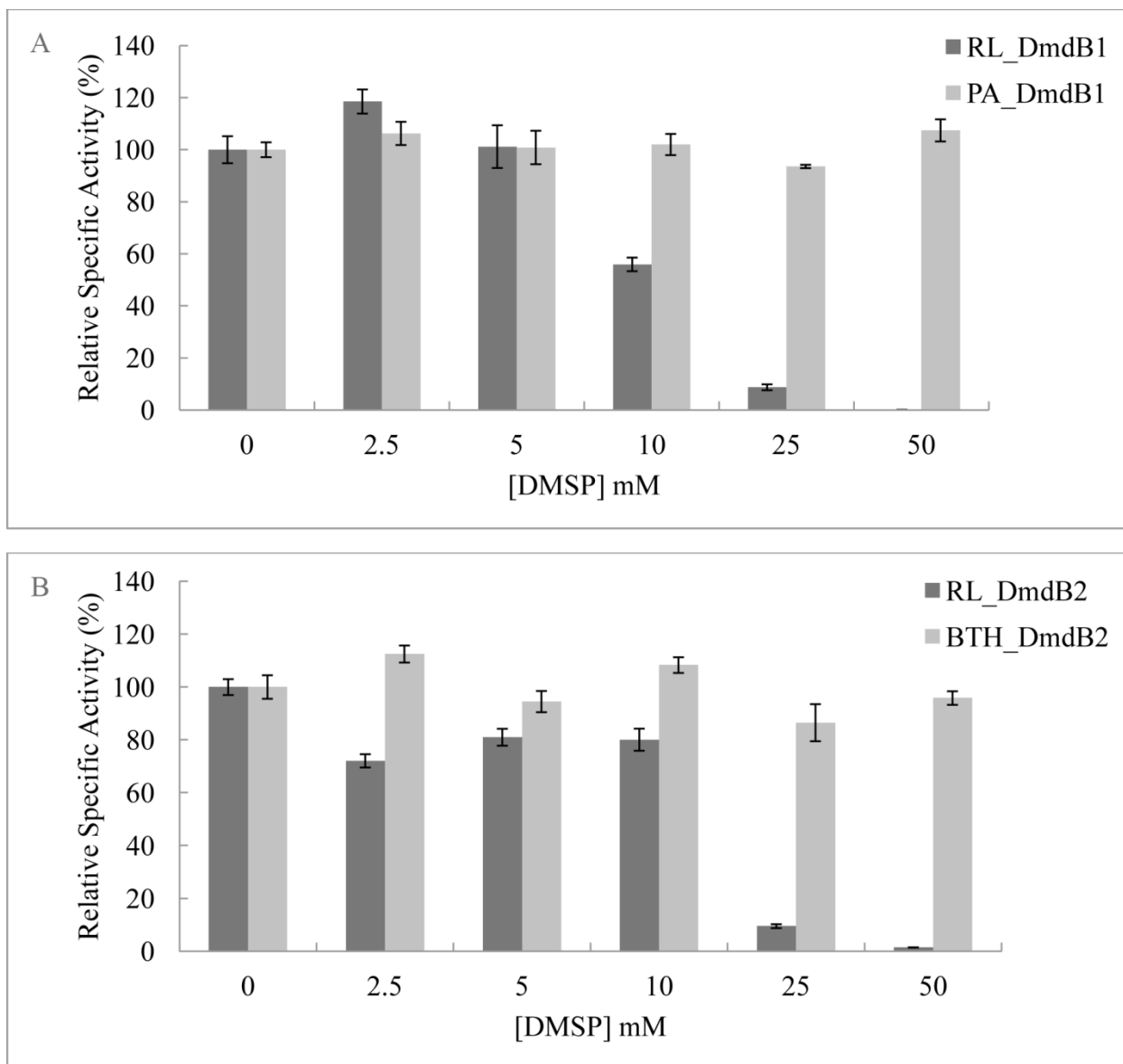


**Figure 2-6.** DMSP inhibition of members of each DmdB clade. A) Inhibition of DmdB activity of DmdB Clade 1 members RL\_DmdB1 and PA\_DmdB1. B) Inhibition of DmdB Clade 2 members RL\_DmdB2 and BTH\_DmdB2. Relative activity values expressed as a percentage of the total measured in the absence of DMSP (100%). Specific activities in units  $\text{mg}^{-1}$  of protein defined as 100% were: RL\_DmdB1:  $25 \pm 5$ ; PA\_DmdB1:  $35 \pm 2$ ; RL\_DmdB2:  $16 \pm 3$ ; and BTH\_DmdB2:  $24 \pm 4$ . Errors are  $\pm$ SE of three replicates.

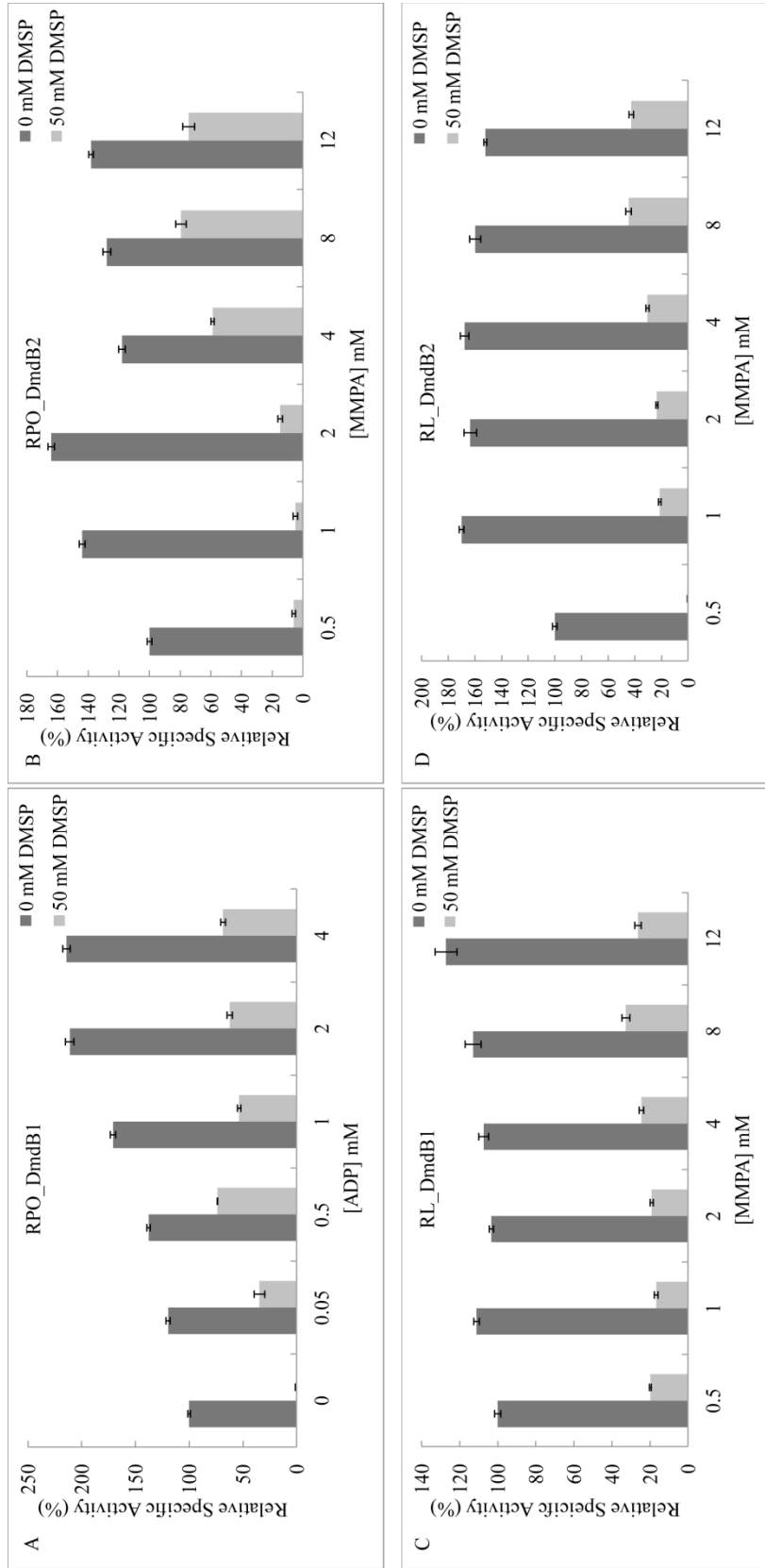


**Figure 2-7.** Protection of DmdB from DMSP inhibition by ADP and MMPA. Effect of ADP on RPO\_DmdB1 (A). Effect of MMPA on RPO\_DmdB2 (B), RL\_DmdB1 (C), and RL\_DmdB2(D). Relative activity expressed as a percentage of the total activity in the absence of DMSP. Specific activities in units  $\text{mg}^{-1}$  of protein defined as 100% were: RPO\_DmdB1:  $14 \pm 2$ ; RPO\_DmdB2:  $13 \pm 2$ ; RL\_DmdB1:  $18 \pm 3$ ; and RL\_DmdB2:  $10 \pm 3$ . Errors are  $\pm$ SE of three replicates.

**Table 2-9.** Expression of RPO\_ *dmdA*, RPO\_ *dmdB1*, and RPO\_ *dmdB2* during steady state growth on DMSP and other carbon sources<sup>a</sup>

	RPO_ <i>dmdA</i>	RPO_ <i>dmdB1</i>	RPO_ <i>dmdB2</i>
<b>DMSP</b>	33.5 <sup>a</sup>	6.3 <sup>a</sup>	19.5 <sup>a</sup>
<b>MMPA</b>	3.6 <sup>b</sup>	2.2 <sup>c</sup>	17.8 <sup>a</sup>
<b>Methionine</b>	2.6 <sup>b</sup>	4.5 <sup>ab</sup>	16.6 <sup>a</sup>
<b>Acetate</b>	4.1 <sup>b</sup>	2.7 <sup>bc</sup>	3.7 <sup>b</sup>

<sup>a</sup>Values within a column with the same superscript were not significantly different with a p value of < 0.05. P-values were calculated using a negative binominal distribution using the CuffDiff program (30). Expression based on Illumina RNAseq reads mapped to RPO\_ *dmdA*, RPO\_ *dmdB1*, and RPO\_ *dmdB2*. Given values are fragments per kilobase per million (FPKM), indicating reads/length of transcript in kb/total number of reads.

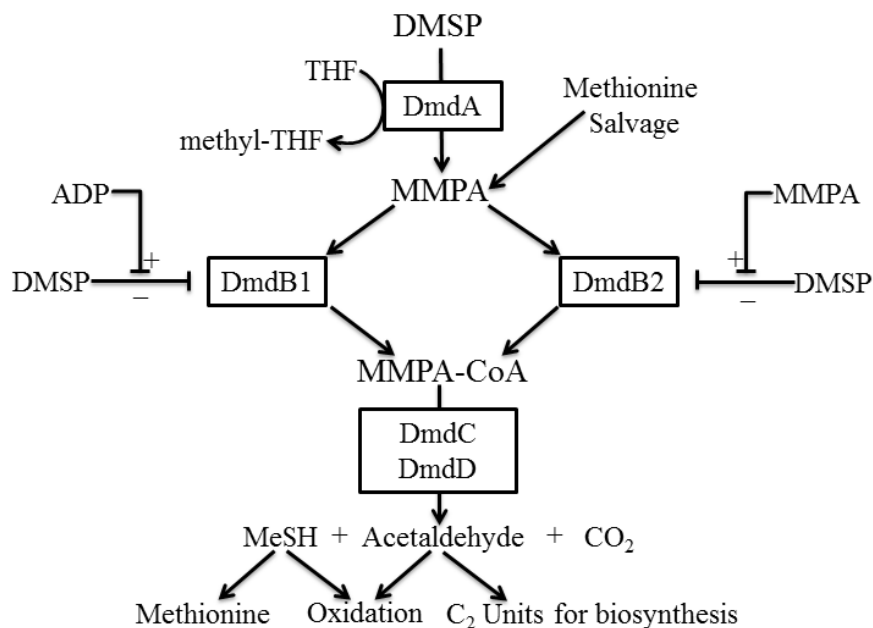


**Figure 2-8:** Model for the regulation of DmdB activity in *Ruegeria pomeroyi* DSS-3. During carbon and energy limitation, DmdB1 overcomes DMSP inhibition as ADP concentrations increase as a result of decreasing cellular energy charge. The resulting stimulation of the demethylation pathway increases the energy charge and lowers ADP concentrations until DMSP inhibition is restored. A different chain of events may explain the role of DmdB2. The levels of DmdA activity and MMPA are likely set by the availability of free THF. During rapid growth, methyl-THF is oxidized, yielding high intracellular levels of free THF and MMPA. The increased levels of MMPA reverse the DMSP inhibition of DmdB2 and leads to rapid production of acetaldehyde and MeSH. These additional energy sources spare the pools of methyl-THF, leading to a depletion of free THF and a decline in MMPA production. In addition, the oxidation of MeSH leads to H<sub>2</sub>O<sub>2</sub> production, resulting in oxidative stress and slowing DMSP-dependent growth. The slowdown in growth reduces the demand for methyl-THF, causing a depletion of free THF. Alternatively, both enzymes may be active during growth on methionine when MMPA is produced in the absence of DMSP.

## CHAPTER 3

ACUH FROM *RUEGERIA LACUSCAERULENSIS* IS A CROTONASE  
SUPERFAMILY ENZYME WITH ACTIVITY TOWARDS  
METHYLTHIOACRYLOYL-COA AND ACRYLOYL-COA<sup>2</sup>

---

<sup>2</sup>Bullock, H.A., Y. Zhu, C.R. Reisch, W.B. Whitman. To be submitted to *Journal of Bacteriology*.

## Abstract

Dimethylsulfoniopropionate (DMSP) produced by marine phytoplankton is an important source of reduced carbon and sulfur for marine bacteria, and the DMSP demethylation pathway is a major mechanism for its assimilation. The final reaction in this pathway is catalyzed by DmdD, a crotonase superfamily enzyme that converts methylthioacryloyl-CoA (MTA-CoA) to acetaldehyde, CO<sub>2</sub>, methanethiol (MeSH) and free CoA. *Ruegeria lacuscaerulensis* metabolizes DMSP, however an ortholog to *dmdD* is not present in its genome. A paralog of DmdD, RL\_AcuH, was isolated from *R. lacuscaerulensis* cell extract based on its activity toward MTA-CoA. Recombinant RL\_AcuH possessed activity with MTA-CoA and crotonyl-CoA, as well as high activity with acryloyl-CoA. Due to its activity with acryloyl-CoA, AcuH is predicted to function in both the demethylation and cleavage pathways in *R. lacuscaerulensis*. Subsequent tests revealed that RL\_AcuH required ADP as a cofactor to maintain the low  $K_m$  of 0.02 mM for MTA-CoA. RL\_acuH was able to complement a *Ruegeria pomeroyi dmdD* deletion in terms of growth and MeSH production. To further verify the MTA-CoA hydratase function of AcuH, orthologs of AcuH from *Dinoroseobacter shibae* DFL12, *Oceanibulbus indolifex* HEL45, *Pseudomonas putida* KT2440, *Burkholderia thailandensis* E264, and *Bacillus subtilis* 168 were analyzed. All had substantial activity towards crotonyl-CoA and all except the *B. subtilis* AcuH had activity towards MTA-CoA. However, the catalytic efficiency exhibited for MTA-CoA hydration was low, indicating this is likely a secondary function. These data indicate that while AcuH is an MTA-CoA hydratase in *R. lacuscaerulensis*, this activity is not uniform across all microorganisms possessing AcuH-like enzymes.

## Introduction

Dimethylsulfoniopropionate (DMSP) is a globally important compound which impacts not only marine biogeochemistry but global sulfur and carbon cycles as well. The high abundance of DMSP in marine environments is due largely to its production by marine phytoplankton and algae for use as an osmolyte, antioxidant, and predator deterrent (1-3). Once released into the ocean, DMSP serves as an important source for reduced carbon and sulfur source for marine microorganisms (4-6). Marine bacteria catabolize DMSP via two competing pathways, the cleavage or the demethylation pathway. The cleavage pathway yields the climatically active gas dimethyl sulfide (DMS) and acrylate. The release of DMS into the atmosphere, where it is oxidized, aids in the formation of cloud condensation nuclei (1, 7-9). The demethylation pathway comprises four consecutive enzymatic reactions to degrade DMSP, the genes of which have been elucidated in the marine roseobacter *Ruegeria pomeroyi* DSS-3 (10). First, DMSP is demethylated by the tetrahydrofolate (THF)-dependent enzyme DmdA, producing 5-methyl-THF and methylmercaptopropionate (MMPA). MMPA is then transformed to MMPA-CoA and subsequently oxidized to methylthioacryloyl-CoA (MTA-CoA) by the MMPA-CoA ligase (DmdB) and MMPA-CoA dehydrogenase (DmdC), respectively. The enoyl-CoA hydratase DmdD catalyzes the final reaction with MTA-CoA to release methanethiol (MeSH), free CoA, CO<sub>2</sub> and acetaldehyde (10, 11).

The demethylation pathway is proposed to explain the majority of DMSP metabolism in marine environments and represents an important pathway for reduced carbon and sulfur acquisition by marine bacteria (10). This conclusion is supported by the wide distribution of homologs of *dmdA*, *dmdB* and *dmdC* in marine bacteria. For instance, assuming no more than one copy of the genes per cell, analyses of the frequency of the *dmdA*, *dmdB* and *dmdC*-like

genes in the 2007 Global Ocean Survey (GOS) metagenomic database indicated that *dmdA* is present in ~27% of marine bacterioplankton, while *dmdB* and *dmdC* are present in ~60% of bacterioplankton, (10, 12, 13). In contrast, homologs of the *R. pomeroyi dmdD* gene are present in only about 1% of marine bacteria, signifying a gap in understanding of the demethylation pathway (10, 13).

To address this gap, the *dmdD*-negative bacterium *Ruegeria lacuscaerulensis* was examined. It metabolizes DMSP via the demethylation pathway, and MTA-CoA hydratase activity was readily detected in cell extracts (10). These results implied that a non-orthologous protein possessing MTA-CoA hydratase activity was present. In this study, the enzyme catalyzing this activity was identified as acryloyl-CoA hydratase or AcuH. Its role in the DMSP demethylation pathway in *R. lacuscaerulensis* and other marine bacteria was examined.

## Methods and Materials

**Strains and Culture Conditions.** *R. lacuscaerulensis* ITI-1157, *R. pomeroyi* DSS-3, *Dinoroseobacter shibae* DFL12, and *Oceanibulbus indolifex* HEL45 were grown on ½ YTSS or in defined marine basal media (MBM) at 30 °C (14, 15). *Pseudomonas putida* KT2440, *Burkholderia thailandensis* E264 and *Bacillus subtilis* 168 were grown on Luria Bertani (LB) or defined M9 salts minimal media at 30°C or 37°C. Recombinant strains of *Escherichia coli* BL21 (DE3) were grown on LB. When minimal medium was used, 6 mM acetate, 3 mM glucose, 3 mM DMSP, or 3 mM MMPA (Alfa Aesar) was added as a sole carbon source. For growth and gas production experiments, cultures were started with 10<sup>6</sup> cells and incubated at 30 °C. Absorbance was measured at 600 nm in a Thermo Scientific Genesys 20 spectrophotometer.

**Plasmid Construction and Expression of Recombinant Proteins.** Nucleotide sequences of genes encoding the AcuH MTA-CoA hydratase from *R. lacuscaerulensis* (RL\_AcuH; EEX08788) (16, 17), *R. pomeroyi* (RPO\_AcuH; AAV93475) (15), *D. shibae* (DS\_AcuH; ABV95103) (18, 19), *O. indolifex* (OI\_AcuH; WP\_007118329) (20), *B. thailandensis* (BTH\_AcuH; AIP28389) (21), *P. putida* (PP\_AcuH; AAK18173) (22), and *B. subtilis* (BS\_AcuH; WP\_003231526) (23) were amplified using PCR from genomic DNA, digested and inserted between the BamHI and HindIII restriction sites on the pTrcHisA vector (Invitrogen). DNA sequences of the cloning site were verified by restriction digest and sequencing with the pTrcHisA forward primer (Applied Biosystems). All of the recombinant protein sequences included a 6× his-tag and an EK cleavage site at the N-terminal. The *R. pomeroyi dmdD* gene was cloned into the pET101 vector from Invitrogen as part of a previous study (10). The plasmids were transformed into *E. coli* BL21 (DE3), and the cells were grown in LB broth at 37°C until cultures reached an optical density at 600 nm of 0.4. The cultures were then induced with 0.4 mM isopropyl β-D-1-thiogalactopyranoside (IPTG). After additional growth for six hours at 30°C, cell pellets were collected by centrifugation at 10,000 ×g, 4°C for 10 min and stored at -20 °C for future use.

**Purification of Native and Recombinant MTA-CoA hydratase.** For the purification of recombinant AcuH from *R. lacuscaerulensis* (RL\_AcuH) and *R. pomeroyi* (RL\_AcuH), frozen *E. coli* cells were suspended in 200 mM sodium HEPES buffer (pH 7.5) with 1 g/L lysozyme (Sigma) and incubated at 30°C for one hour with vigorous shaking. Lysed cells were centrifuged at 30,000 ×g, 4°C for 30 min to remove cell debris from supernatant. Supernatant was applied onto a 1-ml HisTrap HP column (GE Healthcare) equilibrated with Buffer A consisting of 20 mM sodium phosphate (pH 7.4) and 20 mM imidazole (Sigma). Proteins were eluted by washing

the column using a gradient of 20 column volumes from 0-100% Buffer B consisting of 20 mM sodium phosphate (pH 7.4) and 500 mM imidazole. In all cases, the desired protein eluted with 350-450 mM imidazole. The activity of each fraction was determined by DmdD assay with MTA-CoA as substrate (described below) (10). Active fractions were pooled and exchanged into 20 mM Tris-HCl (pH 8.5) containing 200 mM NaCl, 5 mM dithiothreitol (DTT), 1 mM disodium EDTA and 5% (vol/vol) glycerol with Amicon Ultra-15 Centrifugal Filter 3,000 NMWL (Millipore). The N-terminal recombinant sequences of AcuH were cleaved by enterokinase (NEB) according to the manufacturer's protocol. Cleaved AcuH was applied to Sephacryl S200 HR column equilibrated with 200 mM sodium HEPES buffer (pH 7.5) containing 150 mM NaCl at a flow rate of 0.75 ml min<sup>-1</sup> for purification and determination of native molecular mass. The concentrations of purified recombinant enzymes were determined using Nanodrop 1000 (Thermo) at 280 nm, with predicted extinction coefficients of 11,710 M<sup>-1</sup> cm<sup>-1</sup> for RL\_AcuH and 14,690 M<sup>-1</sup> cm<sup>-1</sup> for RPO\_AcuH before storage in aliquots at -20 °C.

His-tagged recombinant putative AcuHs from *D.shibae* (DS\_AcuH), *O. indolifex* (OI\_AcuH), *P. putida* (PP\_AcuH), *B. thailandensis* (BTH\_AcuH), and *B. subtilis* (BS\_AcuH) were purified in a similar manner with a few alterations. Recombinant *E. coli* were suspended in 200 mM sodium HEPES (pH 7.5) and sonicated. Lysed cells were centrifuged at 10,000 ×g, 4 °C for 10 minutes. The supernatants were applied to a 1 ml HisTrap HP column (GE Healthcare) and were resolved as described above. The pTrcHisA vector harboring an unrelated protein, *Pseudomonas aeruginosa* PA\_1833 oxiooreductase, was treated with the same purification protocol for use as a control to assess background crotonyl-CoA activity. The desired proteins eluted with 350-450 mM imidazole. Pooled active fractions were concentrated as described above, brought to 2 mL with 20 mM Tris-HCl (pH 8.5) containing 200 mM NaCl, 5 mM

dithiothreitol (DTT), 1 mM disodium EDTA and 5% (vol/vol) glycerol and stored at -20 °C. The N-terminal recombinant sequences of the AcuHs were not removed.

**Substrate Synthesis.** Methylthioacryloyl-CoA (MTA-CoA) was synthesized enzymatically using *E. coli* BL21 (DE3) cell extracts containing overexpressed SAR11\_0248 (DmdB) and SAR11\_0249 (DmdC) (10). Protein expression and soluble cell extract preparation were performed with the same conditions as described above. MMPA-CoA was first synthesized by DmdB in a reaction containing 200 mM sodium HEPES (pH 7.5), 2 mM MMPA, 2 mM ATP, 2 mM MgCl<sub>2</sub>, 2 mM CoA, and 3 ml soluble cell extract containing recombinant SAR11\_0248 (DmdB) protein prepared from 50 ml of cell culture. The enzymatic assay was incubated at room temperature for 10 min. Product formation was confirmed by HPLC analysis using a 4.6×150 mm, 3 μm particle size, Hypersil Gold column (Thermo-Fisher) developed with a linear gradient of 2–20% acetonitrile in 50 mM ammonium acetate (pH 6) over 10 minutes. MTA-CoA was synthesized by addition of 0.5 mM phenazine methosulfate (PMS) and 3 ml soluble cell extract containing recombinant SAR11\_0249 (DmdC) protein prepared from 50 ml of cell culture to the DmdB reaction. The DmdC reaction was incubated at room temperature for one hour. Formation of MTA-CoA was confirmed by HPLC with the same conditions described above. Synthesized MTA-CoA was purified by reverse phase chromatography (RP-HPLC) using an Ultrasphere ODS preparative column (10×250 mm). The column was equilibrated with 50 mM ammonium acetate (pH 6), containing 2% (vol/vol) acetonitrile and developed by a linear gradient from 2-20% acetonitrile in the same buffer. Elution of MTA-CoA was detected at 254 nm. Fractions containing MTA-CoA were lyophilized and resuspended in nanopure H<sub>2</sub>O. Acryloyl-CoA was synthesized chemically by mixing CoA and acryloyl chloride (Sigma) in 0.2 M KHCO<sub>3</sub>, adjusting the pH to approximately 3 with 1.0 M K<sub>2</sub>CO<sub>3</sub>, and finally adding KCl to 1 M.

Purification of acryloyl-CoA was performed as described above by RP-HPLC, except the column was developed with a gradient of 2–20% acetonitrile in 50 mM sodium phosphate buffer (pH 7.4). Acryloyl-CoA was found to be unstable even upon storage at -20 C and was used within five days.

MTA-CoA and acryloyl-CoA were quantified from the absorbance at 260 nm, assuming the same molar extinction coefficient as for enoyl-CoA with an  $\epsilon_{260} = 22,000 \text{ M}^{-1} \text{ cm}^{-1}$  (24). The purity was analyzed by RP-HPLC with a Hypersil Gold column as described above. DMSP was synthesized as described by Chambers *et al.* 1987 (25). Other reagents were analytical grade or better.

**Enzyme Assays and Kinetic Analyses.** A concentration of 200 mM of the following buffers was used to determine the pH optima for RL\_AcuH and RPO\_AcuH: sodium HEPES (6.5, 7.0, and 7.5), 3-(N-morpholino)propanesulfonic acid (MOPS) (6.5, 7.0, and 7.5), N-Cyclohexyl-2-aminoethanesulfonic acid (CHES) (8.5, 9.0, 9.5, 10.0, and 10.5) and Tris-HCl (7.5, 8.0, 8.5, and 9.0). Activity was determined with 0.5 mM MTA-CoA.

Kinetic analyses to determine substrate specificity of purified RL\_AcuH and RPO\_AcuH were performed in 200 mM sodium HEPES (pH 7.5) with MTA-CoA concentrations ranging from 0.1 mM to 1.25 mM. For each assay, 0.5 or 5  $\mu\text{g}$  of RL\_AcuH or RPO\_AcuH was added, respectively. Assays were incubated at room temperature for 30s, then quenched by addition of 4  $\mu\text{l}$  10%  $\text{H}_3\text{PO}_4$ . Assays with crotonyl-CoA were performed with similar conditions, except that 2.5 ng of RL\_AcuH or RPO\_AcuH was added to the reactions. Acryloyl-CoA assays were performed with substrate concentrations ranging from 5 nM to 20 nM and 2.5 ng of RL\_AcuH or RPO\_AcuH in each reaction. The reaction rates of assays with MTA-, crotonyl- and acryloyl-CoA were calculated based on the formation of reaction products, CoA, 3-hydroxybutyryl-CoA

and 3-hydroxypropionyl-CoA, respectively. Assays to determine the effect of buffers on enzyme kinetics were performed in 200 mM of sodium HEPES (pH 7.5), Tris-HCl (pH 8.0 and 9.0) with MTA-CoA concentrations ranging from 0.1 mM to 0.75 mM under conditions described above.

Kinetic analyses to determine the substrate specificity of RL\_AcuH from *R. lacuscaerulensis* or *E. coli* crude cell extracts were performed with MTA-CoA as described above. Briefly, *R. lacuscaerulensis* cultures were grown in MBM containing 3 mM MMPA and harvested at an absorbance of 0.2. Cultures of *E. coli* BL21 (DE3) expressing RL\_AcuH were grown in LB, induced and harvested in conditions described above. Harvested cells were washed three times with 20 mM Tris-HCl (pH 8.5) and lysed by sonication. Supernatants were collected by centrifugation at 30,000  $\times g$ , 4°C for 30 min. Protein concentrations of the cell extracts were determined using Nanodrop1000 (Thermo) with the general reference setting based on a 1 mg/ml protein solution producing an absorbance at 280 nm of 1.0 A.

Assays to determine the substrate specificity for the AcuHs from *D. shibae*, *O. indolifex*, *P. putida*, *B. thailandensis*, and *B. subtilis* for MTA-CoA and crotonyl-CoA were performed in 200 mM sodium HEPES (pH 7.5) with MTA-CoA concentrations ranging from 0.5 mM to 10 mM and crotonyl-CoA concentrations of 0.1 mM to 2 mM. MTA-CoA hydratase assays contained 0.5  $\mu g$  of protein and were incubated for up to five minutes at room temperature prior to quenching by the addition of 4  $\mu l$  10% H<sub>3</sub>PO<sub>4</sub>. Crotonyl-CoA assays contained between 0.0125  $\mu g$  and 0.05  $\mu g$  protein and were incubated for 30s before being quenched. Reaction rates were determined comparing both the consumption of the reactant, MTA-CoA or crotonyl-CoA, and the formation of the reaction products, free CoA or 3-hydroxybutyryl-CoA. The pTrcHisA vector harboring the *P. aeruginosa* PA\_1833 oxio-reductase was subject to the same analysis described here to determine if any background activity with crotonyl-CoA would bias the kinetic

analyses. There was no background activity with MTA-CoA. The background activity towards crotonyl-CoA was  $6 \mu\text{mol min}^{-1} \text{mg}^{-1}$  of protein, less than 0.75% of the activity shown by the putative AcuHs and, thus, too low to interfere with the kinetic calculations.

All kinetic assays were performed in triplicate. Standard curves of CoA sodium salt (Sigma), 3-hydroxybutryl-CoA, crotonyl-CoA and MTA-CoA were obtained by suspending the necessary range of concentrations of compounds in nanopure H<sub>2</sub>O. All assays were run using a Hypersil Gold C18 column (3 $\mu\text{m}$  particle size, 4.6 x 150 mm, Fisher Scientific). The column was equilibrated with 50 mM ammonium acetate (pH 6), containing 2% (vol/vol) acetonitrile and developed by a linear gradient from 2-20% acetonitrile in the same buffer. Kinetic data were analyzed using SigmaPlot 12.0 with the Enzyme Kinetics module (Systat Software Inc.).

**Dialysis.** AcuH proteins were dialyzed using MWCO 12-14,000 Da Spectra/Por 4 membrane tubing with a flat width of 32 mm (Spectrum Laboratories, Inc.). Three milliliters of cell extract was dialyzed against 300 mL of 50 mM sodium phosphate (pH 7.5). The 50 mM sodium phosphate buffer was exchanged three times, once after two and a half hours, a second time after five hours, and a third time after 10 hours. Samples were left over night after the third buffer exchange. Experiments to identify potential AcuH cofactors contained additions of 2 mM ADP, ATP, AMP, NAD or NADH to the 50 mM sodium phosphate buffer. Once dialyzed in the presence of potential cofactors, kinetic constants were determined for the AcuH samples as previously described.

**SDS-PAGE.** Sodium dodecyl sulfate-polyacrylamide gel electrophoresis (SDS-PAGE) was accomplished using Mini-PROTEAN TGX Precast Gels (Bio-Rad) 4-15% polyacrylamide gradient mini-gels. Gels were stained using Coomassie Blue R-250 (Bio-Rad).

**Complementation of *R. pomeroiyi* DSS-3  $\Delta dmdD$  mutant strain.** The *RL\_acuH*, *DS\_acuH*, *OI\_acuH*, *BTH\_acuH*, and *PP\_acuH* genes were amplified by PCR from their respective genomic DNAs. The amplicons were digested using the NdeI and XbaI restriction enzymes (New England Biolabs) and inserted between these sites in the pSRKKm vector. The constructs were then methylated by CpG methyltransferase per manufacturer instructions (New England Biolabs) and introduced into the *R. pomeroiyi dmdD*<sup>-</sup> (*SPO3805::tet*) strain via electroporation (26). Uptake of the complementation plasmid was verified by growth on ½ YTSS medium containing 80 µg/ml kanamycin.

**Gas Chromatography.** MeSH and DMS production were measured by gas chromatography using a SRI 8610-C gas chromatograph fitted with a Chromasil 330 column (Supleco), using N<sub>2</sub> as a carrier gas at a flow rate of 60 ml min<sup>-1</sup> and an oven temperature of 60°C. Measurements were made using a flame photometric detector and the Peak Simple software (SRI Instruments). MeSH standard curves were produced by flowing N<sub>2</sub> through a permeation tube containing methyl mercaptan (VICI, Valco Instruments) at a flow rate of 0.1 ml/min. After a 24 hr equilibration period, 1 ml of MeSH was removed and diluted into a sealed 250 ml serum bottle from which 1 ml of air had been removed. This procedure was repeated with 160 ml, 60, ml and 10 ml serum bottles. DMS standards were produced by making six 1:10 serial dilutions of a 6 mM liquid stock solution of DMSP in separate 10 ml serum bottles. Serum bottles were sealed and then injected with 1 ml of 5M NaOH to hydrolyze the DMSP to DMS. Bottles were incubated with shaking for one hr at 30°C before analysis. For both MeSH and DMS standards, 1 ml of gas was injected onto the GC using gas tight 1 ml syringes (Henke-Sass, Wolf).

MeSH and DMS production were assessed using cultures grown on MBM or M9 minimal media in 160 ml serum bottles (Wheaton). When growth measurements were required as well, cultures were grown in 160ml serum bottles fitted with 20 ml culture tubes as side arms. One milliliter of headspace was injected onto the GC for analysis.

**Phylogenetic analyses for gene tree.** Initially, the amino acid sequences of RPO\_AcuH (SPO0147/SPO\_RS00755) and RPO\_DmdD (SPO3805/ SPO\_RS19305) from *R. pomeroyi* were used as query sequences for BLASTp searches against the genome sequence of *R. lacuscaerulensis* ITI-1157 for a potential DmdD or AcuH. Once identified, RL\_AcuH (SL1157\_0807) from *R. lacuscaerulensis* was used as a protein query sequence against the refseq\_protein database in NCBI. This yielded 10,000 hits with an expected value  $< e^{-40}$ . All sequences with an expected value  $> e^{-70}$  were discarded before further analysis. To construct the amino acid sequence-based phylogenetic tree, representatives were selected using the range\_fasta\_parse.R script using the following command:

```
./range_fasta_parse.R seqdump_RL0807_DmdD.fasta
```

```
Highlighted_and_annotated_hit_table_RL0807_DmdD_10000_11-12-15.csv 75 60 60 45 45 30
```

10. This command took 10 random samples from percent identity hits from 75 to 60, 60 to 45, and 45 to 30 and was used to ensure unbiased sampling of sequences for alignment and phylogenetic tree construction. Sequences with greater than 75 percent identity were automatically retained for further analysis. DmdD representatives were selected using RPO\_DmdD as a query sequence for BLASTp searches. MEGA 6.06 was used to align the sequences via the MUSCLE algorithm and then for the construction of phylogenetic trees using the Maximum Likelihood method (27).

**Phylogenetic analyses for species tree.** NCBI taxonomic IDs were used to create a species level tree of the organisms represented in the gene tree. The newick tree file was generated using the phyloT phylogenetic tree generator. The presence of the other demethylation pathway proteins (DmdA: SPO1913/SPO\_RS09710; DmdB1, SPO0677/SPO\_RS03420; DmdB2, SPO2045/SPO\_RS10375; DmdC1, SPO3804/SPO\_RS19300; DmdC2, SPO0298/SPO\_RS01515; DmdC3, SPO2915/SPO\_RS14785; DmdD, SPO3805/SPO\_RS19305) was assessed using the *R. pomeroyi* amino acid sequences for these proteins as query sequences. These sequences were serially run through BLASTp against the genome of each represented organism. Hits with e-values of  $< e^{-70}$  were retained. This e-value cut off was chosen to avoid the appearance of false-positives. The species tree was constructed and annotated to contain the demethylation pathway proteins using the iTOL (Interactive Tree of Life) and the Binary dataset template (28).

## Results

### **Identification of MTA-CoA hydratase activity in *R. lacuscaerulensis*.** *R.*

*lacuscaerulensis* grows on DMSP and MMPA, and its genome possesses homologs to all of the genes of the demethylation pathway except *dmdD*. (10, 11). Because extracts of MMPA-grown cells possess abundant MTA-CoA hydratase activity, this activity is likely encoded by a non-orthologous gene (10). To identify this gene the MTA-CoA hydratase activity was purified from cell extracts of MMPA-grown *R. lacuscaerulensis*. At the final step of the purification, fractions with high enzymatic activity were dominated by three proteins. In-gel trypsin digestion and LC-MS identified one of the proteins as SL1157\_0807 (Figure 3-1). SL1157\_0807, referred to subsequently as RL\_AcuH, was annotated as an enoyl-CoA hydratase (ECH) and belonged to the

same ECH enzyme family as DmdD from *R. pomeroyi*, hereafter referred to as RPO\_DmdD. The high similarity to DmdD suggested that it was the source of MTA-CoA hydratase activity. Alignment of the predicted RL\_AcuH amino acid sequence with that of the RPO\_DmdD suggested that 50 amino acids were missing from the N-terminus of RL\_AcuH (Figure 3-2). Examination of the genome sequence of *R. lacuscaerulensis* suggested that a sequencing error wrongly predicted a translation start codon that divided the gene into two adjacent ORFs, SL1157\_0808 and SL1157\_0807. For confirmation, this region of the genomic DNA was PCR amplified and re-sequenced. Upon correction of the genome sequence, this region of the genome was found to encode a single ORF of 258-amino acid residues, with 29% identity and 46% similarity to the amino acid sequence of RPO\_DmdD. In addition, the *R. pomeroyi* genome possessed an ortholog, SPO0147 (SPO\_RS00755), to RL\_AcuH (Figures 3-2, 3-3). This enzyme, hereafter referred to as RPO\_AcuH, had previously been shown to possess high acryloyl-CoA hydratase activity and was predicted to play an important role in the metabolism of acrylate formed from the DMSP cleavage pathway (9). For that reason, these proteins are named here as AcuH for acrylate utalization hydration similar to the acryloyl-CoA reductase AcuI (29, 30).

**Orthologs of AcuH Are Present in Phylogenetically Diverse Organisms.** If the MTA-CoA hydratase activity of AcuH was physiologically important, it would be expected to be widely distributed in bacteria that possess the DMSP demethylation pathway. Orthologs of RL\_AcuH are widely distributed in the Alphaproteobacteria and other prokaryotes (Figure 3-3). They are closely related to the mitochondrial ECHs from the fatty acid  $\beta$ -oxidation pathway (31, 32), PaaFs of the bacterial phenylacetate catabolic pathway (33, 34) as well as some ECHs of unknown function. In addition, *R. lacuscaerulensis* possesses 9 additional paralogous enoyl-CoA

hydratases, which appear as deep branches in this tree (Figure 3-3). DmdA is an indicator of the DMSP demethylation pathway (12, 35, 36), and all of the genomes that encoded DmdA also encoded at least one of the two isozymes for DmdB and one or more of the three isozymes for DmdC (Figure 3-4). Except for *Peligibacter* spp. and *Puniceispirillum* spp., all of the bacterial genomes that encoded DmdA also encoded AcuH. Some also encoded DmdD. A few bacteria that lacked DmdA possessed the other enzymes of the demethylation pathway including AcuH. Presumably, these bacteria are able to metabolize MMPA but not DMSP (37-40). These results were consistent with a physiologically significant role for AcuH in the MTA-CoA hydratase step during DMSP demethylation. However, orthologs of AcuH were also widely distributed in organisms that lacked DmdA and the other enzymes of the demethylation pathway (Figure 3-4). This result suggested that AcuH has additional important physiological functions, especially outside the Alphaproteobacteria. However, even within the Alphaproteobacteria, some marine bacteria that lacked all the other enzymes of the demethylation pathway, such as *Pseudophaeobacter arcticus*, possessed an AcuH ortholog. For that reason, it seemed likely that even within the Alphaproteobacteria, the AcuH orthologs possessed important functions unrelated to the DMSP demethylation pathway.

**Substrate Specificity of AcuH with MTA-CoA and Other CoA Thioesters.** To examine the activities of AcuH, recombinant RL\_AcuH and RPO\_AcuH were expressed in *E. coli* and purified to electrophoretic homogeneity in a single step using a nickel-affinity column. The 31-amino acid N-terminal his-tags of the recombinant proteins were then cleaved off with enterokinase. SDS-PAGE of the denatured proteins showed subunit molecular weights of ~ 27 kDa, consistent with the predicted molecular weight of 28.6 kDa for both proteins (Figure 3-5). Upon gel filtration, the native molecular masses of the enterokinase-treated proteins were ~160

kDa, suggesting that the native enzymes were hexamers (data not shown). Enzymatic activity of the his-tagged proteins was compared with that of the enterokinase-treated proteins, and no significant differences in specific activity or  $K_m$ s were detected using either MTA-CoA or crotonyl-CoA as substrate (data not shown).

ECHs are known to act upon CoA thioesters including crotonyl-CoA and acryloyl-CoA (31). Therefore, the kinetics of RL\_AcuH and RPO\_AcuH were investigated using MTA-CoA, crotonyl-CoA and acryloyl-CoA as substrates in sodium HEPES buffer under the standard conditions for the DmdD assay (10). The kinetics of both enzymes for crotonyl-CoA and acryloyl-CoA were similar, as expected given their high sequence similarity. Moreover, the catalytic efficiency for acryloyl-CoA was three orders of magnitude greater than that of crotonyl-CoA, suggesting that acryloyl-CoA was the major physiological substrate. Although the  $K_m$ s of both AcuH enzymes for MTA-CoA were similar, the turnover number and catalytic efficiency of RL\_AcuH were 60 and 90 times higher, respectively, than that of RPO\_AcuH (Table 3-1). The low activity of RPO\_AcuH was consistent with previous experimental results. Not only was RPO\_DmdD the only MTA-CoA hydratase activity detected during the purification from *R. pomeroyi* cell extracts, but mutants with deletions of RPO\_dmdD failed to grow on MMPA (10). Based on these data, it was evident that RPO\_AcuH did not play a major role in the *R. pomeroyi* demethylation pathway. Although the  $k_{cat}$  of RL\_AcuH for MTA-CoA hydratase activity was comparable to that of RPO\_DmdD, the  $K_m$  for MTA-CoA was over 100 times higher and much higher than expected for a physiological role in the demethylation pathway. As a consequence, the catalytic efficiency of RL\_AcuH was also 500 times lower than that of RPO\_DmdD (Table 3-1).

It remained possible that the kinetic values determined *in vitro* might not be representative of the *in vivo* activity. To determine if the catalytic properties were greatly affected by the assay conditions, the kinetic properties were determined in various buffers at different pHs. These assays were all performed at room temperature. RL\_AcuH showed maximal activity at pH 9.0 in Tris-HCl buffer (data not shown). The  $K_m$ s for MTA-CoA in sodium HEPES (pH 7.5) and Tris-HCl (pH 8.0 and 9.0) buffers were 1.1, 0.4, and 0.4 mM, respectively. In the Tris-HCl buffers,  $V_{max}$ s were 19 and 37  $\mu\text{mol min}^{-1}\text{mg}^{-1}$  at pH 8.0 and 9.0, respectively. Although somewhat more favorable than the kinetic constants determined under standard conditions, the purified AcuH still possessed very low MTA-CoA catalytic efficiencies.

**ADP Alters RL\_AcuH Kinetics with MTA-CoA.** The kinetics of MTA-CoA hydratase activity were examined in *R. lacuscaerulensis* cell extracts to determine if this activity from RL\_AcuH was altered during the purification. The  $K_m$  of the MTA-CoA in *R. lacuscaerulensis* cell extracts was comparable to that of RPO\_DmdD. Similarly, the  $K_m$  of the recombinant RL\_AcuH in cell extracts of *E. coli* was also lower, about 0.02 mM (Table 3-2). These results suggested that the properties of the AcuH changed during purification. To determine if cofactors present in the cell extract affected RL\_AcuH activity, the *E. coli* extract was dialyzed against sodium phosphate buffer to remove potential cofactors, and the  $K_m$  for MTA-CoA increased from 0.02 mM to 0.31 mM (Table 3-2). There was also a two-fold increase in  $V_{max}$ , consistent with the removal of weak inhibitors common in extracts. To identify the cofactors affecting MTA-CoA hydratase activity, the recombinant RL\_AcuH extract was dialyzed against buffers containing common coenzymes: ATP, ADP, AMP,  $\text{NAD}^+$  or NADH. The largest effect was observed following dialysis in the presence of ADP; the  $K_m$  remained similar to that of the undialyzed extract while the  $V_{max}$  increased to the same level observed following dialysis without

coenzymes. In contrast, the  $K_m$  increased 5 to 50-fold in the presence of the other coenzymes (Table 3-2). Interestingly, the  $V_{max}$  also increased 5-fold following dialysis with  $\text{NAD}^+$ .

These results suggested that ADP and possibly  $\text{NAD}^+$  were effectors required for RL\_AcuH to efficiently catalyze reactions with MTA-CoA at physiologically significant concentrations, functioning either as cofactors during the assay or stabilizing a low  $K_m$  form of the enzyme. Because purification of the recombinant enzyme in the presence of ADP failed to yield enzyme with a low  $K_m$  (data not shown), activities in cell extracts was examined further. Following dialysis in either the presence or absence of 0.5 mM ADP, the addition of ADP to the assay increased the  $V_{max}$  to 4-5  $\mu\text{mol}^{-1} \text{min}^{-1} \text{mg}^{-1}$  of protein, or 15-fold higher than the highest activity seen without ADP (Table 3-3). However, a low  $K_m$  was only observed in the absence of ADP in the assay, suggesting that ADP might also be a competitive inhibitor due to its structural similarity to the CoA moiety of MTA-CoA. Experiments are underway to resolve this issue.

***R. lacuscaerulensis* MTA-CoA Hydratase Activity is Regulated During Growth with DMSP and MMPA.** If the MTA-CoA hydratase activity in cell extracts was physiologically significant, it might increase during growth on DMSP and MMPA. Thus, the MTA-CoA hydratase activity in cell extracts was determined in cultures grown in MBM containing either glucose or MMPA as the sole carbon source. Cultures were grown in glucose to exponential phase before being washed and transferred to media containing either glucose or MMPA for continuous growth overnight. MTA-CoA hydratase activity in glucose medium showed a similar amount of activity at different time points, 2.5  $\text{nmol min}^{-1} \text{mg}^{-1}$ . The activity detected from cultures grown on MMPA, however, was more than 10-fold higher than that of glucose-fed cells, 25  $\text{nmol min}^{-1} \text{mg}^{-1}$ . This result indicated that the MTA-CoA hydratase detected in cell extracts

of *R. lacuscaerulensis* was up-regulated during growth on MMPA as expected if the activity was physiologically important.

**Complementation of a *R. pomeroyi dmdD* Deletion by RL\_acuH.** Previous work has shown that a *R. pomeroyi dmdD*<sup>-</sup> (*SPO3805::tet*) strain displayed little or no growth when MMPA was the sole carbon source and slow growth when DMSP was the carbon source (10). These results suggested that RPO\_AcuH was not capable of functioning as a physiologically relevant MTA-CoA hydratase, a result consistent with enzyme's low catalytic efficiency. However, we were unable to further test the role of AcuH by deleting the gene in either *R. pomeroyi* (9) or *R. lacuscaerulensis* (this work). Therefore, to test the hypothesis that the RL\_acuH gene could function in the demethylation pathway, it was used instead to complement the *R. pomeroyi dmdD*<sup>-</sup> (*SPO3805::tet*) mutation. RL\_acuH was introduced into *R. pomeroyi dmdD*<sup>-</sup> (*SPO3805::tet*) on the pSRKKm plasmid to yield the *R. pomeroyi dmdD*<sup>-</sup> plus RL\_acuH complementation strain (pHAB101). Growth of the complementation strain was the same as the deletion strain in MBM supplemented with 6 mM acetate or 3 mM DMSP as a sole carbon source. The complementation partially restored growth on MMPA to a level similar to that observed for *R. lacuscaerulensis* wild-type cells (Figure 3-6).

During growth with DMSP, *R. pomeroyi* releases small amounts of MeSH formed by the demethylation pathway. However, the amount of MeSH is always much less than the amount of DMSP metabolized because most of the MeSH is oxidized (10, 41). The *R. pomeroyi dmdD*<sup>-</sup> strain produced less MeSH than the wild-type strain when grown on DMSP (Table 3-4). The source of the residual MeSH is not known, but it could result from MTA-CoA hydratase activity of RP\_AcuH or another pathway. The complementation strain increased MeSH production 20% over the deletion strain, consistent with an increase in MTA-CoA hydratase activity. For

comparison, the wild-type strain of *R. lacuscaerulensis* also produced small amounts of MeSH (Table 3-4). In contrast, the DMS production of the deletion and complementation strains was very similar.

**AcuHs from Other Microorganisms Have MTA-CoA Hydratase Activity.** To determine if the AcuHs identified from other organisms had MTA-CoA hydratase activity, five *acuH* orthologs were cloned from *Dinoroseobacter shibae* (DS\_AcuH), *Oceanibus indolifex* (OI\_AcuH), *Pseudomonas putida* (PP\_AcuH), *Burkholderia thailandensis* (BTH\_AcuH), and *Bacillus subtilis* (BS\_AcuH). These proteins represented the widespread distribution of AcuH proteins, including both Alphaproteobacteria possessing *dmdA* and, hence, presumptive DMSP-utilizers as well as distantly related bacteria unlikely to encounter DMSP in nature (Figures 3-3, 3-4). Cloned genes were over-expressed in *E. coli* BL21 (DE3), and the resultant proteins were purified to over 95% purity (Figure 3-7). Purified AcuH enzymes were analyzed to determine their kinetic constants for MTA-CoA. Because of the instability of acryloyl-CoA, crotonyl-CoA served as a positive control for activity. In order to control for background ECH activity of *E. coli* towards crotonyl-CoA, an unrelated *Pseudomonas aeruginosa* oxio-reductase gene PA\_1833 cloned in the same expression vector was purified in the same manner as AcuH. In this enzyme preparation, the background crotonase activity was negligible at < 0.75 % of the lowest activity displayed by the AcuH. All enzymes tested had high catalytic efficiencies ( $k_{cat}/K_m$ ) with crotonyl-CoA, ranging from about  $10^3 \text{ mM}^{-1} \text{ s}^{-1}$ , similar to the *Ruegeria* AcuHs, to three orders of magnitude higher, e.g.  $>10^6 \text{ mM}^{-1} \text{ s}^{-1}$  (Table 3-5). Although the  $K_m$ s were higher than the *Ruegeria* enzymes, these values were consistent with others presented in the literature (31).

While BS\_AcuH had no activity with MTA-CoA, the other four putative AcuH enzymes possessed low levels of MTA-CoA hydratase activity (Table 3-5). An alignment of the amino

acid sequences of the AcuHs tested showed that BS\_AcuH was the least similar (Figure 3-2). BS\_AcuH was also the most phylogenetically distant from RL\_AcuH and RPO\_AcuH (Figure 3-3). The remaining enzymes all displayed similar  $k_{cat}$  for MTA-CoA of 1-2 s<sup>-1</sup>, or intermediate between RL\_AcuH and RPO\_AcuH (Table 3-5). However, the  $K_m$ s were much higher, ranging from 2.0 mM to 23 mM. The resulting catalytic efficiencies were all low, comparable to those observed with RPO\_AcuH (Table 3-1). The  $K_m$  for MTA-CoA in *E. coli* cell extracts expressing recombinant DS\_AcuH was reduced to 1.6 mM, similar to the Rlac\_AcuH. In contrast, the  $K_m$ s in cell extracts of the other enzymes were not altered (Table 3-6). Thus, while MTA-CoA may be used by these enzymes when present in sufficient quantities, their *in vivo* activities are likely to be far below that of RPO\_DmdD. Indeed, members of the crotonase superfamily are known for catalyzing a wide range of reactions, and the low MTA hydratase activity may be another example of this superfamily's broad specificity (42, 43).

**Demethylation Activity of Bacteria Possessing AcuH.** Of *O. indolifex*, *D. shibae*, *B. thailandensis*, *P. putida* and *B. subtilis*, only *D. shibae* was able to grow with DMSP or MMPA as sole carbon sources (Figure 3-8). Moreover, when supplemented with acetate, these compounds also greatly enhanced growth. In contrast, the growth of *O. indolifex*, *P. putida* and *B. thailandensis* was not affected by DMSP and MMPA either alone or in the presence of acetate (data not shown).

The ability of these organisms to produce MeSH and DMS was evaluated to further examine their ability to metabolize MMPA and DMSP. Because most of the bacteria did not utilize MMPA and DMSP as sole carbon sources, cultures were grown in MBM with acetate and either DMSP or MMPA. Interestingly, all four bacteria produced small amounts of DMS from DMSP, including the two from non-marine sources where DMSP is not likely to be abundant

(Figure 3-9). *P. putida*, *D. shibae*, and *O. indolifex* possess orthologs of DddP, a widely distributed DMSP lyase (18-20, 22). In contrast, *B. thailandensis* does not possess an ortholog to any of the currently recognized DMSP lyases (21). Thus, there may be additional families of DMSP lyases to be discovered.

Despite being the only bacterium tested that can grow on DMSP and MMPA as sole carbon sources, *D. shibae* produced very little MeSH on either substrate. Presumably, MeSH was consumed as rapidly as it was produced by this bacterium. *B. thailandensis*, *O. indolifex* and *P. putida* all produced MeSH from MMPA, indicating that they possessed MTA-CoA hydratase activity. In *O. indolifex*, MeSH peaked at about 6  $\mu\text{M}$  equivalents (gas produced/L) but then declined, presumably due to consumption. *B. thailandensis* produced the most MeSH from growth with MMPA, nearly 180  $\mu\text{M}$  equivalents, suggesting that it was not readily consumed (Figure 3-9). MeSH production from DMSP by *B. thailandensis* was not detected, as expected because it did not possess the first enzyme of the demethylation pathway, DmdA (Figure 3-4) (21). *P. putida*, which also lacked DmdA, produced small amounts of MeSH, 1.5  $\mu\text{M}$  equivalents from growth with DMSP, suggesting that it possessed low activities for an alternative pathway for DMSP metabolism.

**Complementation of the *R. pomeroyi dmdD* Deletion by Other *acuHs*.** Although the *AcuHs* from *D. shibae*, *O. indolifex*, *B. thailandensis*, and *P. putida* possessed low levels of MTA-CoA hydratase activity, their genes did not complement the *R. pomeroyi dmdD* (*SPO3805::tet*) mutation. During growth on DMSP as a sole carbon source, the complementation strains took 72 hrs to reach the maximum optical density of 0.2 ( $\text{OD}_{600}$ ), while the *R. pomeroyi* wild-type strain reached the same optical density after 48 hrs. The *R. pomeroyi dmdD* (*SPO3805::tet*) strain reached a maximum  $\text{OD}_{600}$  of 0.15 after 72 hrs (Table 3-7). Despite the

slightly increased growth on DMSP as compared to the deletion mutant, none of the complementation strains restored growth on MMPA as a sole carbon source. Because acryloyl-CoA is an intermediate in the DMSP cleavage pathway, the improved growth on DMSP may have resulted from the increased acryloyl-CoA hydratase activity in the complementation strains.

MeSH and DMS production of the complementation strains was also not significantly different from that of the deletion mutant *R. pomeroyi dmdD* (*SPO3805::tet*). Because this mutant did not grow with MMPA as a sole carbon source, cultures were grown on a combination of acetate and either DMSP or MMPA. Both the deletion mutant and complementation strains failed to produce more than background amounts of MeSH from MMPA (Table 3-8). Although the deletion mutant produced small amounts of MeSH from DMSP, complementation did not greatly increase these amounts. Similarly, the DMS production from DMSP was largely unchanged between the deletion mutant and complementation strains. Thus, these *acuH* genes were not able to restore the MTA-CoA hydratase activity in the *R. pomeroyi dmdD* deletion mutant.

## **Discussion**

Although the enzymes of the demethylation pathway have been well established in *R. pomeroyi*, the limited distribution of DmdD orthologs in other DMSP-utilizing bacteria suggests that this activity is catalyzed by paralogous crotonases in many other marine bacteria (10, 13). The newly identified crotonase superfamily enzyme, AcuH, is a good candidate for this role in *R. lacuscaerulensis*. It catalyzes sufficient MTA-CoA hydratase activity to sustain growth and be purified from MMPA-grown cells (10). In the presence of the effector ADP, its catalytic efficiency is likely to be within the physiological range. The gene also provides partial complementation of a *dmdD* deletion mutation in *R. pomeroyi*. Nevertheless, it is unlikely that

the MTA-CoA hydratase activity of the AcuH is its major physiological role. Although AcuH is widely distributed among DMSP-catabolizing bacteria that lack DmdD, it is common in many bacteria that are unable to metabolize DMSP as well, indicating other roles for this enzyme. Phylogenetically AcuH is more closely related to the eukaryotic ECHs involved in fatty acid  $\beta$ -oxidation than to DmdD. AcuH also possess much higher hydratase activity for crotonyl-CoA and acryloyl-CoA than MTA-CoA. Thus, this AcuH is not a specialized MTA-CoA hydratase like DmdD, rather it is an acryloyl-CoA hydratase that also has the ability to hydrolyze MTA-CoA. Interestingly, the presence of this less specialized enzyme is still sufficient to allow *R. lacuscaerulensis* to utilize the demethylation pathway.

RL\_AcuH possesses a substantially lower catalytic efficiency for MTA-CoA hydrolysis ( $11.5 \text{ mM}^{-1} \text{ s}^{-1}$ ) compared with RPO\_DmdD ( $5000 \text{ mM}^{-1} \text{ s}^{-1}$ ). An even lower catalytic efficiency is observed for RPO\_AcuH ( $0.1 \text{ mM}^{-1} \text{ s}^{-1}$ ), explaining why a *R. pomeroyi dmdD*<sup>-</sup> (SPO3805::tet) strain is unable to grown on MMPA as a sole carbon source (10, 44). While RL\_AcuH exhibits sufficient activity to support the slow growth of *R. lacuscaerulensis* on MMPA, RPO\_AcuH alone does not. These results underscore the importance of reaction kinetics for predicting a role in DMSP metabolism. Simply possessing the enzyme activity is not necessarily sufficient to allow for growth on a substrate. In fact, *R. pomeroyi* and *R. lacuscaerulensis* have also adopted very different strategies. *R. pomeroyi* has a dedicated MTA-CoA hydratase in DmdD, and its AcuH has very low MTA-CoA hydratase activity. Moreover, the activity of its DmdD does not appear to be regulated by effectors (44). In contrast, *R. lacuscaerulensis* lacks a specialized DmdD but possesses an AcuH with broad substrate specificity, and the MTA-CoA hydratase activity is regulated by ADP.

ADP and possibly  $\text{NAD}^+$  appear to be major effectors of the MTA-CoA hydratase activity of the RL\_AcuH. To our knowledge, this is the first report of effectors playing a role in the activity of ECHs, and the DmdD of *R. pomeroyi* was not similarly regulated. It is worth noting that the activity of one of the DmdB isozymes but not the DmdD from *R. pomeroyi* is also controlled by ADP (37). The regulation of the demethylation pathway by ADP suggests that the metabolism of DMSP is responsive to cellular energy level (45). When the ATP:ADP ratio is high, marine bacteria would tend to utilize other carbon sources, including sugars, amino acids and inorganic carbon, for growth (15, 45-47). DMSP would then be protected, allowing cells to retain high concentrations for use as an osmolyte. When other carbon sources become depleted, the ATP:ADP ratio would decrease, and DMSP could be utilized as carbon and energy source (11, 48).

Assuming that AcuH's high activity towards acryloyl-CoA plays an important role in the metabolism of acrylate produced from the DMSP cleavage pathway, the use of a multifunctional enzyme that participates in both the cleavage and demethylation pathways may facilitate the balancing these two pathways. While none of the putative AcuHs tested, besides RL\_AcuH, had the ability to complement a *dmdD* deletion in *R. pomeroyi*, they did stimulate growth on DMSP, supporting their role in acrylate metabolism. Acryloyl-CoA is toxic, and its rapid removal by AcuH may be required for growth on DMSP. Previous studies have proposed a similar role for the acryloyl-CoA reductase, AcuI, in DMSP metabolism. The *acuI* gene is frequently found in proximity to *dmdA* and the genes for various DMSP lyases (*dds*), suggesting that the genes are co-regulated (29, 49). A mutant of *acuI* in *R. pomeroyi* was unable to grow solely on acrylate and growth on DMSP was inhibited, indicating a specific role for AcuI in DMSP metabolism (49). AcuI from *Rhodobacter sphaeroides* and *R. pomeroyi*, and YhdH from *E. coli* are known to

catalyze reactions with acryloyl-CoA as part of 3-hydroxypropionate metabolism and also play roles in conferring resistance to acrylate (30, 49).

Based on the results of this study, the ability to catalyze reactions with MTA-CoA has developed only for certain AcuHs. When AcuHs from phylogenetically diverse organisms were analyzed only one did not show activity towards MTA-CoA, the *B. subtilis* AcuH. However, the catalytic efficiencies of the other AcuH orthologs analyzed from *R. pomeroyi*, *O. indolifex*, *D. shibae*, *P. putida*, and *B. thailandensis*, were very low, and the genes for these enzymes failed to complement *dmdD* mutations in *R. pomeroyi*. Two alternative explanations appear likely. While the *R. lacuscaerulensis* AcuH is likely to play a physiological role in the DMSP demethylation pathway, other marine bacteria may have recruited different ECHs for this function. The fact that many bacteria contain more than ten genes from this super family certainly indicates that this explanation is possible. Interestingly, only a single AcuH-like enzyme was identified in *D. shibae*. *D. shibae* was also the only strain tested that was able to grown on DMSP and MMPA as sole carbon sources, indicating that this AcuH may be physiologically important for *D. shibae*. An alternative explanation is that complementation in *R. pomeroyi* is a poor test for the function of these genes under the physiological conditions in the native cells. *R. pomeroyi* is unusual in that it rapidly metabolizes DMSP. In contrast, the other organisms metabolized DMSP or MMPA much more slowly.

*B. thailandensis* and *P. putida* may not encounter DMSP or MMPA in high enough amounts to require highly efficient DMSP and MMPA metabolic enzymes. However, *B. thailandensis* has a functional DmdB as does *Pseudomonas aeruginosa* (37). It is possible that these bacteria are periodically exposed to MMPA and MMPA-like compounds through their interactions with plants and other bacteria in the soil environment. DMSP produced by certain

coastal plants, *Spartina alterniflora* and *Wollastonia biflora*, may be released into the soil (50, 51). Many fruiting plants produce sulfur volatiles which closely resemble MMPA and other soil dwelling microorganisms produce 3-methylthiopropionic acid, which causes bacterial blight in cassava (38, 40, 52). These exposures may influence the development of enzymes similar to those in the DMSP demethylation pathway. This is supported by the data showing DMS and MeSH production when these organisms are grown with DMSP or MMPA.

The data presented here help to further demonstrate the flexibility of the crotonase superfamily of enzymes. This information fosters the hypothesis that enzymes for DMSP and MMPA metabolism have resulted from the evolution and adaptation of preexisting enzymes encoded in the genomes of bacteria which are regularly exposed to DMSP, MMPA, or structurally similar compounds. This appears to be the case with DmdD as well as AcuH. DmdD is a specific MTA-CoA hydratase, allowing *R. pomeroyi* and the other marine bacteria possessing it to efficiently utilize DMSP via the demethylation pathway (10, 44). AcuH, by comparison, allows for metabolic flexibility, enabling use of both the demethylation and cleavage pathways in certain microorganisms when other carbon sources are also available. Despite the wide distribution of the demethylation pathway and AcuH in marine microorganisms, however, a functional homolog of a MTA-CoA hydratase has not been found in *Pelagibacter ubique* of the ubiquitous SAR11 clade bacteria. A DmdD homolog in *P. ubique* HTCC1062 shares only 25% identity with that in *R. pomeroyi* and did not show activity with MTA-CoA (unpublished observation). Still, the identification and characterization of AcuH from *R. lacuscaerulensis* and *R. pomeroyi* as well as the other organisms described here in adds to our understanding of DMSP metabolism in the environment. The abundance of AcuH homologs further helps to clarify utilization of the demethylation pathway in marine microorganisms

lacking *dmdD*. However, not all AcuH enzymes may be physiologically relevant for use in DMSP metabolism. The properties of the AcuHs investigated here indicate that individual microorganisms could have adapted any one of the many ECHs encoded within their genomes for activity towards MTA-CoA.

## References:

1. **Stefels J.** 2000. Physiological aspects of the production and conversion of DMSP in marine algae and higher plants. *J. Sea Res.* **43**:183-197.
2. **Sunda W, Kieber DJ, Kiene RP, Huntsman S.** 2002. An antioxidant function for DMSP and DMS in marine algae. *Nature* **418**:317-320.
3. **Steinke MW, Wolfe GV, Kirst, GO.** 1998. Partial characterization of dimethylsulfoniopropionate (DMSP) lyase isozymes in 6 strains of *Emiliania huxleyi*. *Mar. Ecol. Prog. Ser.* **175**:215-225.
4. **Zubkov MV, Fuchs BM, Archer SD, Kiene RP, Amann R, Burkill PH.** 2001. Linking the composition of bacterioplankton to rapid turnover of dissolved dimethylsulphoniopropionate in an algal bloom in the North Sea. *Environ. Microbiol.* **3**:304-311.
5. **Howard EC, Henriksen JR, Buchan A, Reisch CR, Burgmann H, Welsh R, Ye W, Gonzalez JM, Mace K, Joye SB, Kiene RP, Whitman WB, Moran MA.** 2006. Bacterial taxa that limit sulfur flux from the ocean. *Science* **314**:649-652.
6. **Kiene RP, Linn, LJ, Bruton JA.** 2000. New and important roles for DMSP in marine microbial communities. *J. Sea Res.* **43**:209-224.
7. **Simo RP, Pedros-Alio C, Malin G, Grimalt J.** 2000. Biological turnover of DMS, DMSP, and DMSO in contrasting open-sea waters. *Mar. Ecol. Prog. Ser.* **203**:1-11.
8. **Charlson RL, Lovelock JE, Andreae MO, Warren SG.** 1987. Oceanic phytoplankton, atmospheric sulfur, cloud albedo and climate. *Nature* **326**:655-611.
9. **Reisch CR, Crabb WM, Gifford SM, Teng Q, Stoudemayer MJ, Moran MA, Whitman WB.** 2013. Metabolism of dimethylsulphoniopropionate by *Ruegeria pomeroyi* DSS-3. *Mol. Microbiol.* **89**:774-791.
10. **Reisch CR, Stoudemayer MJ, Varaljay VA, Amster IJ, Moran MA, Whitman WB.** 2011. Novel pathway for assimilation of dimethylsulphoniopropionate widespread in marine bacteria. *Nature* **473**:208-211.
11. **Reisch CR, Moran MA, Whitman WB.** 2008. Dimethylsulfoniopropionate-dependent demethylase (DmdA) from *Pelagibacter ubique* and *Silicibacter pomeroyi*. *J. Bacteriol.* **190**:8018-8024.
12. **Howard EC, Sun S, Biers EJ, Moran MA.** 2008. Abundant and diverse bacteria involved in DMSP degradation in marine surface waters. *Environ. Microbiol.* **10**:2397-2410.

13. **Rusch DB, Halpern AL, Sutton G, Heidelberg KB, Williamson S, Yooseph S, Wu D, Eisen JA, Hoffman JM, Remington K, Beeson K, Tran B, Smith H, Baden-Tillson H, Stewart C, Thorpe J, Freeman J, Andrews-Pfannkoch C, Venter JE, Li K, Kravitz S, Heidelberg JF, Utterback T, Rogers YH, Falcon LI, Souza V, Bonilla-Rosso G, Eguiarte LE, Karl DM, Sathyendranath S, Platt T, Bermingham E, Gallardo V, Tamayo-Castillo G, Ferrari MR, Strausberg RL, Neilson K, Friedman R, Frazier M, Venter JC.** 2007. The Sorcerer II Global Ocean Sampling expedition: northwest Atlantic through eastern tropical Pacific. *PLoS Biol* **5**:e77.
14. **Baumann P, Baumann L.** . 1981. The marine Gram-negative eubacteria: genera *Photobacterium*, *Beneckea*, *Alteromonas*, *Pseudomonas*, and *Alcaligenes*., p. 1302–1331. *In* M. P. Starr HS, H. G. Trüper, A. Balows & H. G. Schlegel (ed.), *The Prokaryotes*. Springer-Verlag, Berlin.
15. **Moran MA, Buchan A, Gonzalez JM, Heidelberg JF, Whitman WB, Kiene RP, Henriksen JR, King GM, Belas R, Fuqua C, Brinkac L, Lewis M, Johri S, Weaver B, Pai G, Eisen JA, Rahe E, Sheldon WM, Ye W, Miller TR, Carlton J, Rasko DA, Paulsen IT, Ren Q, Daugherty SC, Deboy RT, Dodson RJ, Durkin AS, Madupu R, Nelson WC, Sullivan SA, Rosovitz MJ, Haft DH, Selengut J, Ward N.** 2004. Genome sequence of *Silicibacter pomeroyi* reveals adaptations to the marine environment. *Nature* **432**:910-913.
16. **Yi H, Lim YW, Chun J.** 2007. Taxonomic evaluation of the genera *Ruegeria* and *Silicibacter*: a proposal to transfer the genus *Silicibacter Petursdottir* and *Kristjansson* 1999 to the genus *Ruegeria Uchino* et al. 1999. *Int. J. Syst. Evol. Microbiol.* **57**:815-819.
17. **Zinser Buchan A, Ferriera SF, Johnson JJ, Kravitz SK, Beeson KB, Sutton GS, Roger Y, Friedman RF, Frazier MF, Venter JC.** 2008. *Silicibacter lacuscaerulensis* ITI-1157 genome sequence. EMBL/GenBank/DDBJ Databases.
18. **Biebl H, Allgaier M, Tindall BJ, Koblizek M, Lunsdorf H, Pukall R, Wagner-Dobler I.** 2005. *Dinoroseobacter shibae* gen. nov., sp. nov., a new aerobic phototrophic bacterium isolated from dinoflagellates. *Int. J. Syst. Evol. Microbiol.* **55**:1089-1096.
19. **Wagner-Dobler I, Ballhausen B, Berger M, Brinkhoff T, Buchholz I, Bunk B, Cypionka H, Daniel R, Drepper T, Gerdt G, Hahnke S, Han C, Jahn D, Kalhoefer D, Kiss H, Klenk HP, Kyrpides N, Liebl W, Liesegang H, Meincke L, Pati A, Petersen J, Piekarski T, Pommerenke C, Pradella S, Pukall R, Rabus R, Stackebrandt E, Thole S, Thompson L, Tielen P, Tomasch J, von Jan M, Wanphrut N, Wichels A, Zech H, Simon M.** 2010. The complete genome sequence of the algal symbiont *Dinoroseobacter shibae*: a hitchhiker's guide to life in the sea. *ISME J.* **4**:61-77.

20. **Wagner-Dobler I, Rheims H, Felske A, El-Ghezal A, Flade-Schroder D, Laatsch H, Lang S, Pukall R, Tindall BJ.** 2004. *Oceanibulbus indolifex* gen. nov., sp. nov., a North Sea alphaproteobacterium that produces bioactive metabolites. *Int. J. Syst. Evol. Microbiol.* **54**:1177-1184.
21. **Kim HS, Schell MA, Yu Y, Ulrich RL, Sarria SH, Nierman WC, DeShazer D.** 2005. Bacterial genome adaptation to niches: divergence of the potential virulence genes in three *Burkholderia* species of different survival strategies. *BMC Genomics* **6**:174.
22. **Nelson KE, Weinel C, Paulsen IT, Dodson RJ, Hilbert H, Martins dos Santos VA, Fouts DE, Gill SR, Pop M, Holmes M, Brinkac L, Beanan M, DeBoy RT, Daugherty S, Kolonay J, Madupu R, Nelson W, White O, Peterson J, Khouri H, Hance I, Chris Lee P, Holtzapple E, Scanlan D, Tran K, Moazzez A, Utterback T, Rizzo M, Lee K, Kosack D, Moestl D, Wedler H, Lauber J, Stjepandic D, Hoheisel J, Straetz M, Heim S, Kiewitz C, Eisen JA, Timmis KN, Dusterhoft A, Tummeler B, Fraser CM.** 2002. Complete genome sequence and comparative analysis of the metabolically versatile *Pseudomonas putida* KT2440. *Environ. Microbiol.* **4**:799-808.
23. **Kunst F, Ogasawara N, Moszer I, Albertini AM, Alloni G, Azevedo V, Bertero MG, Bessieres P, Bolotin A, Borchert S, Borriss R, Boursier L, Brans A, Braun M, Brignell SC, Bron S, Brouillet S, Bruschi CV, Caldwell B, Capuano V, Carter NM, Choi SK, Cordani JJ, Connerton IF, Cummings NJ, Daniel RA, Denziot F, Devine KM, Dusterhoft A, Ehrlich SD, Emmerson PT, Entian KD, Errington J, Fabret C, Ferrari E, Foulger D, Fritz C, Fujita M, Fujita Y, Fuma S, Galizzi A, Galleron N, Ghim SY, Glaser P, Goffeau A, Golightly EJ, Grandi G, Guiseppi G, Guy BJ, Haga K, Haiech J, Harwood CR, Henaut A, Hilbert H, Holsappel S, Hosono S, Hullo MF, Itaya M, Jones L, Joris B, Karamata D, Kasahara Y, Klaerr-Blanchard M, Klein C, Kobayashi Y, Koetter P, Koningstein G, Krogh S, Kumano M, Kurita K, Lapidus A, Lardinois S, Lauber J, Lazarevic V, Lee SM, Levine A, Liu H, Masuda S, Mauel C, Medigue C, Medina N, Mellado RP, Mizuno M, Moestl D, Nakai S, Noback M, Noone D, O'Reilly M, Ogawa K, Ogiwara A, Oudega B, Park SH, Parro V, Pohl TM, Portelle D, Porwollik S, Prescott AM, Presecan E, Pujic P, Purnelle B, Rapoport G, Rey M, Reynolds S, Rieger M, Rivolta C, Rocha E, Roche B, Rose M, Sadaie Y, Sato T, Scanlan E, Schleich S, Schroeter R, Scoffone F, Sekiguchi J, Sekowska A, Seror SJ, Serror P, Shin BS, Soldo B, Sorokin A, Tacconi E, Takagi T, Takahashi H, Takemaru K, Takeuchi M, Tamakoshi A, Tanaka T, Terpstra P, Togoni A, Tosato V, Uchiyama S, Vandebol M, Vannier F, Vassarotti A, Viari A, Wambutt R, Wedler H, Weitzenegger T, Winters P, Wipat A, Yamamoto H, Yamane K, Yasumoto K, Yata K, Yoshida K, Yoshikawa HF, Zumstein E, Yoshikawa H, **Danchin A.** 1997. The complete genome sequence of the gram-positive bacterium *Bacillus subtilis*. *Nature* **390**:249-256.**
24. **Decker K.** 1959. Die aktivierte Essigsäure. Ferdinand Enke Publisher, Stuttgart, Germany.

25. **Chambers ST, Kunin CM, Miller D, Hamada A.** 1987. Dimethylthetin can substitute for glycine betaine as an osmoprotectant molecule for *Escherichia coli*. J. Bacteriol. **169**:4845-4847.
26. **Henricksen J.** 2008. Physiology of dimethylsulfoniopropionate metabolism in a model marine Roseobacter, *Silicibacter pomeroyi*. University of Georgia, Athens, GA.
27. **Tamura KS, Stencher G, Peterson D, Filipski A, Kumar S.** 2013. MEGA6: Molecular evolutionary genetics analysis Version 6.0. Mol. Biol. Evol. **30**:2725-2729.
28. **Letunic I, Bork P.** 2016. Interactive Tree of Life (ITOL) v3: an online tool for the display and annotation of phylogenetic and other trees. Nucleic Acid Research:1-4.
29. **Sullivan MJ, Curson AR, Shearer N, Todd JD, Green RT, Johnston AW.** 2011. Unusual regulation of a leaderless operon involved in the catabolism of dimethylsulfoniopropionate in *Rhodobacter sphaeroides*. PLoS One **6**:e15972.
30. **Asao M, Alber BE.** 2013. Acrylyl-coenzyme A reductase, an enzyme involved in the assimilation of 3-hydroxypropionate by *Rhodobacter sphaeroides*. J. Bacteriol. **195**:4716-4725.
31. **Agnihotri G, Liu HW.** 2003. Enoyl-CoA hydratase. reaction, mechanism, and inhibition. Bioorg. Med. Chem. **11**:9-20.
32. **Maggio-Hall LA, Keller NP.** 2004. Mitochondrial beta-oxidation in *Aspergillus nidulans*. Mol. Microbiol. **54**:1173-1185.
33. **Teufel R, Mascaraque V, Ismail W, Voss M, Perera J, Eisenreich W, Haehnel W, Fuchs G.** 2010. Bacterial phenylalanine and phenylacetate catabolic pathway revealed. PNAS **107**:14390-14395.
34. **Grishin AM, Ajamian E, Zhang L, Rouiller I, Bostina M, Cygler M.** 2012. Protein-protein interactions in the beta-oxidation part of the phenylacetate utilization pathway: crystal structure of the PaaF-PaaG hydratase-isomerase complex. J. Biol. Chem. **287**:37986-37996.
35. **Varaljay VA, Gifford SM, Wilson ST, Sharma S, Karl DM, Moran MA.** 2012. Bacterial dimethylsulfoniopropionate degradation genes in the oligotrophic north pacific subtropical gyre. Appl. Environ. Microbiol. **78**:2775-2782.
36. **Varaljay VA, Robidart J, Preston CM, Gifford SM, Durham BP, Burns AS, Ryan JP, Marin R, Kiene RP, Zehr JP, Scholin CA, Moran MA.** 2015. Single-taxon field measurements of bacterial gene regulation controlling DMSP fate. ISME J. **9**:1692.
37. **Bullock HA, Reisch CR, Burns AS, Moran MA, Whitman WB.** 2014. Regulatory and functional diversity of methylmercaptopropionate coenzyme A ligases from the

- dimethylsulfoniopropionate demethylation pathway in *Ruegeria pomeroyi* DSS-3 and other proteobacteria. *J. Bacteriol.* **196**:1275-1285.
38. **Ewbank E, Maraite H.** 1990. Conversion of methionine to phytotoxic 3-methylthiopropionic acid by *Xanthomonas campestris* pv. *manihotis*. *J. Gen. Microbiol.* **136**:1185-1189.
  39. **Albers E.** 2009. Metabolic characteristics and importance of the universal methionine salvage pathway recycling methionine from 5'-methylthioadenosine. *IUBMB Life* **61**:1132-1142.
  40. **Perreaux D, Maraite H, Meyer JA.** 1982. Identification of 3(methylthio) propionic acid as a blight inducing toxin produced by *Xanthomonas campestris* pv. *manihotis* *in vitro*. *Physiol. Plant Path.* **20**:313-319.
  41. **Kiene RP, Linn LJ, Gonzalez J, Moran MA, Bruton JA.** 1999. Dimethylsulfoniopropionate and methanethiol are important precursors of methionine and protein-sulfur in marine bacterioplankton. *Appl. Environ. Microbiol.* **65**:4549-4558.
  42. **Hamed RB, Batchelar ET, Clifton IJ, Schofield CJ.** 2008. Mechanisms and structures of crotonase superfamily enzymes--how nature controls enolate and oxyanion reactivity. *Cell Mol. Life Sci.* **65**:2507-2527.
  43. **Holden HM, Benning MM, Haller T, Gerlt JA.** 2001. The crotonase superfamily: divergently related enzymes that catalyze different reactions involving acyl coenzyme a thioesters. *Acc. Chem. Res.* **34**:145-157.
  44. **Tan D, Crabb WM, Whitman WB, Tong L.** 2013. Crystal structure of DmdD, a crotonase superfamily enzyme that catalyzes the hydration and hydrolysis of methylthioacryloyl-CoA. *PLoS One* **8**:e63870.
  45. **Atkinson DE.** 1968. The energy charge of the adenylate pool as a regulatory parameter. Interaction with feedback modifiers. *Biochemistry* **7**:4030-4034.
  46. **DeLorenzo S, Brauer SL, Edgmont CA, Herfort L, Tebo BM, Zuber P.** 2012. Ubiquitous dissolved inorganic carbon assimilation by marine bacteria in the Pacific Northwest coastal ocean as determined by stable isotope probing. *PLoS One* **7**:e46695.
  47. **Law AT, Button DK.** 1977. Multiple-carbon-source-limited growth kinetics of a marine coryneform bacterium. *J. Bacteriol.* **129**:115-123.
  48. **Vila-Costa M, Simo R, Harada H, Gasol JM, Slezak D, Kiene RP.** 2006. Dimethylsulfoniopropionate uptake by marine phytoplankton. *Science* **314**:652-654.

49. **Todd JD, Curson AR, Sullivan MJ, Kirkwood M, Johnston AW.** 2012. The *Ruegeria pomeroyi acul* gene has a role in DMSP catabolism and resembles *yhdH* of *E. coli* and other bacteria in conferring resistance to acrylate. *PLoS One* **7**:e35947.
50. **Kocsis MG, Nolte KD, Rhodes D, Shen TL, Gage DA, Hanson AD.** 1998. Dimethylsulfoniopropionate biosynthesis in *Spartina alterniflora*. Evidence that S-methylmethionine and dimethylsulfoniopropylamine are intermediates. *Plant Physiol.* **117**:273-281.
51. **Hanson AD, Rivoal J, Paquet L, Gage DA.** 1994. Biosynthesis of 3-dimethylsulfoniopropionate in *Wollastonia biflora* (L.) DC. Evidence that S-methylmethionine is an intermediate. *Plant Physiol.* **105**:103-110.
52. **Gonda I, Lev S, Bar E, Sikron N, Portnoy V, Davidovich-Rikanati R, Burger J, Schaffer AA, Tadmor Y, Giovannonni JJ, Huang M, Fei Z, Katzir N, Fait A, Lewinsohn E.** 2013. Catabolism of L-methionine in the formation of sulfur and other volatiles in melon (*Cucumis melo* L.) fruit. *Plant J.* **74**:458-472.

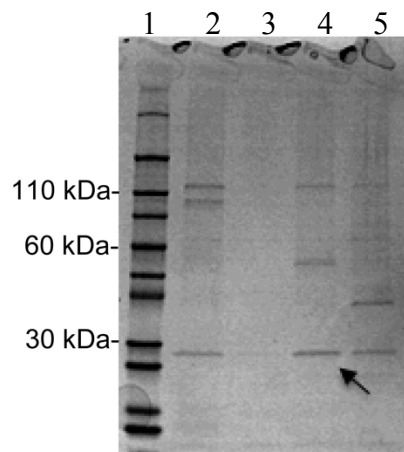


**Figure 3-1.** SDS-PAGE of RL\_AcuH (arrow) isolated from cell extracts of *R. lacuscaerulensis* grown on MMPA-based medium. The Novex Sharp Pre-stained protein marker (Thermo-Fisher) is used in lane 1. The band in lane 4 just under 60 kDa was identified as a DNA gyrase. The band at 110 kDa was not analyzed as it was also present in fractions (Lane 2) that did not possess MTA-CoA hydratase activity.

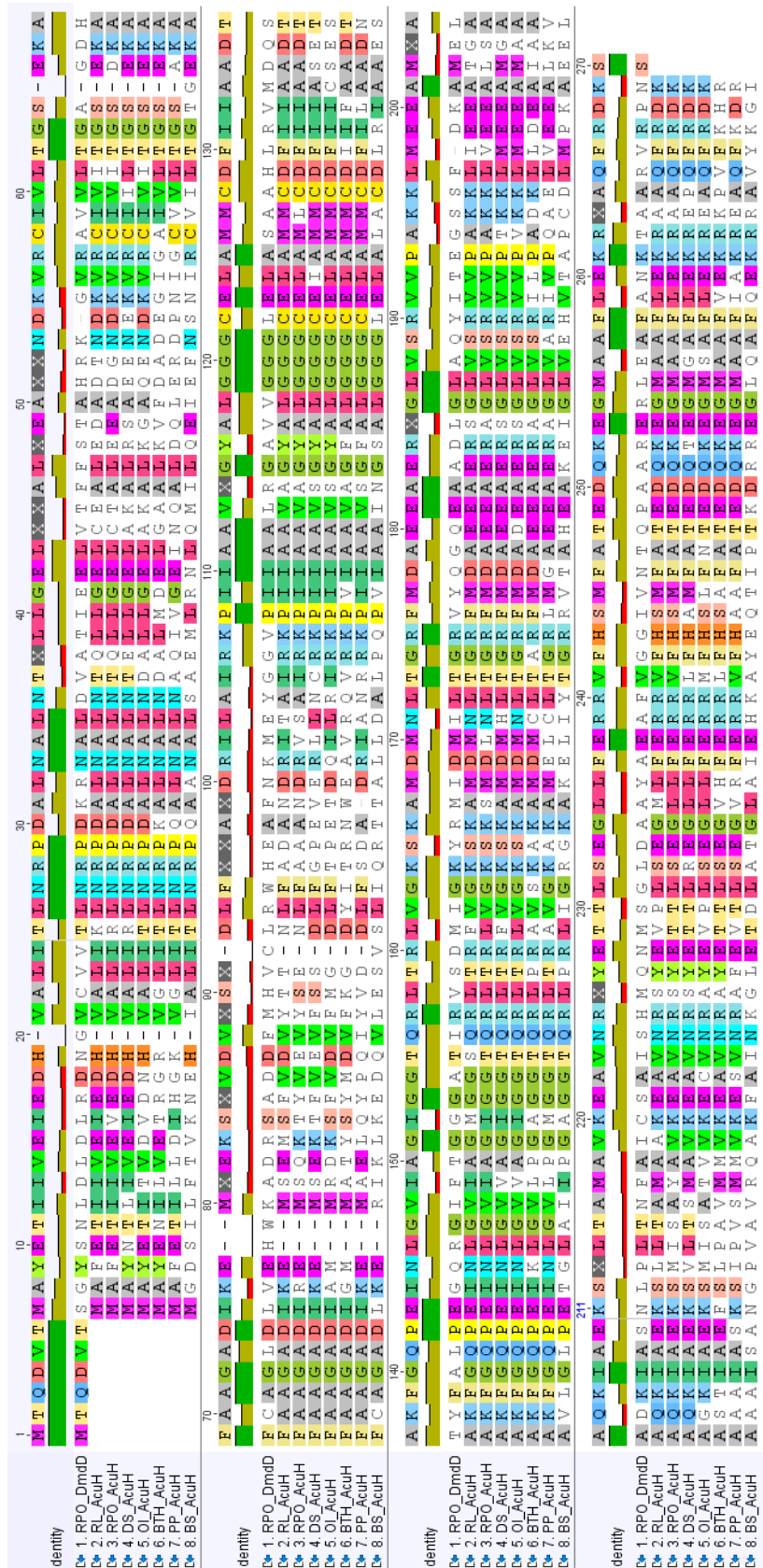


**Figure 3-2.** Protein sequence alignment of RPO\_DmdD, RL\_AcuH, RPO\_AcuH, and other AcuH orthologs. Alignment was assembled using Muscle in the Geneious software pack.

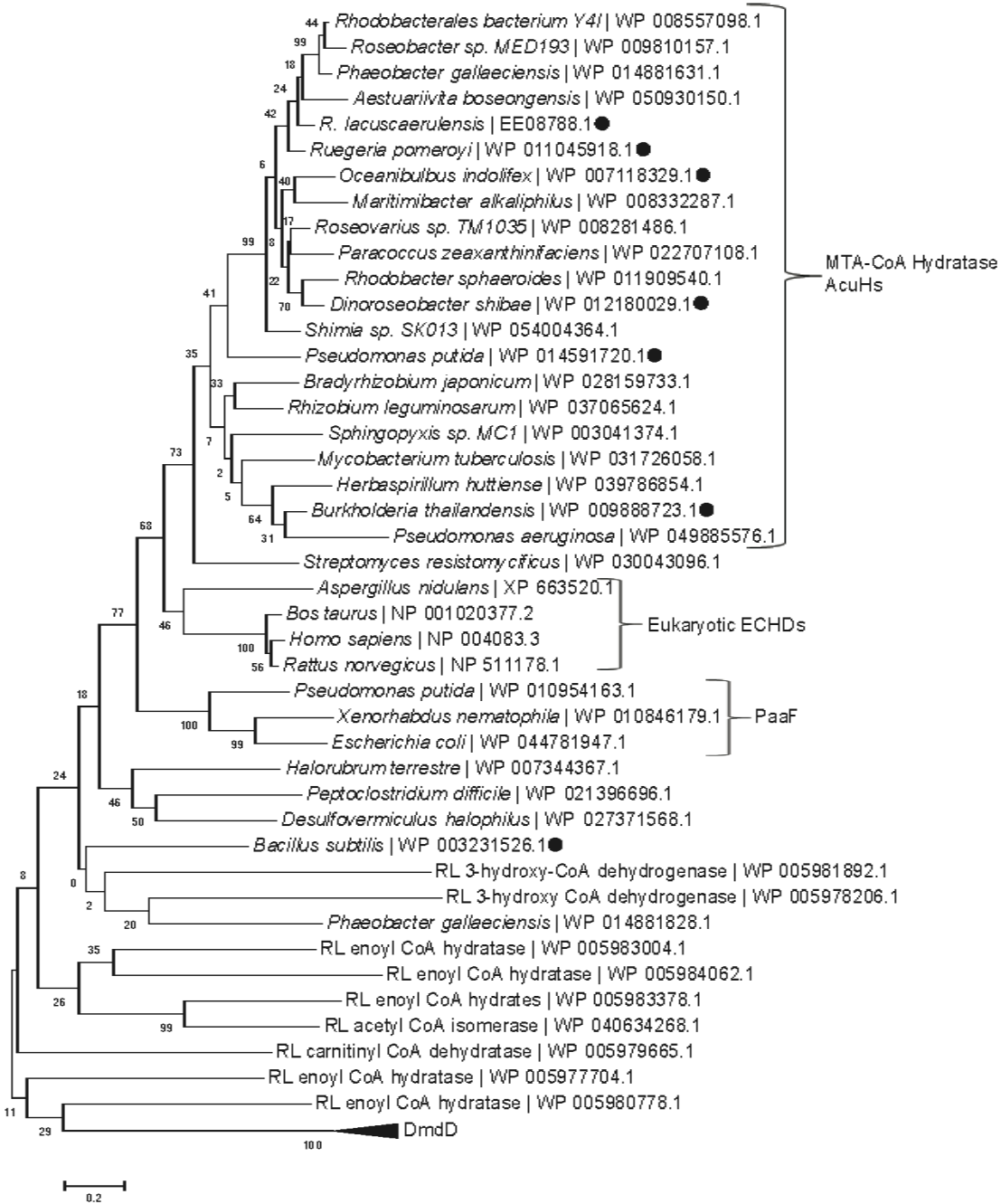


**Figure 3-3.** Phylogeny of representative AcuH homologs and other enoyl-CoA hydratases.

(●) Indicates putative AcuH proteins tested in this study. “RL” indicates the other annotated enoyl-CoA hydratases in the *R. lacuscaerulensis* genome with sequence similarity to AcuH. The phylogenetic tree was constructed using the amino acid sequences and the maximum likelihood method in MEGA 6.06.

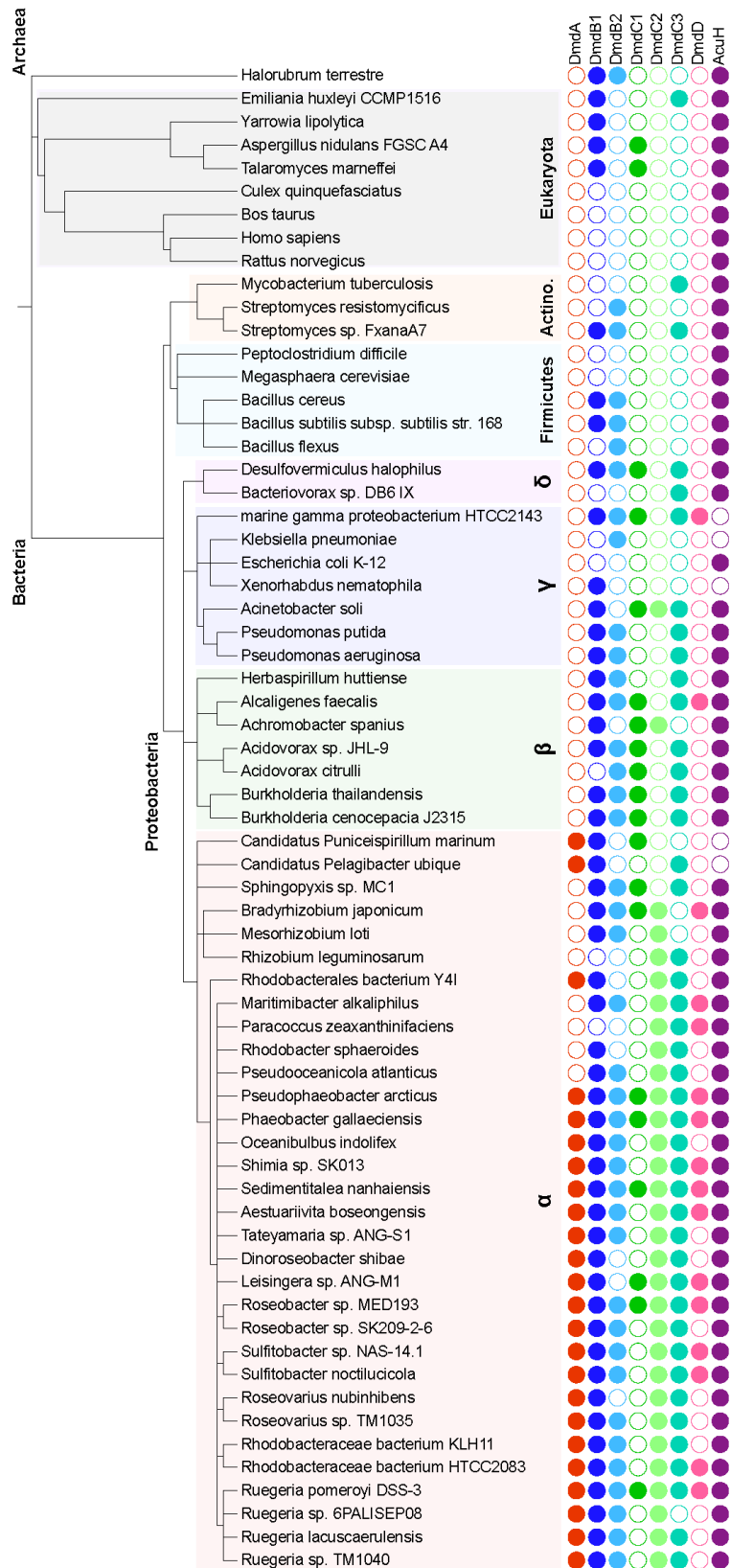


**Figure 3-4:** Distribution of demethylation pathway genes in representative bacteria and eukaryotes. 16S rRNA gene phylogeny of organisms that possess AcuH is shown on the left with the major taxonomic groups indicated. Distances are not drawn to scale. Colored filled circles represent the presence of homologs to AcuH and the other enzymes of the DMSP demethylation pathway as determined by BLAST scores  $< e 10^{-70}$  to the following genes from *R. pomeroyi*: DmdA: SPO1913; DmdB1, SPO0677; DmdB2, SPO2045; DmdC1, SPO3805; DmdC2, SPO0298; DmdC3, SPO2915; and DmdD, SPO3804. For the AcuH, SL1157\_0807, from *R. lacuscaerulensis* was used. Open circles represent the absence of homologs with BLAST scores  $< e 10^{-70}$ .

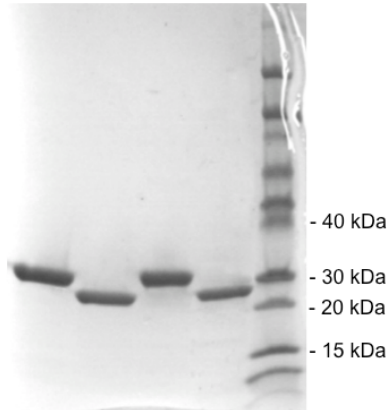


**Figure 3-5.** SDS-PAGE of purified recombinant RL\_AcuH and RPO\_AcuH from *E. coli* BL21. Lane: 1. Purified his<sub>6</sub>- RL\_AcuH; 2. RL\_AcuH after removal of the his-tag; 3. Purified his<sub>6</sub>- RPO-AcuH; 4. RPO-AcuH after removal of the his-tag. 5. Novex Sharp Pre-stained protein marker (Thermo-Fisher).

**Table 3-1.** Apparent kinetic constants for RL\_AcuH, RPO\_AcuH, and RPO\_DmdD with different substrates.

Substrate	Enzyme	$K_m$ (mM) <sup>a</sup>	$k_{cat}$ (s <sup>-1</sup> )	$k_{cat}/K_m$ (mM <sup>-1</sup> s <sup>-1</sup> )
	RL_AcuH	1.1 ± 0.1	12.6 ± 0.6	11.5
MTA-CoA	RPO_AcuH	1.3 ± 0.1	0.2 ± 0.01	0.1
	RPO_DmdD <sup>b</sup>	0.008	44	5.5 x10 <sup>3</sup>
Crotonyl-CoA	RL_AcuH	0.23 ± 0.02	890 ± 68	3.8 x10 <sup>3</sup>
	RPO_AcuH	0.12 ± 0.01	220 ± 9	2.0 x10 <sup>3</sup>
	RPO_DmdD	0.02	42	2.1 x10 <sup>3</sup>
Acryloyl-CoA	RL_AcuH	0.06 ± 0.01	4.2 ± 1.0 x10 <sup>5</sup>	7.4 x10 <sup>6</sup>
	RPO_AcuH	0.07 ± 0.02	3.6 ± 0.8 x10 <sup>5</sup>	5.0 x10 <sup>6</sup>
	RPO_DmdD	ND	ND	ND

<sup>a</sup>  $K_m$  and  $k_{cat}$  (±SD) are representative of three replicate experiments. The  $k_{cat}$  was calculated on the basis of the monomer molecular weight.

<sup>b</sup> The kinetics of RPO\_DmdD were obtained from (44). The  $k_{cat}$  of the RPO\_DmdD for acryloyl-CoA was below the limit of detection, <1.4 x 10<sup>-4</sup> s<sup>-1</sup>.

**Table 3-2.** Apparent kinetic constants for MTA-CoA hydratase activity in cell extracts of *R. lacuscaerulensis* and *E. coli* expressing recombinant AcuH.

Sample	$K_m$ (mM) <sup>a</sup>	$V_{max}$ ( $\mu\text{mol min}^{-1} \text{mg}^{-1}$ )
<i>R. lacuscaerulensis</i> cell extract	$0.01 \pm 0.007$	$0.03 \pm 0.003$
Recombinant RL_AcuH cell extract <sup>b</sup>	$0.02 \pm 0.005$	$0.05 \pm 0.19$
Recombinant RL_AcuH extract dialyzed in buffer with:		
No cofactor	$0.31 \pm 0.21$	$0.12 \pm 0.04$
ADP	$0.02 \pm 0.01$	$0.12 \pm 0.06$
ATP	$0.17 \pm 0.04$	$0.11 \pm 0.04$
AMP <sup>c</sup>	1.12	0.08
NAD	$0.46 \pm 0.08$	$0.47 \pm 0.08$
NADH <sup>c</sup>	0.11	0.03

<sup>a</sup> $K_m$  and  $V_{max}$  values ( $\pm$ SD) are representative of three replicate experiments performed using separate cell extracts and separate dialysis experiments.

<sup>b</sup> Cell extract of *E. coli* strain expressing recombinant RL\_AcuH.

<sup>c</sup>  $K_m$  and  $V_{max}$  values are representative of a single experiment performed using cell extracts collected from a single dialysis experiment.

**Table 3-3.** Effect of ADP on MTA-CoA kinetics of recombinant RL\_AcuH cell extracts.

Sample	$K_m$ (mM) <sup>a</sup>	$V_{max}$ ( $\mu\text{mol min}^{-1} \text{mg}^{-1}$ )
Recombinant RL_AcuH extract dialyzed with ADP:		
Assayed without ADP <sup>b</sup>	$0.03 \pm 0.005$	$0.25 \pm 0.03$
Assayed with ADP	$0.18 \pm 0.02$	$3.92 \pm 0.85$
Recombinant RL_AcuH extract dialyzed without ADP:		
Assayed without ADP	$0.28 \pm 0.01$	$0.04 \pm 0.008$
Assayed with ADP	$0.28 \pm 0.02$	$5.84 \pm 0.91$

<sup>a</sup>  $K_m$  and  $V_{max}$  values ( $\pm$ SD) are representative of three replicate experiments performed using cell extracts collected from a single dialysis experiment.

<sup>b</sup> Addition of 0.5 mM ADP made to enzyme assay where noted.

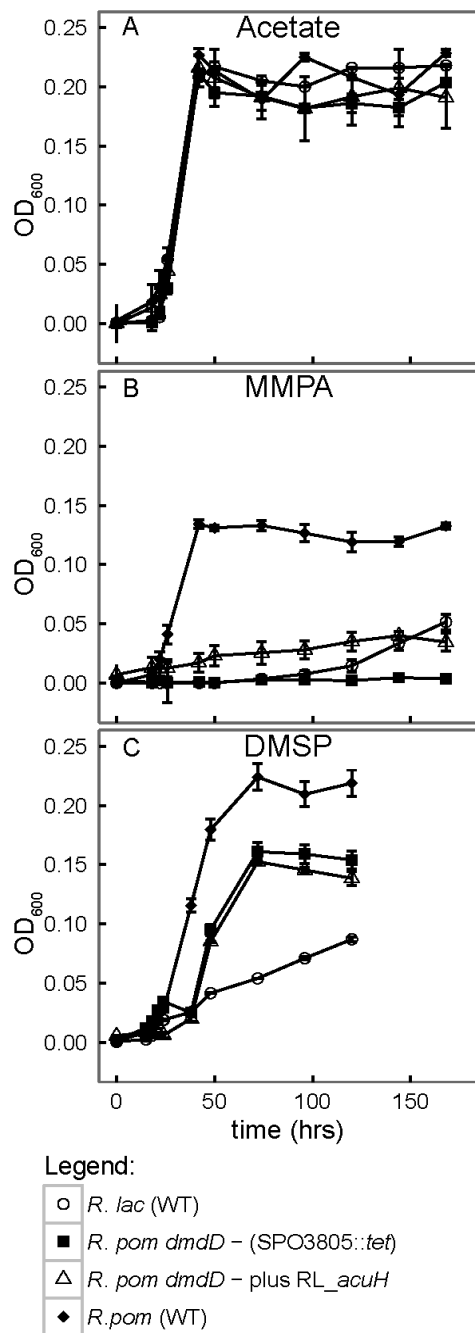


**Figure 3-6.** Growth of *R. pomeroyi* strains on acetate, MMPA, and DMSP. (●) *R. pomeroyi* wild-type (WT); (○) *R. lacuscaerulensis* wild-type (WT); (△) *R. pomeroyi dmdD*<sup>-</sup> mutant (*SPO3805::tet*); and (▲) *R. pomeroyi dmdD*<sup>-</sup> mutant complemented with *RL\_acuH*. Growth on 6 mM acetate (A), 3 mM MMPA (B), and 3 mM DMSP (C). Errors bars are ± SD of three replicates.

**Table 3-4.** Gas production during growth on DMSP and MTA-CoA hydratase specific activities of cell extracts *R. pomeroyi*, *R. lacuscaerulensis*, and *R. pomeroyi dmdD*<sup>-</sup> mutant.

	Gas Production (mM) <sup>a</sup>	
	MeSH	DMS
<i>R. pomeroyi</i>	0.08 ± 0.01	0.50 ± 0.01
<i>R. lacuscaerulensis</i>	0.02 ± 0.001 <sup>b</sup>	0.01 ± 0.001 <sup>c</sup>
<i>R. pomeroyi dmdD</i> <sup>-</sup> (SPO3805::tet)	0.036 ± 0.007	0.31 ± 0.04
<i>R. pomeroyi dmdD</i> <sup>-</sup> plus RL_acuH	0.053 ± 0.006	0.34 ± 0.04

<sup>a</sup> Gas production was measured after 96 hrs of growth on 3 mM DMSP in MBM. Errors are ± SD of three replicates.

<sup>b</sup> MeSH and DMS production of *R. lacuscaerulensis* after 300 hrs growth on DMSP was 0.03 mM ± 0.001 and 0.20 mM ± 0.13, respectively.

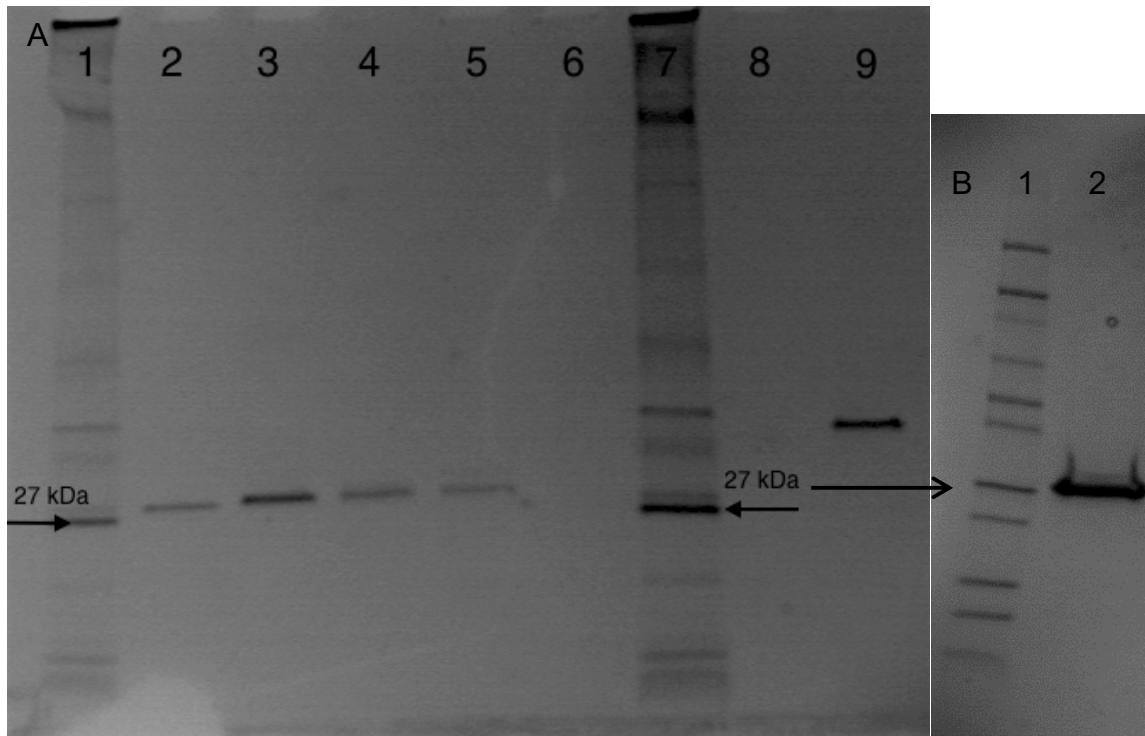


**Figure 3-7.** SDS-PAGE of His-Tag purified recombinant AcuH proteins. A: Lane 1: 2-212 kDa protein marker (NEB). Lane 2: *O. indolifex* AcuH. Lane 3: *D. shibae* AcuH. Lane 4: *P. putida* AcuH. Lane 5: *B. thailandensis* AcuH. Lane 6: Blank. Lane 7: 2-212 kDa protein marker (NEB). Lane 8. Blank. Lane 9: Purified pTricHisA vector harboring an unrelated protein, PA\_1833 oxioeducatse, from *P. aeruginosa*.

B: SDS-PAGE of His-Tag purified recombinant AcuH proteins. Lane 1: Novex Sharp Pre-stained protein marker (Thermo-Fisher). Lane 2: *B. thailandensis* AcuH.

**Table 3-5.** Apparent kinetic constants of putative AcuH enzymes for MTA-CoA and crotonyl-CoA

Substrate	Enzyme	$K_m$ (mM) <sup>a</sup>	$k_{cat}$ (s <sup>-1</sup> )	$k_{cat}/K_m$ (mM <sup>-1</sup> s <sup>-1</sup> )
MTA-CoA	OI_AcuH	8.2 ± 3.0	1.8 ± 0.3	0.21
	DS_AcuH	23 ± 12	2.0 ± 0.6	0.09
	PP_AcuH	2.0 ± 0.9	1.1 ± 0.3	0.56
	BTH_AcuH	3.7 ± 1.3	1.4 ± 0.2	0.38
	BS_AcuH	ND <sup>b</sup>	ND	ND
Crotonyl-CoA <sup>c</sup>	OI_AcuH	1.0 ± 0.3	2.5 ± 1.2 x10 <sup>6</sup>	2.6 x10 <sup>6</sup>
	DS_AcuH	2.9 ± 1.1	2.1 ± 0.5 x10 <sup>3</sup>	0.7 x10 <sup>3</sup>
	PP_AcuH	1.3 ± 0.8	3.8 ± 1.3 x10 <sup>5</sup>	2.8 x10 <sup>5</sup>
	BTH_AcuH	0.5 ± 0.1	1.0 ± 0.1 x10 <sup>6</sup>	2.0 x10 <sup>6</sup>
	BS_AcuH	0.7 ± 0.3	1.7 ± 0.6 x10 <sup>4</sup>	2.4 x10 <sup>4</sup>

<sup>a</sup> $K_m$  and  $k_{cat}$  (±SD) are representative of three replicate experiments.  $k_{cat}$  and  $k_{cat}/K_m$  values were calculated based off the molecular weight of the protein monomers

<sup>b</sup>No detectable activity (below the limit of detection, <1.4 x 10<sup>-4</sup> s<sup>-1</sup>).

<sup>c</sup>The background activity for this substrate for recombinant proteins purified from BL21 (DE3) was < 0.75% of the activity exhibited by the putative AcuH proteins in all cases. BL21 (DE3) cells do not have activity with MTA-CoA.

**Table 3-6.** Apparent kinetic constants for MTA-CoA hydratase activity in cell extracts of *E. coli* expressing recombinant AcuH.

	$K_m$ (mM) <sup>a</sup>	$V_{max}$ ( $\mu\text{mol min}^{-1} \text{mg}^{-1}$ )
RPO_AcuH	2.2	0.9
DS_AcuH	1.6	1.1
OI_AcuH	8.9	0.8
BTH_AcuH	2.5	1.5
PP_AcuH	4.8	1.7

<sup>a</sup> $K_m$  and  $V_{max}$  values are representative of the average of two replicate experiments performed using cell extracts from a single dialysis experiment.

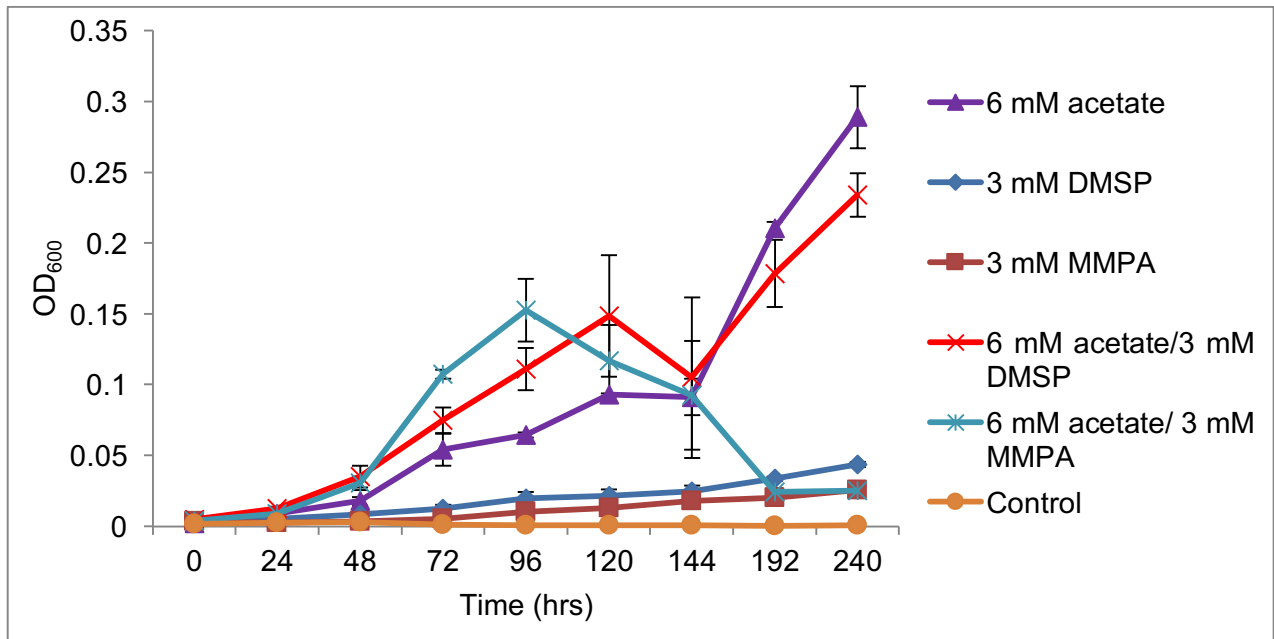


**Figure 3-8.** Growth phenotypes of *D. shibae* grown on MBM with 3 mM DMSP, 3mM MMPA, 6 mM acetate or a combination of 6mM acetate/3mM DMSP or 6 mM acetate/MMPA. The control contains *D. shibae* cells in MBM with vitamin supplement but no carbon source. Errors bars are  $\pm$  SD of three replicates.

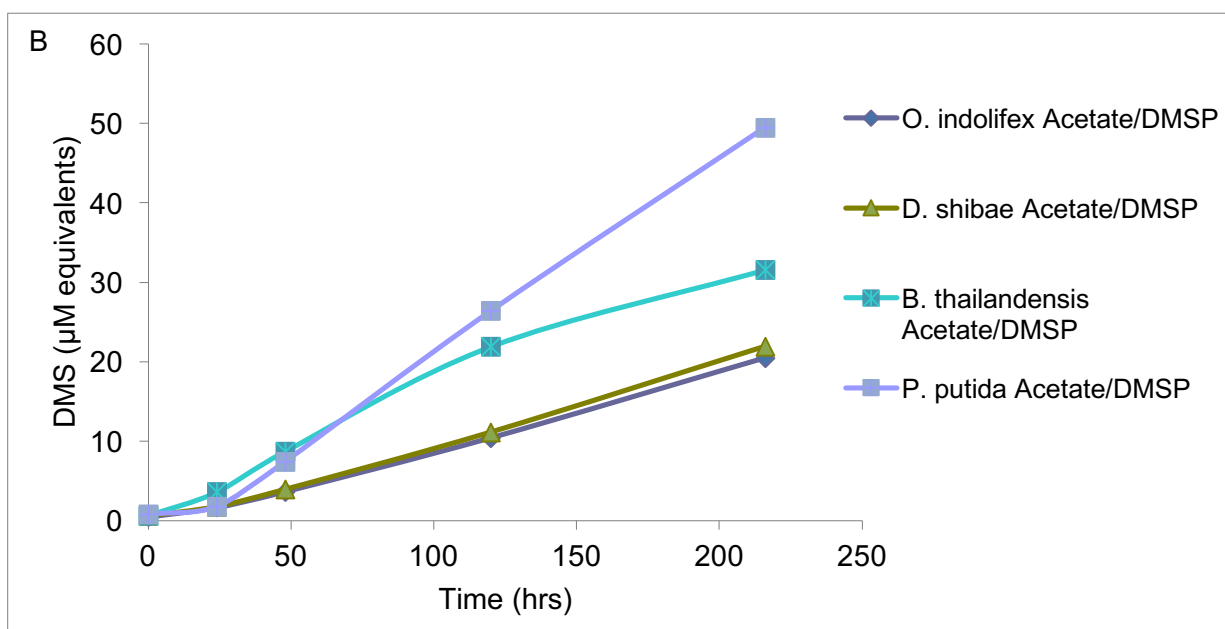
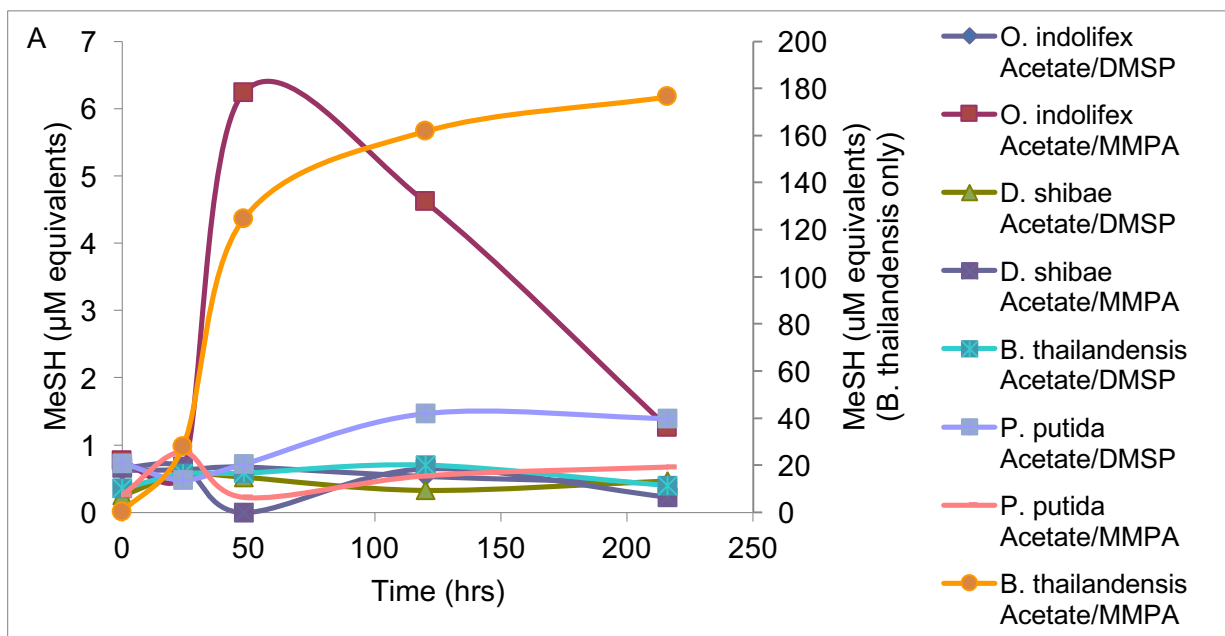


**Figure 3-9.** MeSH (A) and DMS (B) production by *O. indolifex*, *D.shibae*, *B. thailandensis* and *P. putida*. *O. indolifex* and *D.shibae* were grown on MBM with a combination of 6mM acetate/3mM DMSP or 6 mM acetate/3mM MMPA. *B. thailandensis* and *P. putida* were grown on M9 Salts with a combination of 6mM acetate/3mM DMSP or 6 mM acetate/3mM MMPA. Values are the average of two replicates. “µM equivalents” of the gaseous products were equal to

$\mu\text{mol}$  of gas per L of culture. Control samples with 6 mM acetate as a sole carbon source did not produce any gases. Cultures grown on MMPA produced no DMS.

**Table 3-7.** Growth of the *R. pomeroyi dmdD*<sup>-</sup> mutant (delD) complemented with *acuHs* from *O. indolifex* (OI), *D.shibae* (DS), *B. thailandensis* (BTH), and *P. putida* (PP).

	Acetate <sup>a</sup>	Acetate/MMPA	Acetate/DMSP
	OD <sub>600</sub> (48 hrs) <sup>b</sup>	OD <sub>600</sub> (72 hrs)	OD <sub>600</sub> (72 hrs)
<i>R. pomeroyi</i> (WT)	0.270 ± 0.004	0.183 ± 0.002	0.193 ± 0.011 (48 hrs)
<i>R. pomeroyi dmdD</i> - (SPO3805::tet)	0.272 ± 0.010	0.005 ± 0.001	0.149 ± 0.006
<i>R. pomeroyi dmdD</i> - plus BTH_ <i>acuH</i>	0.232 ± 0.002 (72 hrs)	0.003 ± 0.001	0.191 ± 0.002 (96 hrs)
<i>R. pomeroyi dmdD</i> - plus OI_ <i>acuH</i>	0.250 ± 0.006	0.002 ± 0.001	0.185 ± 0.008
<i>R. pomeroyi dmdD</i> - plus DS_ <i>acuH</i>	0.217 ± 0.004	0.004 ± 0.001	0.181 ± 0.004
<i>R. pomeroyi dmdD</i> - plus PP_ <i>acuH</i>	0.208 ± 0.008	0.005 ± 0.003	0.186 ± 0.005

<sup>a</sup> Growth on a combination of 6mM acetate/3mM DMSP or 6 mM acetate/3mM MMPA in MBM. Errors are ± SD of three replicates.

<sup>b</sup> Absorbance reported is the highest absorbance recorded for each set of samples. Variations in the time point reported are noted.

**Table 3-8.** MeSH and DMS production of the *R. pomeroyi dmdD*<sup>-</sup> mutant (delD) complemented with *acuHs* from *O. indolifex* (OI), *D.shibae* (DS), *B. thailandensis* (BTH), and *P. putida* (PP).

	Gas Production ( $\mu\text{M}$ ) <sup>a</sup>		
	Acetate/MMPA	Acetate/DMSP	
	MeSH	MeSH	DMS
<i>R. pomeroyi</i> (WT)	490 $\pm$ 5.1	204 $\pm$ 10	940 $\pm$ 34
<i>R. pomeroyi dmdD</i> <sup>-</sup> (SPO3805::tet)	7.13 $\pm$ 0.4	69.1 $\pm$ 5.7	502 $\pm$ 22
<i>R. pomeroyi dmdD</i> <sup>-</sup> plus BTH_ <i>acuH</i>	11.2 $\pm$ 0.7	43.3 $\pm$ 2.1	466 $\pm$ 19
<i>R. pomeroyi dmdD</i> <sup>-</sup> plus OI_ <i>acuH</i>	11.2 $\pm$ 0.2	65.4 $\pm$ 11	477 $\pm$ 37
<i>R. pomeroyi dmdD</i> <sup>-</sup> plus DS_ <i>acuH</i>	6.30 $\pm$ 1.1	103 $\pm$ 12	593 $\pm$ 33
<i>R. pomeroyi dmdD</i> <sup>-</sup> plus PP_ <i>acuH</i>	9.98 $\pm$ 2.2	77.7 $\pm$ 4.3	532 $\pm$ 13

<sup>a</sup> Gas production was measured after 96 hrs of growth on a combination of 6mM acetate/3mM DMSP or 6 mM acetate/3mM MMPA in MBM. Errors are  $\pm$  SD of three replicates.

Control samples with 6 mM acetate as a sole carbon source did not produce any gases. Samples grown on acetate/MMPA produced no DMS.

## CHAPTER 4

### POTENTIAL REGULATORS OF DIMETHYLSULFONIOPROPIONATE DEMETHYLATION IN *RUEGERIA POMEROYI* DSS-3: TETRAHYDROFOLATE AVAILABILITY AND DMDB ACETYLATION

#### **Introduction**

The marine Alphaproteobacteria *Ruegeria pomeroyi* DSS-3 is able to metabolize dimethylsulfoniopropionate (DMSP) via either the demethylation pathway or the cleavage pathway (1-3). Since DMSP metabolized via the cleavage pathway produces the climatically active gas dimethyl sulfide (DMS), any factors that affect use of this pathway or the demethylation pathway will also affect the input of DMS to the atmosphere (4, 5). The proposed uses of DMSP by *R. pomeroyi* include roles as carbon and reduced sulfur sources (2, 6, 7) as well as an osmolyte and antioxidant (8-10). The use of DMSP may vary based on the physiological status of the bacterial cell or outside environmental factors. The recent identification of the enzymes of the DMSP demethylation and cleavage pathways has provided greater insight into potential points for the regulation of these pathways (2, 11-13).

A model for the regulation of the DmdB isozymes in *R. pomeroyi*, with implications for the regulation of the demethylation pathway as a whole, was proposed in (14), reproduced here as Chapter 2. In this model, the DmdB isozymes (RPO\_DmdB1 and RPO\_DmdB2) appear to be major regulatory points in DMSP metabolism. While both enzymes were inhibited by high cellular concentrations of DMSP, RPO\_DmdB1 regained activity in the presence of increasing ADP concentrations, suggesting that it was responsive to cellular energy charge, and

RPO\_DmdB2 regained activity in the presence of high levels of MMPA (14, 15). In the case of RPO\_DmdB1, it was predicted that carbon and energy limitation would result in a decrease in cellular energy charge, increasing ADP levels, which would stimulate RPO\_DmdB1 activity (14). Stimulation of RPO\_DmdB2 activity would be a result of changes in DmdA activity affecting the concentration of MMPA. The availability of free tetrahydrofolate (THF) and the turnover of methyl-THF in *R. pomeroiyi* were proposed to set DmdA activity levels and affect use of the demethylation pathway (14). THF is used as the methyl acceptor by DmdA in the reaction producing MMPA (6, 10). It is predicted that limiting the concentration of free THF available to *R. pomeroiyi* or slow turnover of methyl-THF will block the demethylation and cause increased utilization of the cleavage pathway.

In addition to the role of THF, another possible regulatory mechanism is the reversible acetylation of the active site residue  $N^\epsilon$ -lysine (Lys) of the DmdB isozymes. Reversible  $N^\epsilon$ -Lys acetylation is a form of post translational modification that has been shown to regulate carbon metabolism, protein synthesis, and transcription in many organisms. This method of modulating protein activity regulates CoA ligases as well as many other proteins (16-18). Acetyl-CoA dependent acetyltransferases, called Gcn5-like protein *N*-acetyltransferases (GNATs or Pats) are members of the histone acetyltransferase superfamily and are conserved in all domains of life (18). GNATs use acetyl-CoA to acetylate CoA ligases via transfer of the acetyl group to an  $N^\epsilon$ -Lys of the protein, either reducing or eliminating the target CoA ligase activity. This regulation is thought to be a rapid means of dealing with changes in homeostasis, with the goal of maintaining the energy balance within the cell (19, 20). Acetylation may be reversed by a deacetylase in a  $NAD^+$  dependent reaction (18, 21).

This chapter describes the initial steps to verifying the DmdB regulation model and further investigating potential regulators of the demethylation pathway.

## Materials and Methods

**Strains and Culture Conditions.** *R. pomeroyi* DSS-3 was grown on ½ YTSS or in defined marine basal minimal medium (MBM) at 30 °C (22, 23). *Escherichia coli*, including recombinant strains, were grown on Luria Bertani (LB) or defined M9 salts minimal medium at 30°C or 37°C. When minimal medium was used, 6 mM acetate, 3 mM glucose, DMSP, or MMPA (Alfa Aesar) was added as a sole carbon source. For growth experiments, cultures were incubated at 30 °C, and the absorbance was measured at 600 nm in a Thermo Scientific Genesys 20 spectrophotometer. DMSP was synthesized using the method described in Chambers *et al.*, 1987 (24).

**Construction of In-frame deletions.** This method was adapted from a *Rhodopseudomonas palustris* deletion protocol provided by C. VanDrisse from the Escalante lab. An overview of the processes is provided in Figure 4-1A. Primers sets were designed to amplify regions 1 kb upstream (Primers delA and delB) and 1 kb downstream (Primers delC and delD) of the target gene, either SPO0677 (RPO\_ *dmdB1*) or SPO2045 (RPO\_ *dmdB2*). Primers delB and delC were designed to contain an overlapping region of 20-24 bases from the gene to be deleted that comprised the fusion site (Figure 4-1B). The upstream and downstream fragments were amplified by PCR. The resultant amplicons were then fused using overlap-extension PCR and primers delA and delD (25). The fusion product was cloned in the vector pK18*obsacB* using the BamHI and XbaI restriction sites and then transformed via heat shock into TOP10 cells. Uptake of pK18*obsacB* was selected for in LB medium + 25 µg/µl kanamycin (kan).

Once propagated in the TOP10 cells, the pK18*mobsacB* deletion plasmid was methylated using CpG methyltransferase (M. SssI) per manufacturer instructions (NEB) and electroporated into *R. pomeroyi* (26). Cells were suspended in 400  $\mu$ l  $\frac{1}{2}$  YTSS and incubated at 30°C for 3 hrs prior to plating on  $\frac{1}{2}$  YTSS + 80  $\mu$ g/ $\mu$ l kan. Plates were incubated at 30°C for up to one week, though colonies typically began appearing after three days. Colonies were restreaked onto MBM containing 3 mM sucrose and MBM containing 6 mM acetate + 80  $\mu$ g/ $\mu$ l kan. Growth on 3 mM sucrose selected for loss of the pK18*mobsacB* plasmid as the *sacB* gene conveys sensitivity to sucrose. Colonies that grew on the sucrose containing plates were picked using sterile toothpicks and patched onto  $\frac{1}{2}$  YTSS and  $\frac{1}{2}$  YTSS + 80  $\mu$ g/ $\mu$ l kan. Kanamycin-sensitive colonies were screen for loss of the target gene by colony PCR and later verified by sequencing.

**RPO\_DmdB Purification and Activity Assays.** RPO\_DmdB1 and RPO\_DmdB2 were purified using the same protocols described in Chapter 2 (14). DmdB activity assays were performed as described in Chapter 2 (14). Briefly, reactions contained the 0.2mM CoA, 2 mM ATP, MgCl<sub>2</sub>, MMPA, and 10  $\mu$ l of the acetylated DmdB sample. Reactions were run for two or five minutes and quenched by the addition of 4  $\mu$ l 10% phosphoric acid. MMPA-CoA production was analyzed by HPLC as previously described.

**Identification, Cloning, and Purification of Potential *R. pomeroyi* Acetylase and Deacetylases.** Potential GNATs were initially identified from the *R. pomeroyi* genome using the Function Search on [img.jgi.doe.gov](http://img.jgi.doe.gov) with Pfam00583 as the protein family query for GNATs. All proteins annotated as acetyltransferases in the *R. pomeroyi* genome were also checked for GNAT domains. Potential deacetylases were identified based on amino acid sequence similarity to known deacetylases from *Rhodospseudomonas palustris*, *Salmonella enterica*, and *Streptomyces lividins*. All potential GNATs were amplified from the *R. pomeroyi* genome and cloned into the

pTEV6 vector by C. VanDrissie using the method described in Galloway *et al.*, 2013 (27).

Deacetylases were cloned into pET101 by H. Bullock using the standard protocol from Invitrogen. Deacetylases and GNATs were cloned to include an N-terminal his-tag. All proteins were overexpressed in *E. coli* BL21 (DE3) cells and purified using Ni-NTA resin.

**Acetylation Assays.** Acetylation assays were performed by C. VanDrissie using the standard Escalante lab protocol. Reactions were performed in 50 mM sodium HEPES buffer at pH 7 and included 1 mM Tris(2-carboxyethyl)phosphine HCl (TCEP), 20  $\mu$ M radiolabeled [ $^{14}$ C] acetyl-CoA, 1  $\mu$ M *Rhodospseudomonas palustris* Pat (*RpPat*), 1  $\mu$ M of RPO\_Dmdb1 or RPO\_Dmdb2 from *R. pomeroyi*, and H<sub>2</sub>O for a total reaction volume of 100  $\mu$ l. Controls for self-acetylation included all reaction components except for *RpPat*. A positive control included the benzoyl-CoA synthetase BadA from *R. palustris*. All samples were incubated at 37°C for one hour. Once samples had cooled to room temperature, DNA loading dye (Fermentas) was added to the samples. Samples were analyzed by SDS-PAGE, the resulting gels were stained with Coomassie Blue, exposed overnight, and imaged using the Typhoon Biomolecular Imager. Preparations of acetylated RPO\_Dmdb2 to check the CoA ligase activity were treated using the same protocol but with unlabeled acetyl-CoA.

**Deacetylation Assays.** Deacetylation assays were performed by C. VanDrissie using the standard Escalante lab deacetylation protocol. RPO\_Dmdb2 was first acetylated using the protocol described above. The RPO\_Dmdb2 acetylation reaction sample was subjected to buffer exchange using 10 mM sodium HEPES (pH 7) prior to initiation of the deacetylase assays. Deacetylation reactions were performed in 50 mM sodium HEPES buffer (pH 7) with 1x of the acetylated RPO\_Dmdb2 mixture, 1  $\mu$ M of the purified deacetylase, and H<sub>2</sub>O up to a volume of

25  $\mu$ l. The positive control contained the CobB deacetylase in place of the putative deacetylase from *R. pomeroyi*. The negative control contained no deacetylase.

**Effect of Trimethoprim on Growth and Gas Production.** Trimethoprim (Sigma) at concentrations of 0, 0.5, 1.0, 2.0, or 4.0  $\mu$ g/ml was added to *R. pomeroyi* cultures growing on MBM with 3 mM DMSP or 3 mM acetate provided as the sole carbon sources. Growth was measured at Abs 600 nm. The 3 ml cultures were inoculated with 1,000 *R. pomeroyi* cells that had been initially grown in MBM with 3 mM acetate. When required, 0.025 mM adenine, 0.025 mM guanine, and 0.1 mM methionine (Sigma) were added at the start of the growth experiment.

MeSH and DMS production were measured by gas chromatography using a SRI 8610-C gas chromatograph fitted with a Chromasil 330 column (Supleco). The carrier gas was N<sub>2</sub> at a flow rate of 60 ml min<sup>-1</sup> and an oven temperature of 60°C. Measurements were made using a flame photometric detector and the Peak Simple software (SRI Instruments). MeSH and DMS standard curves were produced as described in Chapter 3. MeSH and DMS production were measured using cultures grown on MBM in 160ml serum bottles fitted with 20 ml side arms for monitoring absorbance. One milliliter of headspace was injected onto the GC using gas tight 1 ml syringes (Henke-Sass, Wolf).

#### **Sapelo Island Environmental Sample Collection and Treatment with Trimethoprim.**

One hundred milliliters of seawater was added to 160 ml serum bottles. Bottles were sealed immediately after the addition of the seawater. The sterile serum bottles contained 0  $\mu$ M, 2  $\mu$ M, or 20  $\mu$ M DMSP and 0  $\mu$ g/ml, 0.1  $\mu$ g/ml, or 1  $\mu$ g/ml TMP. Each combination (e.g 2  $\mu$ M DMSP + 0  $\mu$ g/ml TMP, 2  $\mu$ M DMSP + 0.1  $\mu$ g/ml TMP, 2  $\mu$ M DMSP + 1  $\mu$ g/ml TMP) was prepared and analyzed in triplicate. In the killed cell control samples, a final concentration of 2% borate-

buffered formalin was added immediately after the addition of the 100 ml seawater sample.

MeSH and DMS production were measured in the manner described above.

**Assays of THF-dependent enzymes.** *R. pomeroyi* cells were grown in MBM with 6 mM acetate or 3 mM DMSP as a sole carbon source. Cells were harvested and lysed via sonication and then stored under nitrogen gas for the assays. All the reagents and components for the enzyme assays were prepared anaerobically and stored under nitrogen gas once removed from the anaerobic chamber. Cuvettes used for the enzyme assays were sealed with red stoppers, and all additional reactions components not added in the chamber were added using a syringe. This helped to ensure that the reactions were exposed to as little oxygen as possible. In all cases, a sample without the addition of crude cell extract was run to correct for any background activity.

**Formate Dehydrogenase Assay.** Enzyme assay was carried out as described in the Sigma Aldrich Enzymatic Assay of Formate Dehydrogenase protocol (28). The assay was adapted to a 1 ml volume. Assays included 50 mM NaHPO<sub>4</sub> buffer (pH 7), 4 mM sodium formate, 60 μM NAD, and 1 μg of crude cell extract. The reaction was catalyzed by the addition of the crude cell extract and incubated at 37°C in the spectrophotometer while tracking the change in absorbance at 340 nm for the conversion of NAD to NADH.

**Methylene-THF Reductase.** Enzyme assay was performed as described by Matthews and Haywood 1979 (29). The reverse reaction was assayed: NADPH + H<sup>+</sup> +methylene-THF →NADP<sup>+</sup> + methyl-THF. Methylene-THF was prepared by the method described in (29, 30). Briefly, THF was dissolved anaerobically in 0.05 M ammonium carbonate (pH 9) in 50 mM formaldehyde. The concentration of methylene-THF was calculated at absorbance 300nm using the extinction coefficient 32000 M<sup>-1</sup> cm<sup>-1</sup>. The enzymatic reaction was carried out at 37°C in 50 mM NaHPO<sub>4</sub> buffer (pH 7) with 0.3 mM EDTA, 1 μg FAD, 50 mM β-mercaptoethanol, 60 μM

methylene-THF, and 0.2 mM NADPH. Assays were initiated by the addition of 20  $\mu$ M crude cell extract. Activity was measured by the change in absorbance at 340 nm. Rates were calculated using the NADPH extinction coefficient, 6,220  $M^{-1} \text{ cm}^{-1}$  (31).

**Methylene-THF Dehydrogenase.** Enzyme assays were performed as described by (32). Reactions contained 50 mM  $\text{NaHPO}_4$  buffer (pH 7), 60  $\mu$ M methylene-THF, synthesized as described above, 0.2 mM  $\text{NADP}^+$ , and 1  $\mu$ g crude cell extract. After addition of the enzyme, the reaction mixture was incubated for 10 minutes at 37°C, and then the reaction was stopped by the addition of 10% HCl. Samples were centrifuged to remove the precipitated protein, and then the absorbance was read at 350 nm. The amount of methenyl-THF produced was calculated using the extinction coefficient of 24,900  $M^{-1} \text{ cm}^{-1}$ .

**Methenyl-THF Cyclohydrolase.** Enzyme assays were performed as described by (33). Reactions were performed in 200 mM potassium maleate buffer (pH 7.5), with 50 mM  $\beta$ -mercaptoethanol, methenyl-THF formed by the methylene-THF dehydrogenase reaction, and 1  $\mu$ g crude cell extract. The change in absorbance at 350 nm was observed to calculate enzyme activity. The change in concentration of methenyl-THF was calculated using the extinction coefficient of 24,900  $M^{-1} \text{ cm}^{-1}$ . This assay was coupled with the previous methylene-THF dehydrogenase assay due to the instability of the methenyl-THF intermediate. When coupled assays were run to measure methenyl-THF cyclohydrolase activity, the methylene-THF assay was not stopped with 10% HCl, but run until the substrate methylene-THF was exhausted.

## Results

**In-frame Deletions of RPO\_ *dmdB1* and RPO\_ *dmdB2*.** Attempts were made to create in-frame deletions of RPO\_ *dmdB1* (SPO0677) and RPO\_ *dmdB2* (SPO2045) in *R. pomeroyi* to

assess the effect each of these have on the use of the demethylation pathway. Multiple in-frame deletion systems were tested, including the RED recombinase system, Flp-*FRT* recombination system, and a method using *sacB* counter-selection for generation of a markerless in-frame deletion (34-38). The RED recombinase and Flp-*FRT* recombination systems were unsuccessful in *R. pomeroyi* as removal of the antibiotic resistance gene was not achieved. The method utilizing *sacB*, which conveys sensitivity to sucrose, initially appeared to have been successful. However, analysis of the growth phenotypes of mutants generated using this system yielded unexpected and unlikely results, described below. When verified by sequencing, the genome possessed the expected scar sequences for the deletions of RPO\_ *dmdB1* and RPO\_ *dmdB2*.

The growth of the RPO\_ *dmdB1*<sup>-</sup> and RPO\_ *dmdB2*<sup>-</sup> deletion mutants was then examined on MBM with 3 mM glucose, 6 mM acetate, 3 mM DMSP, or 3 mM MMPA as sole carbon sources. A RPO\_ *dmdB1*<sup>-</sup> deletion strain was unable to grow on any carbon source other than glucose (Figure 4-2). The growth of the RPO\_ *dmdB1*<sup>-</sup> deletion strain on glucose also displayed a lower final OD<sub>600</sub> than the *R. pomeroyi* wild-type. The in-frame deletion of RPO\_ *dmdB2* showed much the same result. Growth on glucose, while delayed ~8 hours in the mutant compared with the wild-type, ultimately reached the same final OD<sub>600</sub> as the wild-type. The RPO\_ *dmdB2*<sup>-</sup> deletion strain eventually grew on acetate after 53 hours but not on DMSP or MMPA (Figure 4-3). These results were unexpected as previous experiments had shown the deletion of RPO\_ *dmdB2* using the SLIC system resulted in no change in phenotype for growth on DMSP and only a slight delay in growth on MMPA (2). As *R. pomeroyi* possess two *dmdBs*, it is unexpected that deleting one would result in total loss of the ability to grown on DMSP or MMPA. The deletion of either *dmdB* was also not expected to substantially affect growth on acetate. Based on these results, it was concluded that the *sacB* based counter selection step had

resulted in selection for mutations elsewhere in the genome, as had been noted in previous studies (39, 40). If in-frame deletions are to be a part of future studies, another method will have to be identified.

**Effect of free THF Availability on DMS Production.** In the model presented in Figure 2-8 (DmdB model), it is predicted that the availability of free THF and the turnover of CH<sub>3</sub>-THF in *R. pomeroyi* play regulatory roles in the DMSP methylation pathway. To test this hypothesis, the final step of THF biosynthesis, mediated by the enzyme dihydrofolate reductase, was repressed using the bacteriostatic inhibitor trimethoprim (TMP). It was predicted that limitation of the availability of free THF would inhibit the demethylation pathway, leading to relatively more DMSP processed by the cleavage pathway. Additions of TMP less than or equal to 1.0 µg/ml to *R. pomeroyi* cultures grown in MBM with 3mM acetate did not significantly affect growth. However, 1 µg/ml of TMP was somewhat inhibitory towards growth on DMSP yet still allowed for sufficient growth to examine effects on DMS production (Figure 4-4).

DMS production was measured in *R. pomeroyi* cultures grown on DMSP with 0, 0.1 , or 1.0 µg/ml TMP. Cultures that contained 0.1 µg/ml TMP produced higher amounts of DMS than cultures with 1 µg/ml or 0 µg/ml TMP (Figure 4-5 A). Peak DMS production was reached after just 48 hrs of growth in the 0.1 µg/ml TMP samples while the 0 µg/ml and 1.0 µg/ml TMP samples only reached peak DMS production after 96 hrs of growth. The similar DMS production exhibited by the 0 µg/ml TMP and 1.0 µg/ml TMP cultures may have been a consequence of the growth inhibition caused by the higher TMP concentration (Figure 4-4). These data suggested that changes to the available THF in the cell impacted use of the demethylation pathway. To further test this hypothesis, 0.025 mM adenine, 0.025 mM guanine, and 0.1 mM methionine were added to cultures. These additions were intended to reduce the demand for methyl-THF for

adenine, guanine, and methionine biosynthesis (35) (41). The addition of adenine, guanine, and methionine resulted in increased DMS production in the 0  $\mu\text{g/ml}$  and 1.0  $\mu\text{g/ml}$  TMP samples (Figure 4-5 A). This may be due to decreased availability of free THF or an increase in the growth yield of the cultures due to the addition of adenine, guanine, and methionine (Figure 4-5 (B) dotted lines).

**Effect of TMP on DMS Production in Environmental Samples.** Ocean water samples from Sapelo Island, GA were used to test whether the effect of TMP on DMS production in pure laboratory cultures was also observed in environmental samples. Samples were incubated with 0  $\mu\text{M}$ , 2  $\mu\text{M}$ , or 20  $\mu\text{M}$  DMSP, and the addition of 0  $\mu\text{g/ml}$ , 0.1  $\mu\text{g/ml}$ , or 1.0  $\mu\text{g/ml}$  of TMP. Slightly increased DMS production in samples containing 0.1  $\mu\text{g/ml}$  TMP was observed for the 2  $\mu\text{M}$  and 20  $\mu\text{M}$  DMSP samples (Figure 4-6). The 20  $\mu\text{M}$  DMSP samples displayed a pattern most similar to that observed in the pure culture samples. In this case, the 0.1  $\mu\text{g/ml}$  TMP treatment produced the most DMS, while the 1.0  $\mu\text{g/ml}$  TMP treatment produced the least, potentially due to inhibition of the bacteria cells within the sample (Figure 4-6). However, several inconsistencies in the data make this experiment difficult to interpret. The production of DMS by the killed cell samples and the production of nearly 50  $\mu\text{M}$  DMS by the 20  $\mu\text{M}$  DMSP samples indicate potential problems with the experiment. The higher DMS levels produced by the killed cells and the 20  $\mu\text{M}$  DMSP samples may be caused by extra DMSP/DMS added to the bottles from the environment or an error during experimental setup. Additionally, when samples were hydrolyzed at the conclusion of the experiment only small amounts of DMS were observed in the killed cell samples when nearly all of the originally DMSP added to the serum bottles should have been hydrolyzed to DMS (Figure 4-6). This experiment will need to be repeated for further verification.

**Methyl-THF Utilization.** The turnover of methyl-THF is hypothesized to be involved in the regulation of the demethylation pathway in *R. pomeroyi*. RNA-Seq analysis of the expression levels for genes involved in THF biosynthesis and oxidation revealed that their expression was not significantly altered during growth on DMSP as compared with acetate, with the exception of formate-THF ligase and formate dehydrogenase. However, the activity of the enzymes involved in methyl-THF oxidation may be altered during growth on DMSP (Figure 4-7, overview). The activities of methylene-THF reductase, methylene-THF dehydrogenase, methenyl-THF cyclohydrolase, and formate dehydrogenase were analyzed after growth on DMSP. The specific activities of the methylene-THF reductase and formate dehydrogenase were two-fold higher in cell-free extracts of DMSP-grown cells compared with acetate grown cells. The same pattern, however, was not observed for the other THF oxidation enzymes tested (Figure 4-8). The specific activities of methylene-THF dehydrogenase and methenyl-THF cyclohydrolase from cells grown on acetate or DMSP were not significantly different. These experiments were only conducted once, replication will be needed before they results can be verified. The use of chemostat, rather than batch culture, grown cells may also produce a different result and will need to be tested.

**Acetylation of DmdB.** Acetylation is a form of post-translational modification that is often used to slow consumption of ATP and CoA as the availability of cellular energy decreases. The following experiments were conducted in collaboration with the Escalante Lab at the University of Georgia. Experiments performed by Chelsey VanDrisse are noted. The susceptibility of RPO\_DmdB1 and RPO\_DmdB2 to regulation by acetylation was originally tested by C. VanDrisse using known protein acetyltransferases (Pats) from other microorganisms, including *Rhodospseudomonas palustris* (*RpPatA*), *Salmonella enterica* (*SePat*),

*Bacillus subtilis* (AcuA), and *Streptomyces lividans* (SIPatA and SIPatPro). These Pats are a GCN-5 type N-acetyltransferases (GNATs) which catalyze the reversible acetylation of the N<sup>ε</sup>-lysine of proteins. This is accomplished via the transfer of an acetyl group from acetyl-CoA to the primary amine of a protein. Only *RpPat* was able to acetylate RPO\_Dmdb2 (Figure 4-9, bottom gel). *R. palustris* is an Alphaproteobacteria and the most genetically similar to *R. pomeroyi*. The presence of a band in the bottom gel of Figure 4-9 indicates the acetylation of the protein, based on the presence of the radiolabeled acetyl group from acetyl-CoA. The positive controls for all other Pats worked correctly, indicating that a lack of functionality of the other Pats was not the reason they failed to acetylate RPO\_Dmdb2 (Figure 4-9). C. VanDrisse verified this initial result with RPO\_Dmdb2 and tested the ability of *RpPat* to acetylate RPO\_Dmdb1 (Figure 4-10). Purified RPO\_Dmdb1, however, was not stable enough for the acetylation experiments. Further experiments were only conducted using RPO\_Dmdb2.

The acetylation of RPO\_Dmdb2 was expected to substantially decrease CoA ligase activity. RPO\_Dmdb2 was acetylated using unradiolabeled acetyl-CoA so that the activity of the protein could be tested using the HPLC enzyme assay (14). These assays all used MMPA as a substrate. Activity assays of RPO\_Dmdb2 acetylated by *RpPat* show a 60% decreased in CoA ligase activity compared with the un-acetylated control (Figure 4-11). Controls that included only RPO\_Dmdb2 with *RpPat* or with only acetyl-CoA did not show any change in RPO\_Dmdb2 activity. Likewise, assays to test for “acetylation” by MMPA (MMPAylation) did not affect RPO\_Dmdb2 activity nor did the treatment of RPO\_Dmdb2 with the same reaction mixture used for acetylation but without *RpPat* or acetyl CoA. Assays were run for two and five minutes to ensure that the results were consistent over time.

***R. pomeroyi* GNATs.** A total of 28 acetyltransferases with GNAT domains were identified from the *R. pomeroyi* genome (Table 4-1). These were cloned into the pTEV5 vector, over-expressed in *E. coli* BL21 (DE3), and purified by C. VanDrisse. However, none of the 21 acetyltransferases from *R. pomeroyi* tested thus far have catalyzed the acetylation of RPO\_DmdB2 (Figure 4-12). Five GNATs showed reduced expression during growth on DMSP or MMPA based on RNA-Seq data (SPO2003, SPO3248, SPO3628, SPO3249, and SPO3247), suggesting that these could play a role in acetylating RPO\_DmdB2 when DMSP and MMPA are not present. However, these GNATs also did not acetylate RPO\_DmdB2.

**DmdB Deacetylation.** The acetylation of a protein may be reversible by a deacetylase. Potential deacetylases were selected based on amino acid sequence similarity to known deacetylases and upregulation during growth on DMSP in RNA-Seq expression data (Table 4-2). Potential deacetylases were cloned into *E. coli* BL21 (DE3) using the Champion pET101 cloning kit (Invitrogen). Acetylation and deacetylation assays were performed by C. VanDrisse and RPO\_DmdB2 activity assays were performed by H. Bullock. The acetylation of RPO\_DmdB2 was reversed by the deacetylases SPO3195 and SPO0872 as well as the CobB deacetylase from *S. enterica*. Deacetylation by SPO0872 restored RPO\_DmdB2 activity to 100% while SPO3195 and CobB restored up to 80% of the activity (Figure 4-13). These data suggest that RPO\_DmdB2 could be regulated by acetylation but the correct GNAT/Pat protein still needs to be identified.

## **Discussion**

The enzymes involved in the demethylation pathway have only recently been identified, as a result the work towards understanding the regulation of this pathway has just begun (2). Since DMSP has many proposed roles within the bacteria cell, as a(n) carbon source, reduced

sulfur source (2, 6, 7), osmolyte, and antioxidant (8-10), the rate of DMSP metabolism and choice of pathway could vary greatly depending upon the environmental conditions. The high intracellular concentration of DMPS maintained in *R. pomeroyi* cells (around 70 mM), would be useful if DMSP was needed as an antioxidant or osmolyte (10). This stored DMSP may also be used as carbon and energy source when necessary, as proposed in Bullock *et al.*, 2014 (14), or simply as a supplementary carbon and sulfur source. The changing dynamics of DMSP concentration in the marine environment means that at times DMSP can be an abundant carbon and sulfur source, while at other points it may be scarce. As a result, it would be important for marine bacteria like *R. pomeroyi* to be able to control the activity level of the DMSP metabolic pathways. Since any DMSP that is metabolized via the demethylation pathway will not produce DMS, understanding the factors that influence the use of the demethylation or cleavage pathways is key to fully understanding the role of DMSP in the global sulfur cycle and climate. Based on the previous study of the DmdB enzymes, it appears that DmdB is a major regulatory point in *R. pomeroyi* DMSP metabolism (14). The model proposed for the regulation of the DmdB isozymes in *R. pomeroyi* suggests that these isozymes are regulated by cellular energy charge in the case of RPO\_DmdB1 and MMPA levels in the case of RPO\_DmdB2. The MMPA levels within the cell are set by the activity of DmdA. It is predicted that the levels of DmdA activity are set by the availability of THF and methyl-THF (14).

The initial approach planned for analyzing the roles of the two DmdBs in *R. pomeroyi* was to create in-frame, markerless deletions of RPO\_ *dmdB1* and RPO\_ *dmdB2* individually and then create a double *dmdB* deletion strain. As a successful in-frame and markerless deletion system for *R. pomeroyi* has not yet been identified, other methods were used to investigate the regulation of DmdB. Since the activity of DmdA will play a role in the activity of the DmdB

isozymes, we first looked into effect that the availability of free THF has on the use of the demethylation pathway. The availability of free THF does appear to have some influence on the use of the demethylation pathway as inhibition of THF biosynthesis by TMP increase the production of DMS during growth on DMSP. This increase in DMS production indicates increased use of the cleavage pathway.

The turnover of methyl-THF is also proposed to influence levels of DmdA activity. The activities of methylene-THF dehydrogenase and methenyl-THF cyclohydrolase varied little between *R. pomeroyi* cultures grown on DMSP or acetate as the sole carbon source. The activities of methylene-THF reductase, which catalyzes the conversion of 5-methyl-THF to 5,10-methylene-THF, and formate dehydrogenase were two-fold higher in cells grown on DMSP compared with those grown on acetate. Methyl-THF is used in the biosynthesis of methionine by methionine synthase, though the methyl group for methionine biosynthesis may also come from MeSH via the enzyme cystathionine gamma synthase (42-44). The turnover of this methyl-THF for methionine biosynthesis or via oxidation to 5,10-methylene-THF will affect the rates of DmdA activity and thus the amount of MMPA produced by the cell. If a cell needs to grow largely on DMSP for any reason it will be important for the cell to be able to continually turnover methyl-THF to maintain DmdA activity at high levels.

Formate dehydrogenase activity also increased in cell extracts grown on DMSP. This could be a result of the formation of formaldehyde from the oxidation of MeSH during the final reaction of the demethylation pathway (2, 45). Formaldehyde may be oxidized to formate via various reactions (46). Formaldehyde may also react with tetrahydrofolate to produce 5,10-methylene-THF. In some bacterial species, the oxidation of formaldehyde directly to formate has been observed, catalyzed by a formaldehyde dehydrogenase (46, 47). It has been noted in

methanotrophs and methylotrophs that the THF- linked pathway for formaldehyde detoxification is upregulated when methane or methanol is present, likely due to the potential for formaldehyde formation from the oxidation of these compounds (48). This follows nearly the same pathway outlined in Figure 4-7. Formyl-THF is hydrolyzed by the formate THF-ligase to produce formate and free THF. These data support the proposed model for the regulation of DmdB activity.

One avenue that had not previously been investigated is the possibility that the DmdB enzymes are regulated by post-translational modification. Acetylation, one type of post-translational modification, by a GCN-5 type N-acetyltransferase (GNAT) is one possibility (18). The GNAT-type acetyltransferases catalyze the reversible acetylation of proteins by the transfer of an acetyl group from acetyl-CoA to the N<sup>ε</sup>-lysine of the primary amine of a protein. This will either inactivate or substantially lower the activity of the target protein. In the case of ATP-dependent CoA ligases like DmdB, acetylation can slow the use of ATP and CoA as cellular energy decreases or potentially if there is an imbalance in the CoA pools within the bacterial cell. Protein acetylation by GNATs has been noted in many bacterial species (18, 19, 49). RPO\_DmdB2 was able to be acetylated by a known Pat from *R. palustris*, *RpPat*, causing a 60% reduction in RPO\_DmdB2 activity. RPO\_DmdB1 was not stable enough for the acetylation assays. The acetylation of RPO\_DmdB2 could also be reversed by two deacetylases from *R. pomeroyi* as well as a deacetylase from *B. subtilis*. However, the *R. pomeroyi* GNAT acetyltransferase responsible for acetylating RPO\_DmdB2 was not identified out of the 20 that have been cloned and purified thus far. The correct GNAT may be within the 20 that have been tested, but the conditions for the acetylation to take place may not have been tested.

The results with the *RpPat* and the various deacetylase appear to indicate that RPO\_DmdB2 is able to be regulated by acetylation. We can now begin to adjust our DmdB

regulatory model. Acetylation is proposed to occur when there are imbalances in cellular energy or the CoA:acetyl-CoA ratio (19, 50). This fits in well with the proposed regulatory model for the DmdB enzymes. RPO\_DmdB2 may be acetylated while DMSP is being stored in the cell for use as an osmolyte and antioxidant. Both enzymes will remain inactive due to DMSP-based inhibition. When DMSP is needed as a carbon or energy source, ADP levels in the cell begin to rise, causing RPO\_DmdB1 to increase in activity. When sufficient amounts of MMPA are produced RPO\_DmdB2 is deacetylated and begins converting MMPA to MMPA-CoA. Once the energy charge of the cell is restored, RPO\_DmdB1 activity lowers. RPO\_DmdB2 continues to function until it is once again acetylated due to imbalances in the availability of free CoA. RPO\_DmdB2 activity levels may also decrease as the turnover rate of DmdA slows due to decreased availability of free THF or slower turnover of methyl-THF.

The regulation of DMSP metabolism in *R. pomeroyi* appears to be complex, and involves delicate balances of vital cell resources like THF and CoA. All of the potential uses of DMSP in *R. pomeroyi* will affect its metabolism within the cell. RPO\_DmdB1 and RPO\_DmdB2 are not the only regulatory point for the DMSP demethylation pathway. DmdA is the gatekeeper of the demethylation pathway, but all subsequent steps also require careful control to ensure efficient functioning and maintenance of homeostasis within the bacterial cell. While these experiments have provided insight into the regulation of this pathway, they have not yielded any concrete conclusions.

## References

1. **Kiene RP.** 1996. Production of methanethiol from dimethylsulfoniopropionate in marine surface waters. *Mar. Chem.* **54**:69-83.
2. **Reisch CR, Stoudemayer MJ, Varaljay VA, Amster IJ, Moran MA, Whitman WB.** 2011. Novel pathway for assimilation of dimethylsulphoniopropionate widespread in marine bacteria. *Nature* **473**:208-211.
3. **Simo R.** 2001. Production of atmospheric sulfur by oceanic plankton: biogeochemical, ecological and evolutionary links. *Trends Ecol. Evol.* **16**:287-294.
4. **Charlson RL, Lovelock JE, Andreae MO, Warren SG.** 1987. Oceanic phytoplankton, atmospheric sulfur, cloud albedo and climate. *Nature* **326**:655-611.
5. **Lovelock JE, Maggs RJ, Rasmussen RA.** 1972. Atmospheric dimethyl sulfide and natural sulfur cycle. *Nature* **237**:452.
6. **Howard EC, Henriksen JR, Buchan A, Reisch CR, Burgmann H, Welsh R, Ye W, Gonzalez JM, Mace K, Joye SB, Kiene RP, Whitman WB, Moran MA.** 2006. Bacterial taxa that limit sulfur flux from the ocean. *Science* **314**:649-652.
7. **Kiene RL, Linn LJ, Bruton, JA.** 2000. New and important roles for DMSP in marine microbial communities. *J. Sea Res.* **43**:209-224.
8. **Salgado P, Kiene R, Wiebe W, Magalhaes C.** 2014. Salinity as a regulator of DMSP degradation in *Ruegeria pomeroyi* DSS-3. *J. Microbiol.* **52**:948-954.
9. **Lesser MP.** 2006. Oxidative stress in marine environments: biochemistry and physiological ecology. *Annu. Rev. Physiol.* **68**:253-278.
10. **Reisch CR, Moran MA, Whitman WB.** 2008. Dimethylsulfoniopropionate-dependent demethylase (DmdA) from *Pelagibacter ubique* and *Silicibacter pomeroyi*. *J. Bacteriol.* **190**:8018-8024.
11. **Reisch CR, Crabb WM, Gifford SM, Teng Q, Stoudemayer MJ, Moran MA, Whitman WB.** 2013. Metabolism of dimethylsulphoniopropionate by *Ruegeria pomeroyi* DSS-3. *Mol. Microbiol.* **89**:774-791.
12. **Curson AR, Todd JD, Sullivan MJ, Johnston AW.** 2011. Catabolism of dimethylsulphoniopropionate: microorganisms, enzymes and genes. *Nat. Rev. Microbiol.* **9**:849-859.
13. **Johnston AW, Green RT, Todd JD.** 2016. Enzymatic breakage of dimethylsulfoniopropionate—a signature molecule for life at sea. *Curr. Opin. Chem. Biol.* **31**:58-65.

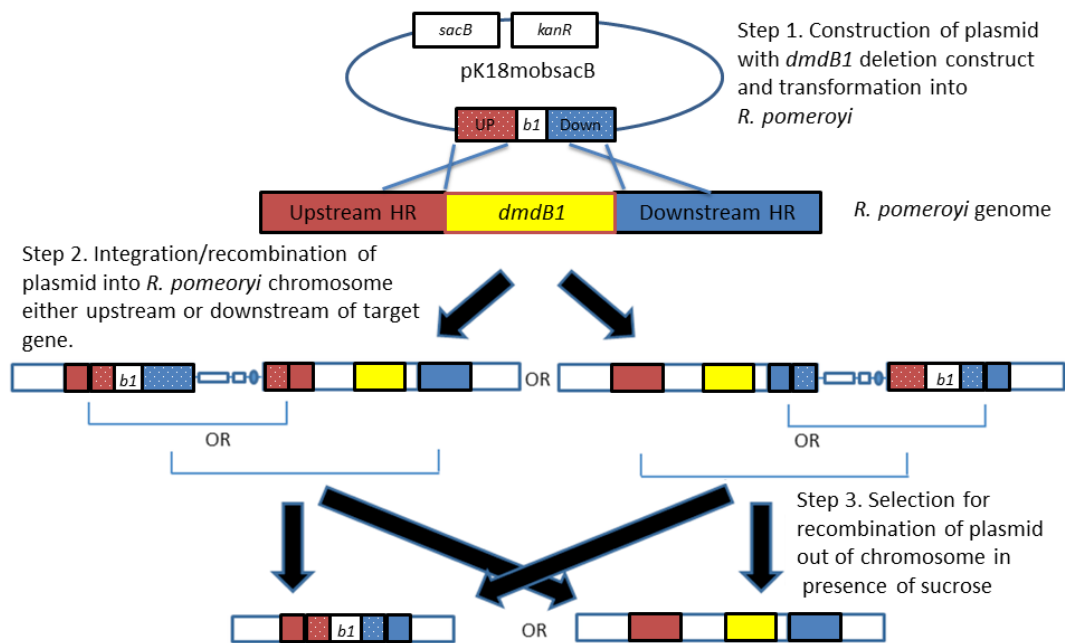
14. **Bullock HA, Reisch CR, Burns AS, Moran MA, Whitman WB.** 2014. Regulatory and functional diversity of methylmercaptopropionate coenzyme A ligases from the dimethylsulfoniopropionate demethylation pathway in *Ruegeria pomeroyi* DSS-3 and other proteobacteria. *J. Bacteriol.* **196**:1275-1285.
15. **Atkinson DE.** 1968. The energy charge of the adenylate pool as a regulatory parameter. Interaction with feedback modifiers. *Biochemistry* **7**:4030-4034.
16. **Starai VJ, Celic I, Cole RN, Boeke JD, Escalante-Semerena JC.** 2002. Sir2-dependent activation of acetyl-CoA synthetase by deacetylation of active lysine. *Science* **298**:2390-2392.
17. **Wang Q, Zhang Y, Yang C, Xiong H, Lin Y, Yao J, Li H, Xie L, Zhao W, Yao Y, Ning ZB, Zeng R, Xiong Y, Guan KL, Zhao S, Zhao GP.** 2010. Acetylation of metabolic enzymes coordinates carbon source utilization and metabolic flux. *Science* **327**:1004-1007.
18. **Thao S, Escalante-Semerena JC.** 2011. Control of protein function by reversible N-epsilon-lysine acetylation in bacteria. *Curr. Opin. Microbiol.* **14**:200-204.
19. **Chan CH, Garrity J, Crosby HA, Escalante-Semerena JC.** 2011. In *Salmonella enterica*, the sirtuin-dependent protein acylation/deacylation system (SDPADS) maintains energy homeostasis during growth on low concentrations of acetate. *Mol. Microbiol.* **80**:168-183.
20. **Thao S, Escalante-Semerena JC.** 2011. Biochemical and thermodynamic analyses of *Salmonella enterica* Pat, a multidomain, multimeric N(epsilon)-lysine acetyltransferase involved in carbon and energy metabolism. *MBio.* **2**.
21. **Brandl A, Heinzl T, Kramer OH.** 2009. Histone deacetylases: salesmen and customers in the post-translational modification market. *Biol. Cell* **101**:193-205.
22. **Baumann P, Baumann L.** 1981. The marine gram-negative eubacteria: genera *Photobacterium*, *Beneckeia*, *Alteromonas*, *Pseudomonas*, and *Alcaligenes*., p 1302–1331. In M. P. Starr HS, H. G. Trüper, A. Balows & H. G. Schlegel (ed), *The Prokaryotes*. Springer-Verlag, Berlin.
23. **Moran MA, Buchan A, Gonzalez JM, Heidelberg JF, Whitman WB, Kiene RP, Henriksen JR, King GM, Belas R, Fuqua C, Brinkac L, Lewis M, Johri S, Weaver B, Pai G, Eisen JA, Rahe E, Sheldon WM, Ye W, Miller TR, Carlton J, Rasko DA, Paulsen IT, Ren Q, Daugherty SC, Deboy RT, Dodson RJ, Durkin AS, Madupu R, Nelson WC, Sullivan SA, Rosovitz MJ, Haft DH, Selengut J, Ward N.** 2004. Genome sequence of *Silicibacter pomeroyi* reveals adaptations to the marine environment. *Nature* **432**:910-913.

24. **Chambers ST, Kunin CM, Miller D, Hamada A.** 1987. Dimethylthetin can substitute for glycine betaine as an osmoprotectant molecule for *Escherichia coli*. J. Bacteriol. **169**:4845-4847.
25. **Horton RM, Ho SN, Pullen JK, Hunt HD, Cai Z, Pease LR.** 1993. Gene splicing by overlap extension. Methods Enzymol. **217**:270-279.
26. **Henricksen J.** 2008. Physiology of dimethylsulfoniopionate metabolism in a model marine Roseobacter, *Silicibacter pomeroyi*. PhD. University of Georgia, Athens, GA.
27. **Galloway NR, Toutkoushian H, Nune M, Bose N, Momany C.** 2013. Rapid cloning for protein crystallography using type IIS restriction enzymes. Cryst. Growth Des. **13**: 2833-2839.
28. **Hopner T, Knappe J.** 1974. Formate: determination with formate dehydrogenase. Methods of Enzymatic Analysis **3**:1551-1555.
29. **Matthews RG, Haywood BJ.** 1979. Inhibition of pig liver methylenetetrahydrofolate reductase by dihydrofolate: some mechanistic and regulatory implications. Biochemistry **18**:4845-4851.
30. **Sheppard CA, Trimmer EE, Matthews RG.** 1999. Purification and properties of NADH-dependent 5, 10-methylenetetrahydrofolate reductase (MetF) from *Escherichia coli*. J. Bacteriol. **181**:718-725.
31. **Bergmeyer HU.** 1972. Standardization of enzyme assays. Clin. Chem. **18**:1305-1311.
32. **D'Ari L, Rabinowitz JC.** 1991. Purification, characterization, cloning, and amino acid sequence of the bifunctional enzyme 5,10-methylenetetrahydrofolate dehydrogenase/5,10-methenyltetrahydrofolate cyclohydrolase from *Escherichia coli*. J. Biol. Chem. **266**:23953-23958.
33. **de Mata ZS, Rabinowitz JC.** 1980. Formyl-methenyl-methylenetetrahydrofolate synthetase(combined) from yeast. Biochemical characterization of the protein from an *ade3* mutant lacking the formyltetrahydrofolate synthetase function. J. Biol. Chem. **255**:2569-2577.
34. **Datsenko KA, Wanner BL.** 2000. One-step inactivation of chromosomal genes in *Escherichia coli* K-12 using PCR products. PNAS **97**:6640-6645.
35. **Quenee L, Lamotte D, Polack B.** 2005. Combined *sacB*-based negative selection and *cre-lox* antibiotic marker recycling for efficient gene deletion in *Pseudomonas aeruginosa*. Biotechniques **38**:63-67.
36. **Schafer A, Tauch A, Jager W, Kalinowski J, Thierbach G, Puhler A.** 1994. Small mobilizable multi-purpose cloning vectors derived from the *Escherichia coli* plasmids

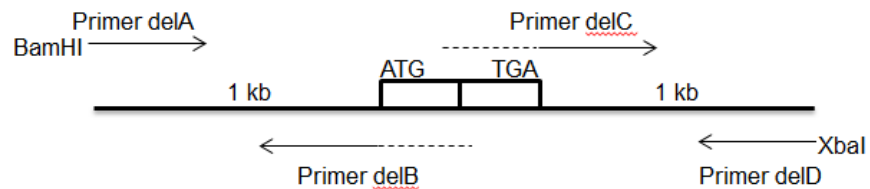
- pK18 and pK19: selection of defined deletions in the chromosome of *Corynebacterium glutamicum*. *Gene* **145**:69-73.
37. **Hoang TT, Karkhoff-Schweizer RR, Kutchma AJ, Schweizer HP.** 1998. A broad-host-range F<sub>1</sub>p-FRT recombination system for site-specific excision of chromosomally-located DNA sequences: application for isolation of unmarked *Pseudomonas aeruginosa* mutants. *Gene* **212**:77-86.
  38. **Tracy E, Ye F, Baker BD, Munson RS, Jr.** 2008. Construction of non-polar mutants in *Haemophilus influenzae* using FLP recombinase technology. *BMC Mol. Biol.* **9**:101.
  39. **Keller KL, Bender KS, Wall JD.** 2009. Development of a markerless genetic exchange system for *Desulfovibrio vulgaris* Hildenborough and its use in generating a strain with increased transformation efficiency. *Appl. Environ. Microbiol.* **75**:7682-7691.
  40. **Fu R, Voordouw G.** 1998. ISD1, an insertion element from the sulfate-reducing bacterium *Desulfovibrio vulgaris* Hildenborough: structure, transposition, and distribution. *Appl. Environ. Microbiol.* **64**:53-61.
  41. **Hartman SC, Buchanan JM.** 1959. The biosynthesis of the purines. *Ergeb Physiol* **50**:75-121.
  42. **Koutmos M, Datta S, Pattridge KA, Smith JL, Matthews RG.** 2009. Insights into the reactivation of cobalamin-dependent methionine synthase. *PNAS* **106**:18527-18532.
  43. **Kiene RP, Linn LJ, Gonzalez J, Moran MA, Bruton JA.** 1999. Dimethylsulfoniopropionate and methanethiol are important precursors of methionine and protein-sulfur in marine bacterioplankton. *Appl. Environ. Microbiol.* **65**:4549-4558.
  44. **Ferla MP, Patrick WM.** 2014. Bacterial methionine biosynthesis. *Microbiology* **160**:1571-1584.
  45. **Gould WD, Kanagawa T.** 1992. Purification and properties of methyl mercaptan oxidase from *Thiobacillus thioparus* TK-m. *J. Gen. Microbiol.* **138**:217-221.
  46. **Chen NH, Djoko KY, Veyrier FJ, McEwan AG.** 2016. Formaldehyde stress responses in bacterial pathogens. *Front. Microbiol.* **7**:257.
  47. **Liao Y, Chen S, Wang D, Zhang W, Wang S, Ding J, Wang Y, Cai L, Ran X, Wang X, Zhu H.** 2013. Structure of formaldehyde dehydrogenase from *Pseudomonas aeruginosa*: the binary complex with the cofactor NAD<sup>+</sup>. *Acta. Crystallogr. Sect. F. Struct. Biol. Cryst. Commun.* **69**:967-972.
  48. **Vorholt JA.** 2002. Cofactor-dependent pathways of formaldehyde oxidation in methylotrophic bacteria. *Arch. Microbiol.* **178**:239-249.

49. **Starai VJ, Escalante-Semerena JC.** 2004. Identification of the protein acetyltransferase (Pat) enzyme that acetylates acetyl-CoA synthetase in *Salmonella enterica*. *J. Mol. Biol.* **340**:1005-1012.
50. **Galdieri L, Zhang T, Rogerson D, Lleshi R, Vancura A.** 2014. Protein acetylation and acetyl coenzyme a metabolism in budding yeast. *Eukaryot. Cell* **13**:1472-1483.
51. **Reisch CR, Moran MA, Whitman WB.** 2011. Bacterial catabolism of dimethylsulfoniopropionate (DMSP). *Front. Microbiol.* **2**:172.

(A)

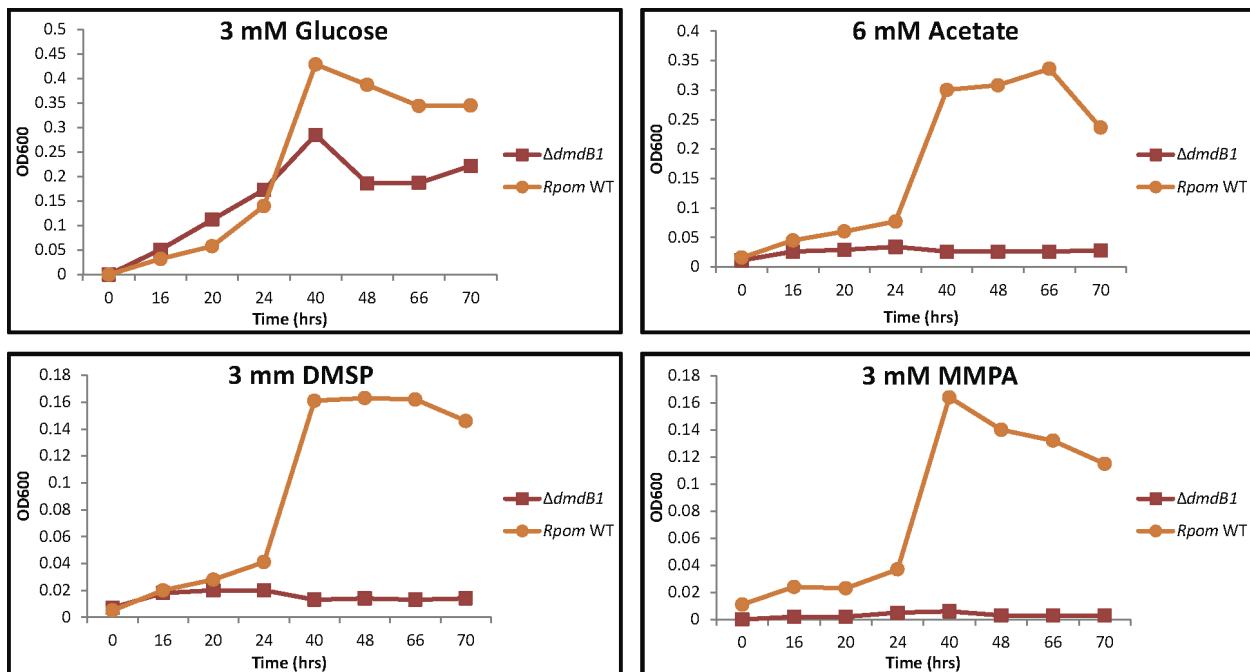


(B)

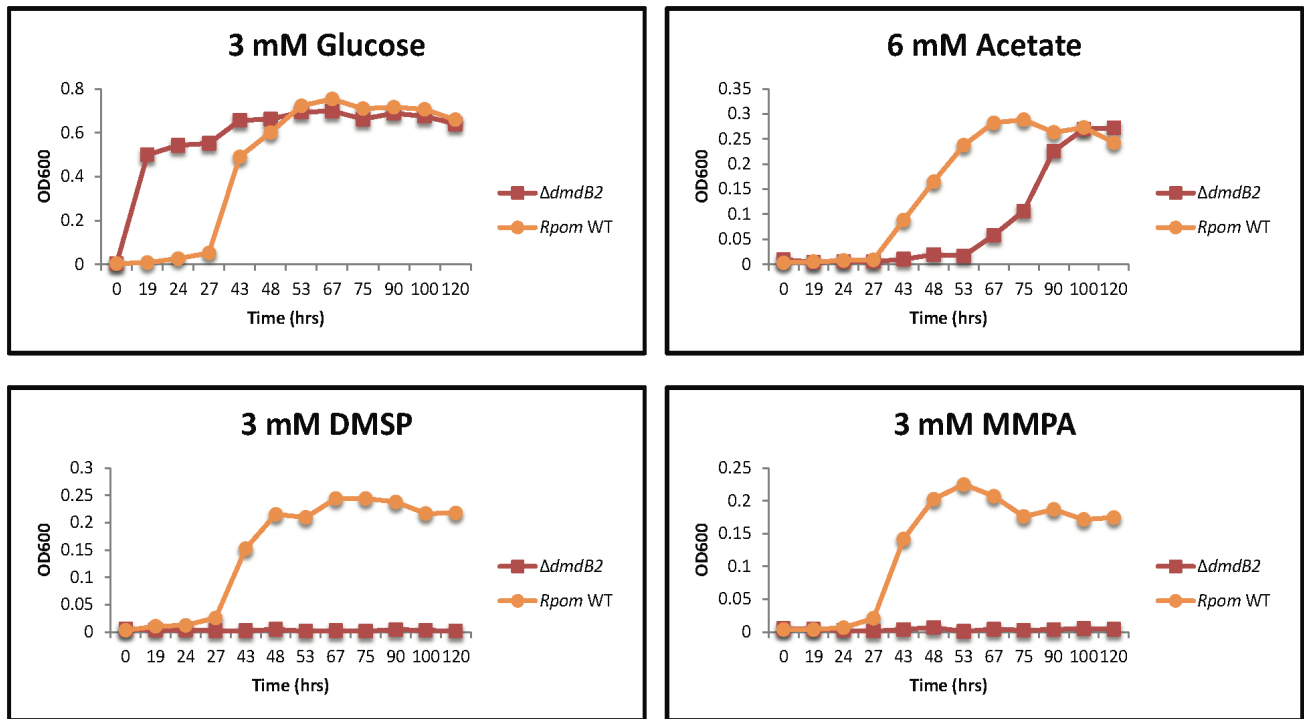


**Figure 4-1.** (A). An overview of the in-frame, markerless deletion system for DmdB1 (*b1*) and DmdB2 using positive selection by kanamycin resistance (*kan<sup>R</sup>*) followed by negative selection with sucrose sensitivity, mediated by *sacB*. Both genes are encoded in the pK18mobsacB plasmid. Once the pK18mobsacB plasmid with deletion construct has been transformed into *R.*

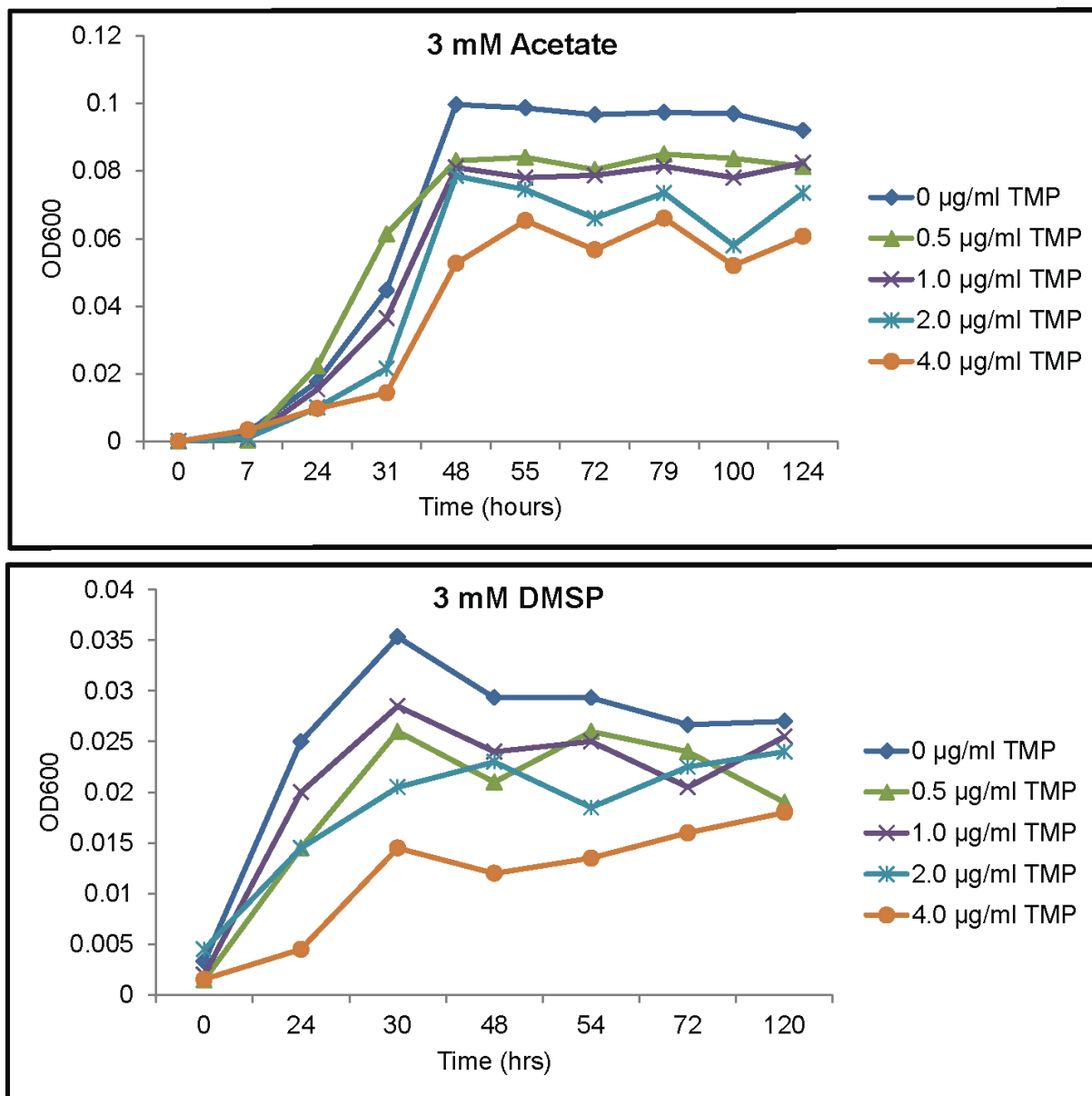
*pomeroyi* (Step 1), integration of the plasmid into the *R. pomeroyi* chromosome via a single crossover event is selected for by resistance to kanamycin (Step 2). This occurs either upstream or downstream of the target gene to be deleted. After verification of plasmid integration, recombination of the plasmid out of the chromosome is accomplished via negative selection with sucrose sensitivity from the *sacB* gene (Step 3). This recombination results in either the deletion of the target gene or reversion to the wild-type, depending on where the initial crossover event occurred. (B) Primer amplification regions and creation of the fusion product for gene deletion.



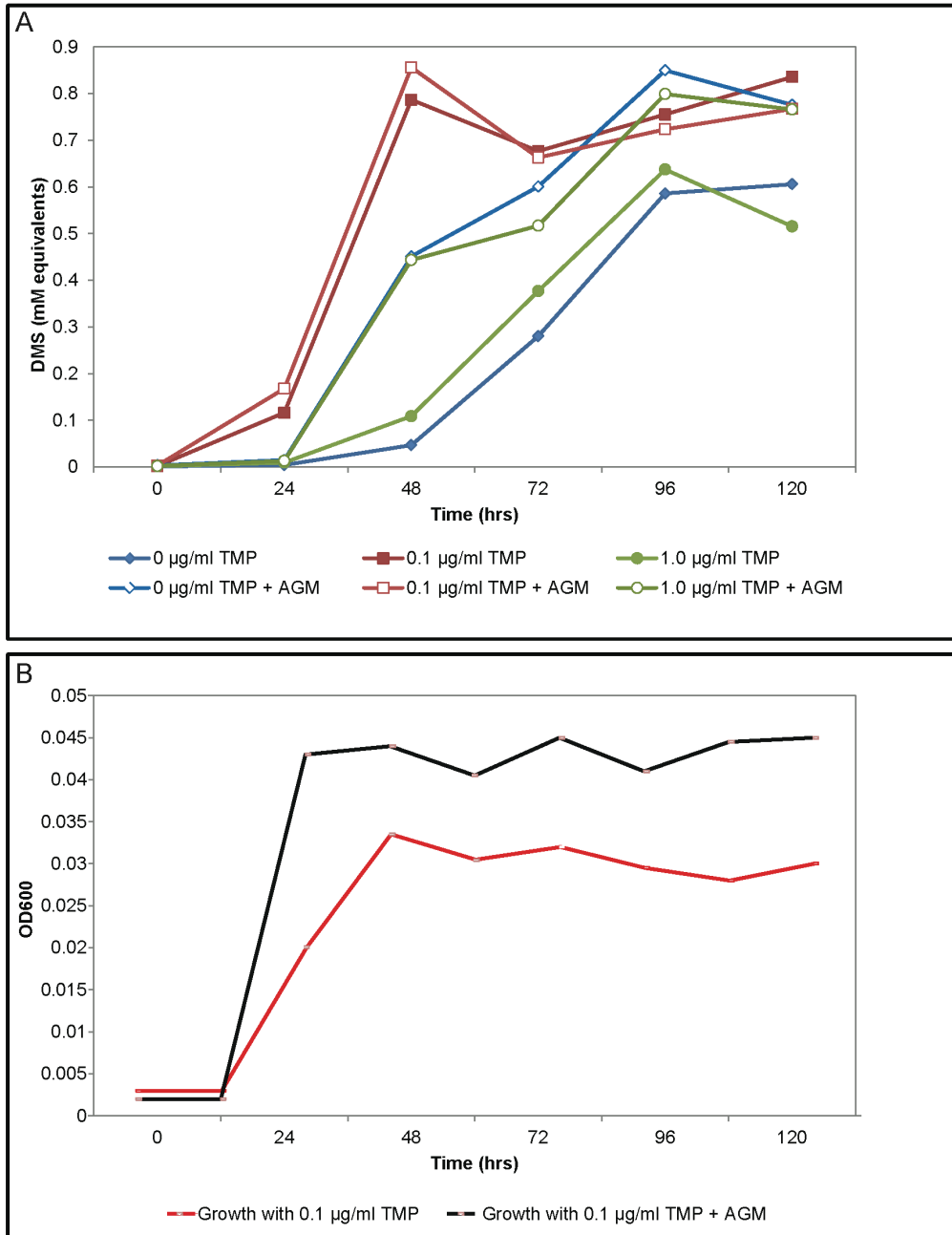
**Figure 4-2.** Growth phenotypes of the *R. pomeroyi* wild-type compared with the in-frame deletion of RPO\_ *dmdB1* ( $\Delta dmdB1$ ). Cultures were grown in 3 ml MBM with the addition of the indicated carbon source. Initial inoculum was 1,000 *R. pomeroyi* cells that had been grown in MBM with 3 mM glucose.



**Figure 4-3.** Growth phenotypes of the *R. pomeroyi* wild-type compared with the in-frame deletion of RPO\_ *dmdB2* ( $\Delta dmdB2$ ). Cultures were grown in 3 ml MBM with the addition of the indicated carbon source. Initial inoculum was 1,000 *R. pomeroyi* cells that had been grown in MBM with 3 mM glucose.



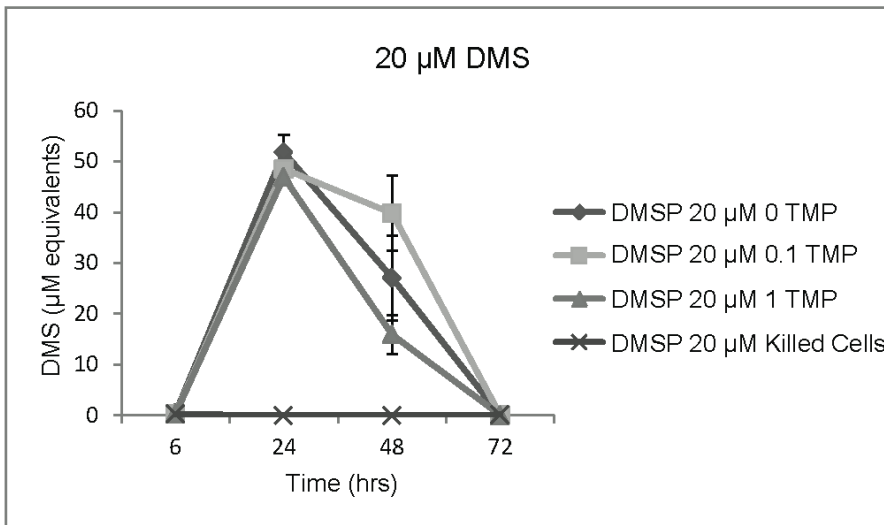
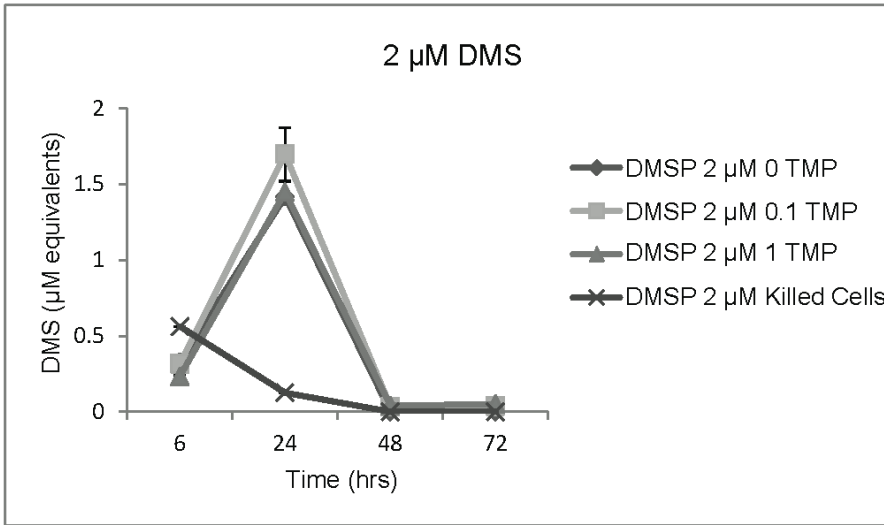
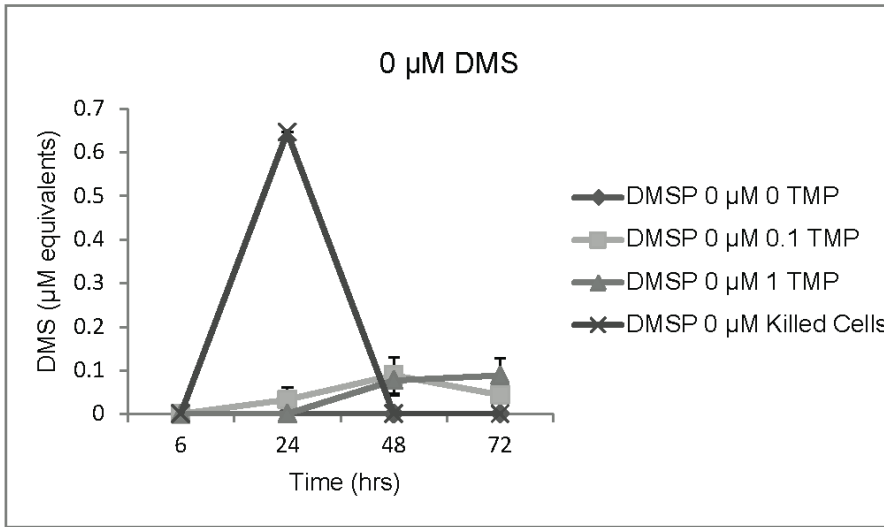
**Figure 4-4.** Growth of *R. pomeroyi* on MBM with 3 mM acetate or 3 mM DMSP in the presence of varying concentrations of the dihydrofolate reductase inhibitor trimethoprim (TMP). Initial inoculum was 1,000 *R. pomeroyi* cells that had been grown in MBM with 3 mM acetate.

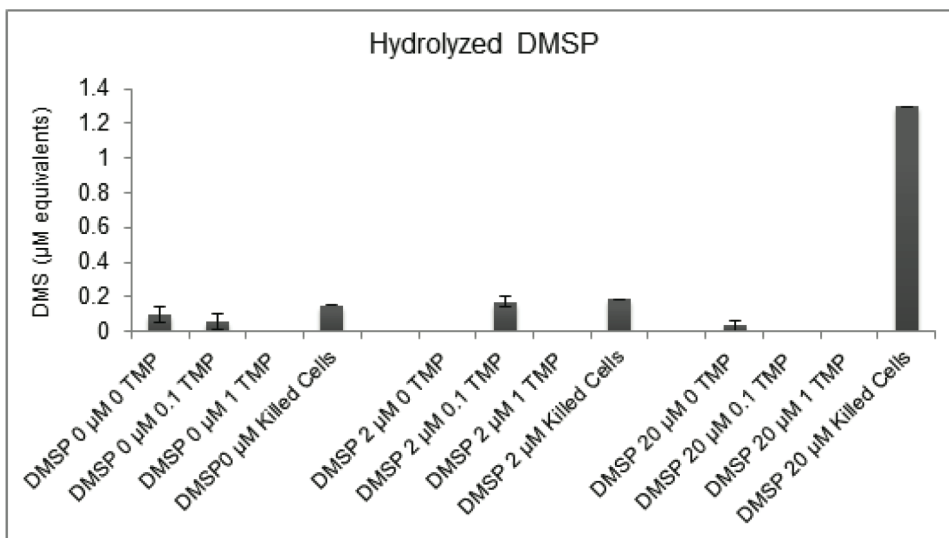


**Figure 4-5.** (A) Effect of TMP additions on DMS production of *R. pomeroyi* grown on 2 mM DMSP. AGM represents additions of 0.025 mM adenine, 0.025 mM guanine, and 0.1 mM methionine. (B) Growth of *R. pomeroyi* on DMSP with 0.1 µg/ml TMP (red) and *R. pomeroyi* on DMSP with 0.1 µg/ml and additions of adenine, guanine, and methionine (black). DMS

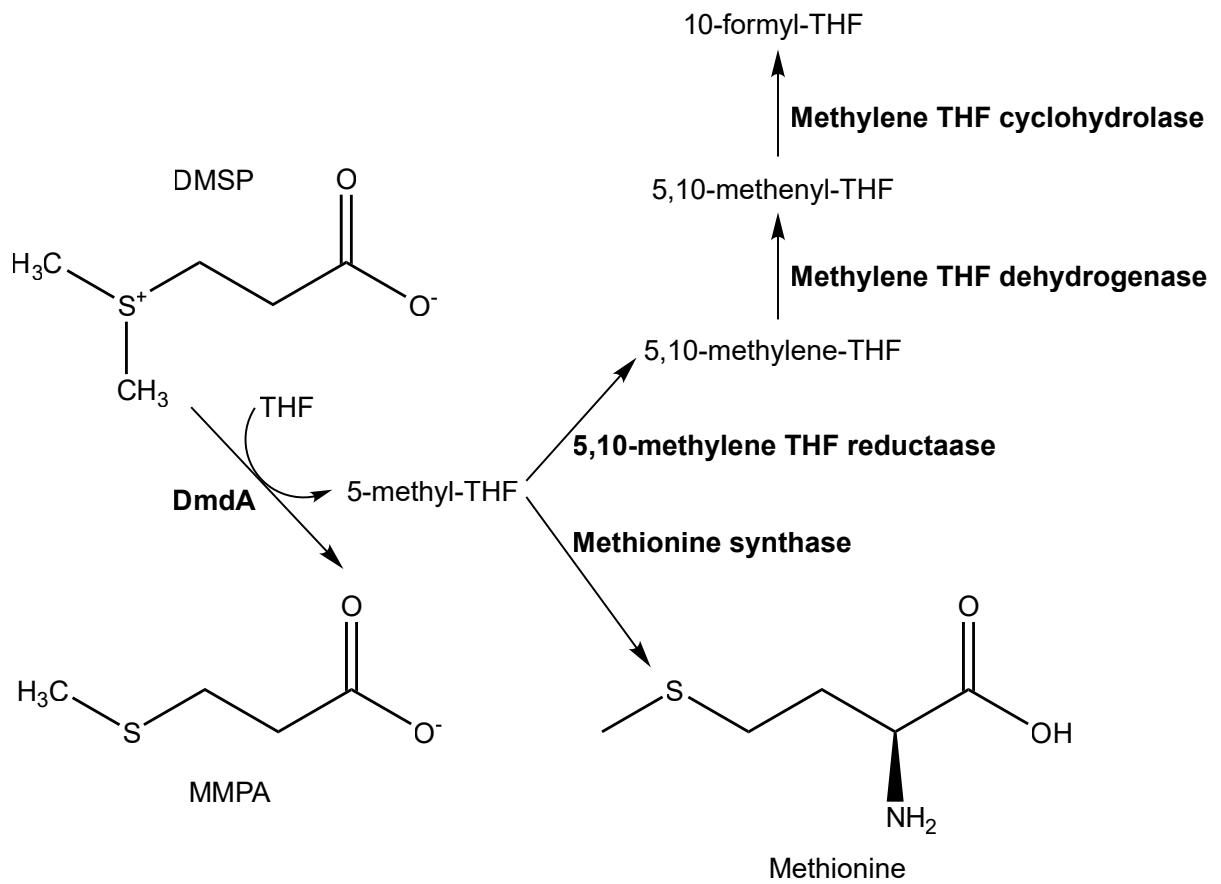
production is given in mM equivalents, the concentration of gas produced per liter of culture.

Initial inoculum was 1,000 *R. pomeroyi* cells that had been grown in MBM with 3 mM acetate.

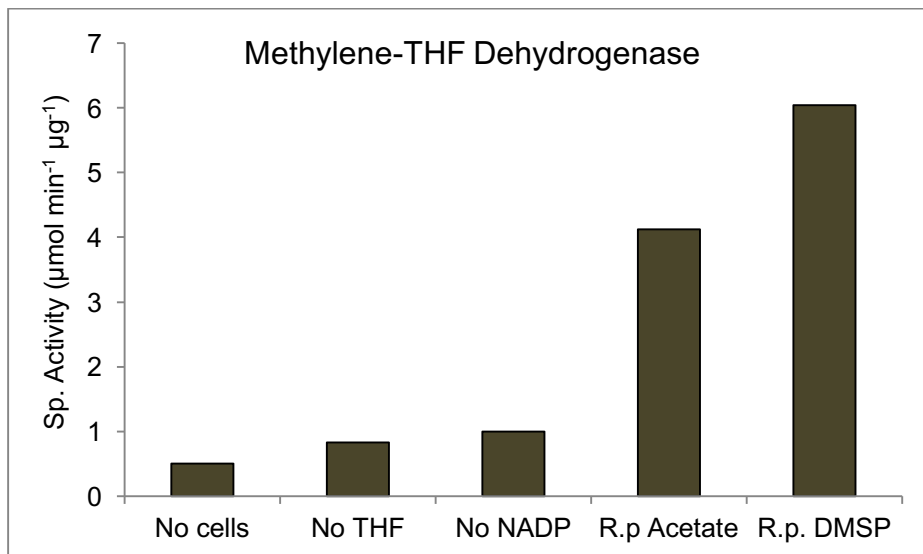
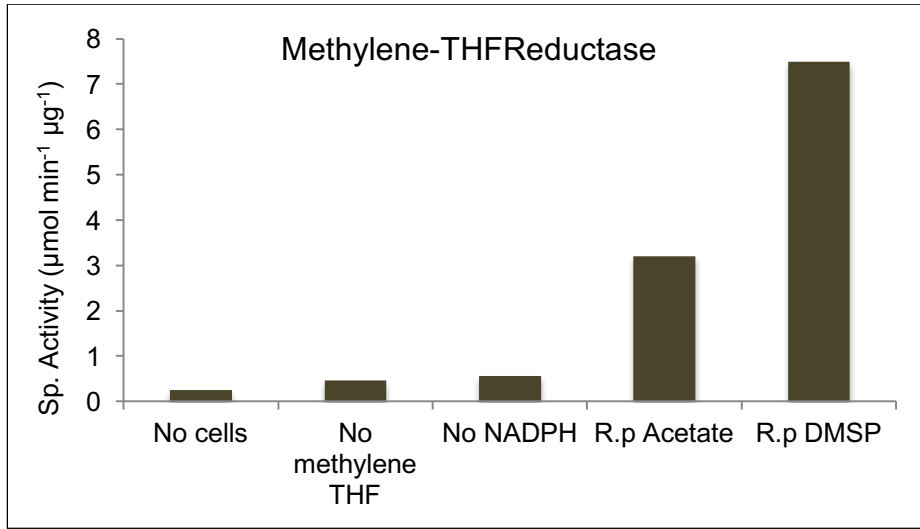




**Figure 4-6.** Effect of TMP additions on DMS productions from seawater samples taken from Sapelo Island, GA. DMS production is given in  $\mu\text{M}$  equivalents, the concentration of gas produced per liter of culture. Samples were hydrolyzed using 5 M NaOH at the conclusion of study to quantify the amount of DMSP remaining (bar graph).



**Figure 4-7:** Overview of the oxidation of methyl-THF to 10-formyl-THF and the responsible enzymes. Adapted from (51).



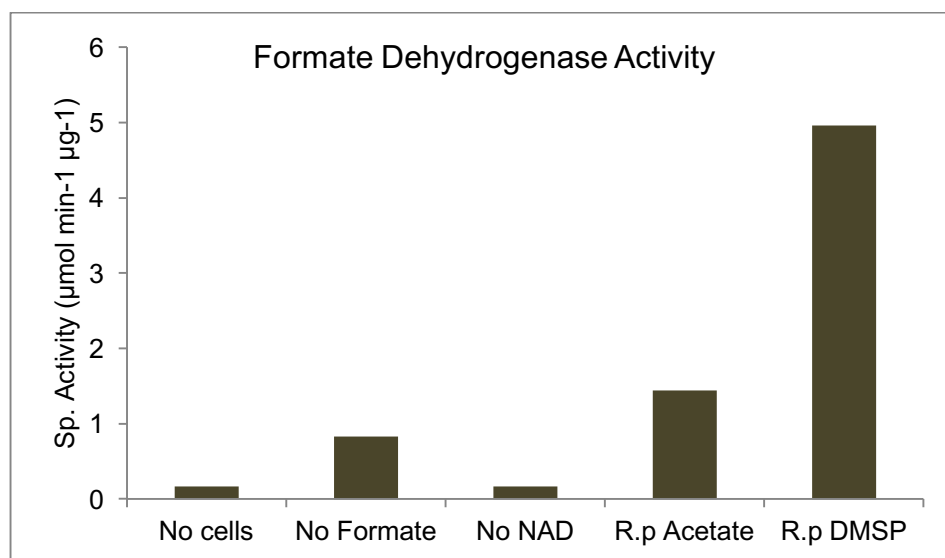
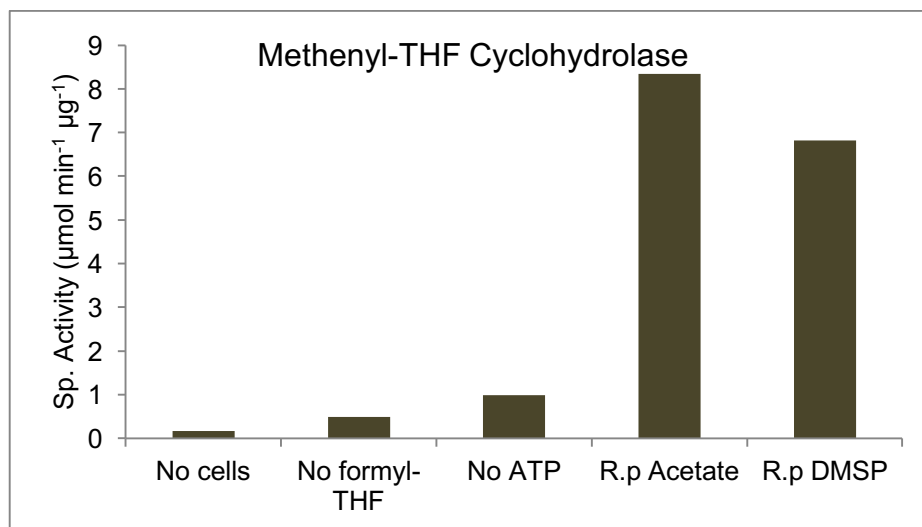


**Figure 4-8.** Specific activity of enzymes involved in the oxidation of methyl-THF to formyl-THF and formate dehydrogenase. Bars represent a single experiment. *R. pomeroyi* cells were grown in MBM with either acetate or DMSP as the sole carbon source. Specific activities between technical replicates displayed a variance of  $\leq 10\%$ .

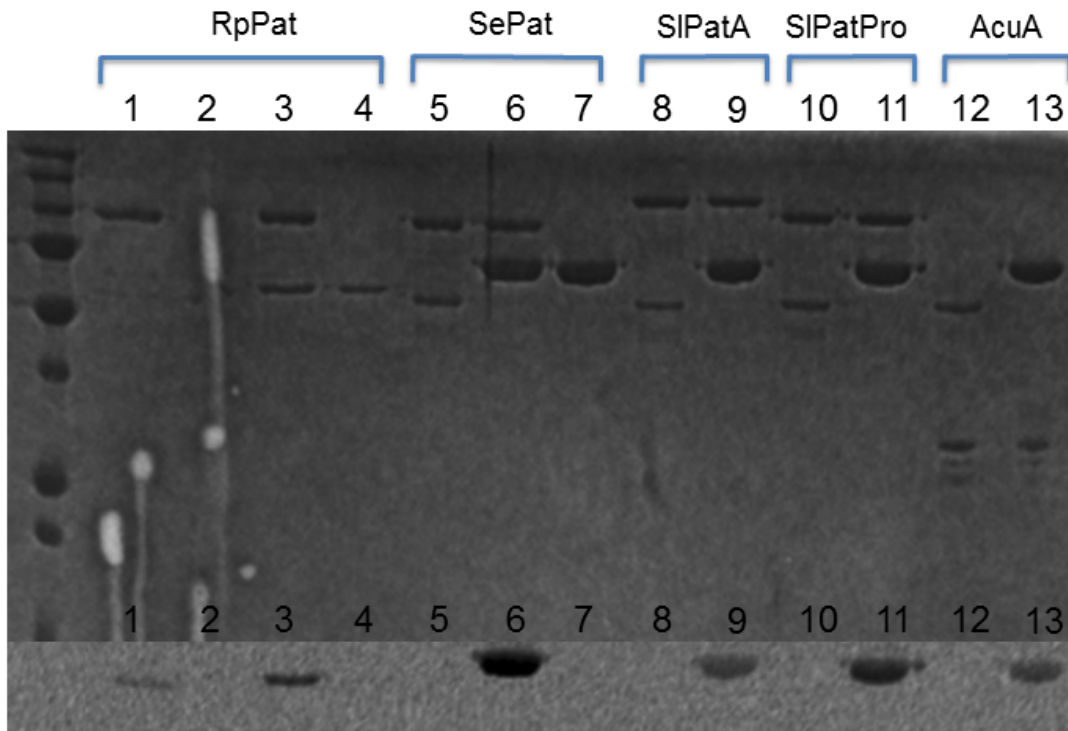


**Figure 4-9.** Acetylation of RPO\_DmdB2 with known protein acetyltransferases (Pats) from *R. palustris* (*RpPat*), *S. enterica* (*SePat*), *S. lividans* (*SIPatA*, *SIPatPro*), and *B. subtilis* (*AcuA*). The top gel is a SDS-PAGE, the bottom gel is a phosphor image of the radiolabeled acetyl-CoA. Acetylation is indicated by the presence of a band in the phosphor image. Lanes 1: RPO\_DmdB2 + *RpPat*, 2: RPO\_DmdB2 alone (negative control), 3: BadA + *RpPat* (positive control), 4: BadA alone (negative control), 5: RPO\_DmdB2 + *SePat*, 6: Acs + *SePat* (positive control), 7: Acs alone (negative control), 8: RPO\_DmdB2 + *SIPatA*, 9: Acs + *SIPatA* (positive control), 10: RPO\_DmdB2 + *SIPatPro*, 11: Acs + *SIPatPro* (positive control), 12: RPO\_DmdB2 + *AcuA*, 13: Acs+ *AcuA* (positive control). BadA: Benzoate CoA ligase, Acs: acetyl-CoA synthetase. Experiment was performed by C. VanDrisse.

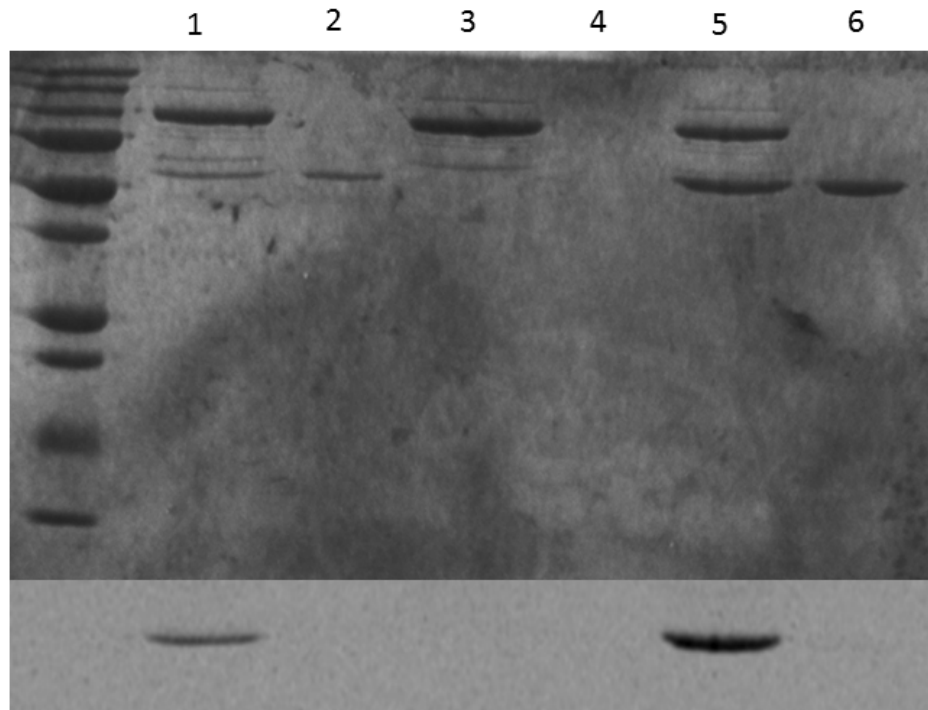


**Figure 4-10.** Acetylation of RPO\_DmdB1 and RPO\_DmdB2 with *RpPat*. The top gel is a SDS-PAGE, the bottom gel is a phosphor image of the radiolabeled acetyl-CoA. Acetylation is indicated by the presence of a band in the phosphor image. Lane 1: RPO\_DmdB2 + *RpPat*, 2: RPO\_DmdB2 alone (negative control), 3: RPO\_DmdB1 + *RpPat*, 4: RPO\_DmdB1 alone (negative control), 5: BadA + *RpPat* (positive control), 6: BadA alone (negative control). Experiment performed by C. VanDrisse.

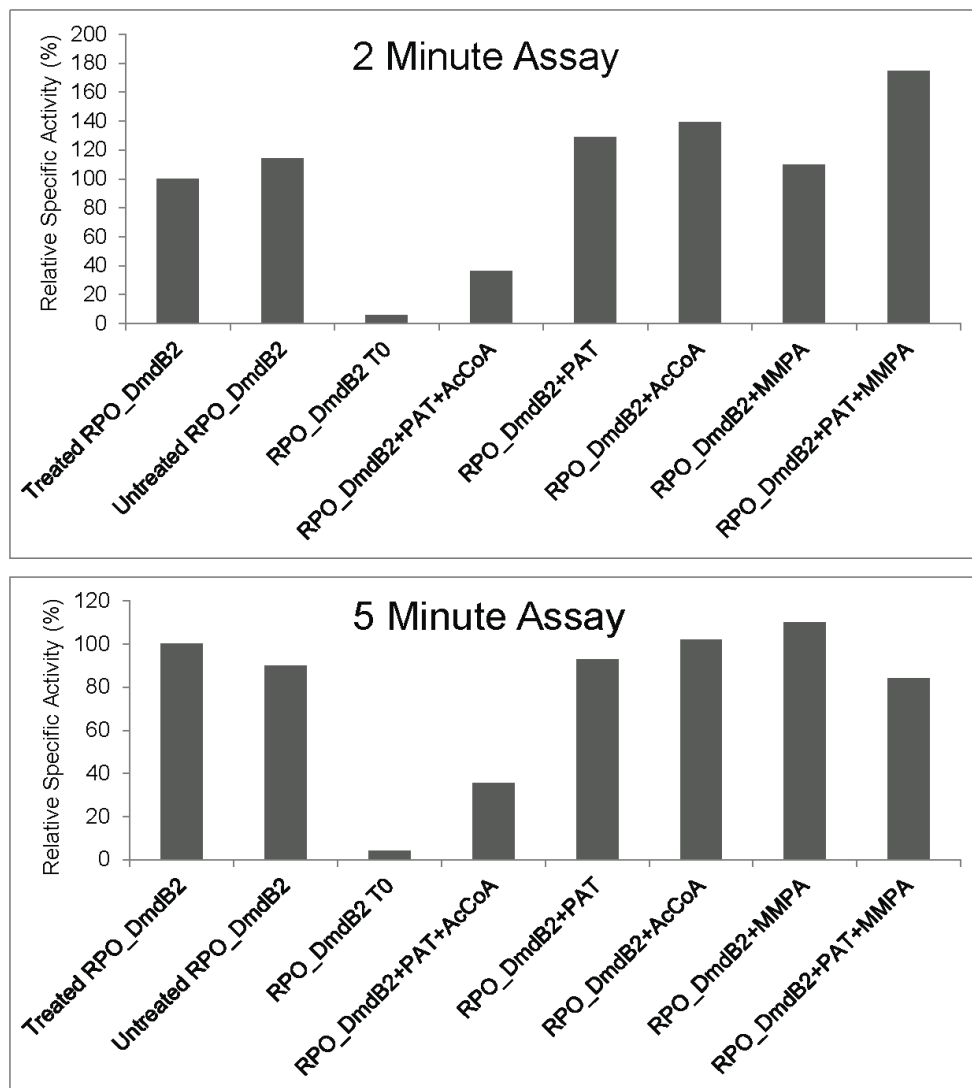


**Figure 4-11.** Relative specific activity with MMPA of RPO\_DmdB2 acetylated with *RpPat*. RPO\_DmdB2 assays were run for two minutes or five minutes as indicated. Bars represent the average of two replicates. Values for replicates were all within 3% of each other. The specific activity designated as 100% activity was  $15.1 \mu\text{mol min}^{-1} \text{mg}^{-1}$ , the specific activity of RPO\_DmdB2 that had been treated in the same conditions as the acetylated samples but without *RpPat* or acetyl-CoA (AcCoA). T0 reactions were stopped immediately after the addition of RPO\_DmdB2 to catalyze the reaction. Acetylation reactions were performed by C. VanDrisse. Activity assays were performed by H. Bullock.

**Table 4-1.** GNAT family acetyltransferases from the *R. pomeroyi* genome.

Locus Tag	Gene Product	Notes
SPO0481	Acetyltransferase, GNAT family	
SPO0888	Acetyltransferase, GNAT family	
SPO1767	Acetyltransferase, GNAT family	
SPO2003	Acetyltransferase, GNAT family	Reduced expression following growth on DMSP
SPO2447	Acetyltransferase, GNAT family	
SPO2622	Acetyltransferase, GNAT family	
SPO3758	Acetyltransferase, GNAT family	
SPOA0075	Hypothetical protein	
SPO2273	Acetyltransferase, GNAT family	
SPO1987	Acetyltransferase, GNAT family	
SPO3250	Acetyltransferase, GNAT family	Reduced expression following growth on DMSP and MMPA
SPO3248	Acetyltransferase, GNAT family	Reduced expression following growth on DMSP and MMPA
SPO3249	Acetyltransferase, GNAT family	Reduced expression following growth on DMSP and MMPA
SPO3551	Acetyltransferase, GNAT family	
SPO3247	Acetyltransferase, GNAT family	Reduced expression following growth on DMSP
SPO1676	Acetyltransferase, GNAT family	

---

Locus Tag	Gene product	Notes
SPO3628	Acetyltransferase, GNAT family	
SPO2063	Acetyltransferase, GNAT family	
SPO0965	Acetyltransferase, GNAT family	
SPO2094	<i>actC</i> domain protien	

---

**Table 4-2.** Deacetylases identified from the *R. pomeroyi* genome.

Locus Tag	Gene Product
SPO0250	Histone deacetylase
SPO0871	LpxC, N-acetylglycosamine deacetylase
SPO0872	Polysaccharide deacetylase
SPO0978	CobB, NAD-dependent deacetylase
SPO3195	Histone deacetylase
SPO1205	LpxC, N-acetylglycosamine deacetylase
SPO2535	AcuC, Histone deacetylase

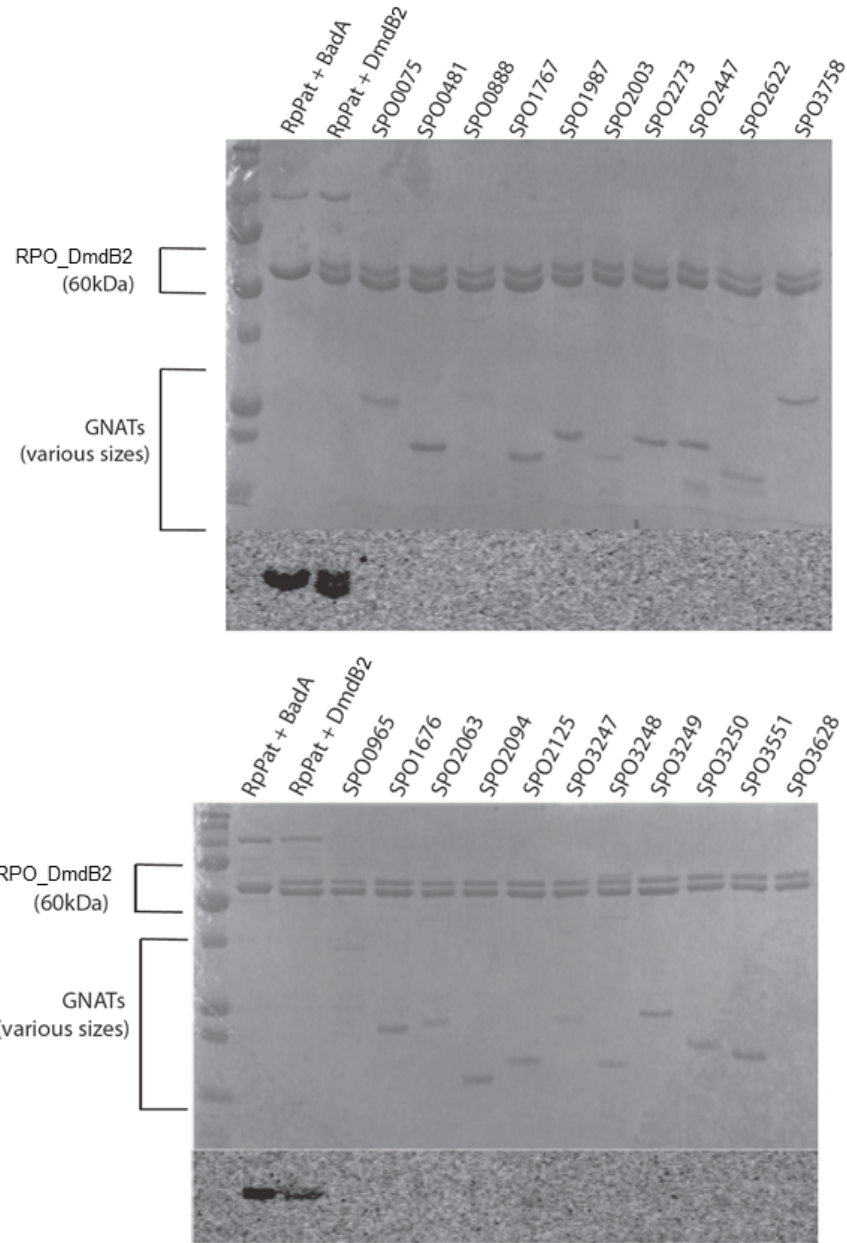


**Figure 4-12.** Acetylation of RPO\_DmdB2 with predicted GNATs from *R. pomeroyi*. The top portion of each gel is a SDS-PAGE and the bottom portion of each gel is a phosphor image of radiolabeled acetyl-CoA. The two high molecular weight bands in the second and third lanes of the top gel are RpPat. Acetylation is indicated by the presence of a band in the phosphor image. RPO\_DmdB2 and BadA acetylated with *RpPat* were positive controls. Experiment performed by C. VanDrise.

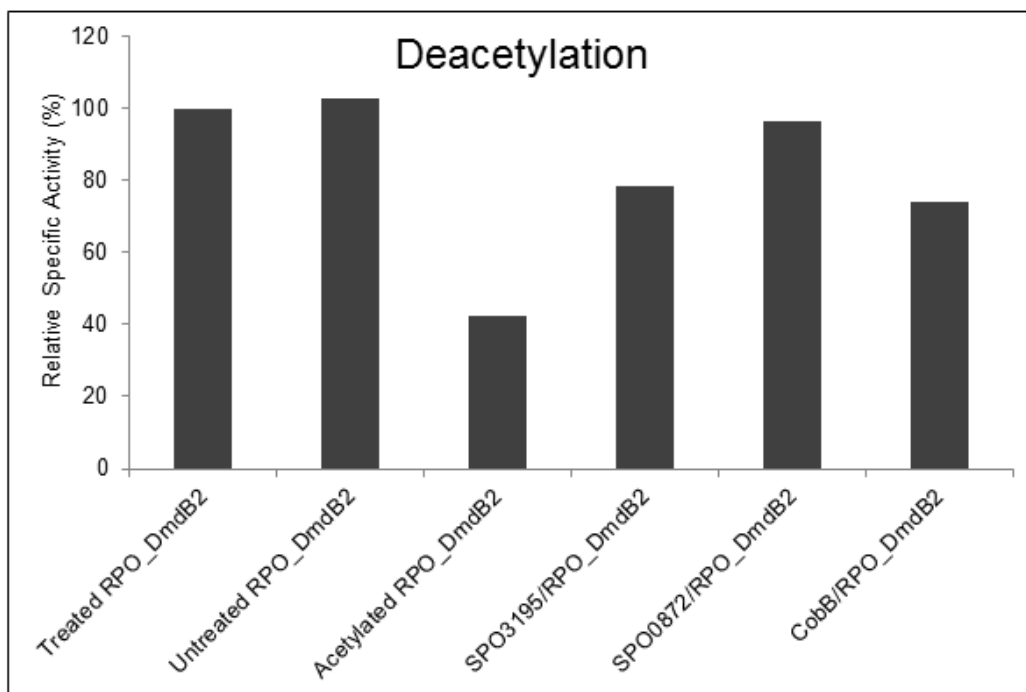


**Figure 4-13.** Relative specific activity of RPO\_DmdB2 after acetylated with *RpPat* and then deacetylation. SPO3195 and SPO0872 are annotated deacetylases in the *R. pomeroyi* genome. CobB is a known deacetylases functioning as a positive control. Bars represent the average of two replicates. Values for replicates were all within 3% of each other. The specific activity designated as 100% activity was  $15.5 \mu\text{mol min}^{-1} \text{mg}^{-1}$ , the specific activity of RPO\_DmdB2 that had been treated in the same conditions as the acetylated/deacetyled samples but without *RpPat*, acetyl-CoA (AcCoA), or the deacetylases. Acetylation and deacetylation assays were performed by C. VanDrise. Activity assays were performed by H. Bullock

## CHAPTER 5

### CONCLUSIONS

The elucidation of steps of the dimethylsulfoniopropionate (DMSP) demethylation and cleavage pathways has made in-depth study of the enzymes responsible for the catalysis of these pathways possible. The purpose of this study was to investigate the kinetic and regulatory properties of the demethylation pathway enzymes and their isozymes. The results shed light on the details of the demethylation pathway, its regulation, and likely roots in other metabolic pathways.

The second step of the demethylation pathway is catalyzed by the methylmercaptopropionate (MMPA)-CoA ligase DmdB. In Chapter 2, the DmdB isozymes from *Ruegeria pomeroyi* as well as representatives from *Pelagibacter ubique*, *Ruegeria lacuscaerulensis*, *Pseudomonas aeruginosa*, and *Burkholderia thailandensis* were investigated. The characterization of the DmdB isozymes from *R. pomeroyi*, RPO\_DmdB1 and RPO\_DmdB2, provided insights into the specialization of enzymes with broad substrate specificities. Both RPO\_DmdB1 and RPO\_DmdB2 were able to catalyze reactions with a range of short chain fatty acids in addition to MMPA. While RPO\_DmdB2 displayed its lowest  $K_m$  for MMPA (0.07 mM), RPO\_DmdB1 had lower  $K_m$ s for propionate (0.04 mM) and butyrate (0.02 mM) than for MMPA (0.08 mM). Despite this variation, both enzymes possessed regulatory mechanisms related to DMSP metabolism. RPO\_DmdB1 and RPO\_DmdB2 were both inhibited by physiologically relevant concentrations of DMSP, but this inhibition was reversible by increasing ADP levels in the case of RPO\_DmdB1 and increasing MMPA levels in the case of RPO\_DmdB2. The DmdB

enzymes from *R. lacuscaerulensis* were sensitive to the presence of DMSP in a manner similar to those from *R. pomeroyi*. By contrast, additions of up to 50 mM DMSP had no effect on the activity of DmdB enzymes from *P. aeruginosa* and *B. thailandensis*. This indicates that sensitivity to DMSP is likely to be an adaptation of marine bacteria or bacteria that degrade DMSP and may be part of a regulatory mechanism.

One of the gaps in our knowledge of the demethylation pathway in marine systems is the lack of homologs to the methylthioacryloyl (MTA)-CoA hydratase *dmdD* in marine metagenomes. The identification of the acrylate utilization hydratase AcuH, discussed in Chapter 3, helps to close this gap. AcuH was found to be widely distributed among likely DMSP-utilizers as well as microorganisms unlikely to encounter DMSP. The AcuH isolated from *R. lacuscaerulensis* had sufficient MTA-CoA hydratase activity to support growth on DMSP and MMPA as sole carbon sources and partially complement a *R. pomeroyi dmdD* (*SPO3805::tet*) deletion strain. However, this was not true for all AcuHs investigated, and all AcuHs tested had substantially higher activity with crotonyl-CoA and acryloyl-CoA than with MTA-CoA. Thus, this enzyme is not a specialized MTA-CoA hydratase but instead an acryloyl-CoA hydratase that also has the ability to hydrolyze MTA-CoA. While AcuH in *R. lacuscaerulensis* allows for utilization of the demethylation pathway, it is probable that AcuH also has other functions and has only adapted for use in DMSP metabolism in certain microorganisms. Interestingly, the *R. lacuscaerulensis* AcuH, like RPO\_DmdB1, responded to the presence of ADP, displaying a lower  $K_m$  when dialyzed in the presence ADP (0.02 mM) than when dialyzed without ADP (0.31 mM). This result further implicates a role for cellular energy charge in DMSP metabolism that will need to be investigated further.

In Chapter 4, we built upon the model for the regulation of the DMSP demethylation pathway proposed in Chapter 2. This model proposed two different methods of regulation for the two *R. pomeroyi* DmdB isozymes. In the first method, RPO\_DmdB1 responds to decreasing cellular energy charge during carbon and energy limitation to overcome DMSP based inhibition and to stimulate use of the demethylation pathway. Once the energy charge has increased back to the appropriate level, DMSP inhibition of RPO\_DmdB1 is restored. To further investigate this regulatory mechanism, the role of acetylation by Gcn5-like protein *N*-acetyltransferase (GNATs) was analyzed. Acetylation is thought to occur as a result of imbalances in cellular energy or the CoA:acetyl-CoA ratio. While tests with RPO\_DmdB1 were unsuccessful due to protein instability, RPO\_DmdB2 was able to be acetylated by the *Rhodospseudomonas palustris* *N*-acetyltransferase *RpPat* *in vitro*. This resulted in a decrease in MMPA-CoA ligase activity by approximately 60% compared with the wild-type. However, none of the more than 20 *R. pomeroyi* acetyltransferases were able to acetylate RPO\_DmdB2 *in vitro*. The deacetylases from the *R. pomeroyi* genome were able to reverse the acetylation by *RpPat* and restore enzyme activity to nearly wild-type levels. Although the results were inconclusive, it is still possible that acetylation may play a regulatory role in DmdB under some conditions yet to be discovered.

An additional method of DmdB regulation is based on levels of DmdA activity. The inhibition of RPO\_DmdB2 by DMSP is reversed by increasing levels of MMPA as a result of increased DmdA activity. DmdA activity levels likely depend on the availability of free tetrahydrofolate (THF) and the turnover of methyl-THF. To test this hypothesis, THF biosynthesis was inhibited using the dihydrofolate reductase inhibitor trimethoprim (TMP). The inhibition of THF biosynthesis in *R. pomeroyi* increased DMS production and, thus, use of the cleavage pathway. Although samples with 0.1  $\mu\text{g/ml}$  of TMP also increased DMS production in

water samples containing natural populations of DMSP-utilizers taken from Sapelo Island, GA, this experiment warrants repetition to verify the results. Additionally, the enzymes formate dehydrogenase and methylene-THF reductase showed a two-fold increase in activity when cells were grown on DMSP as a sole carbon source compared with acetate. Both of these enzymes would be involved in the turnover of methyl-THF. However, the other enzymes involved in the turnover of methyl-THF, methylene-THF dehydrogenase and methenyl-THF cyclohydrolase, did not show increased activity in the presence of DMSP.

The characterization of the DmdB and AcuH enzymes and their potential regulation has yielded new insights into the metabolism of DMSP. Exposure to DMSP has resulted in the adaption of these enzymes to function within the demethylation pathway, allowing for metabolic flexibility and the ability to use a sometimes abundant carbon and sulfur source. The regulation of the demethylation pathway is complex and multifaceted, a result of needing to balance the various role of DMSP in the cell as well as the levels of resources like THF and CoA. The next step will be to build on the information presented here to more fully understand the dynamics between the use of the demethylation and cleavage pathways.